Summer 2011

Automatic High-Fidelity 3D Road Network Modeling

Jie Wang
Old Dominion University

AUTOMATIC HIGH-FIDELITY 3D ROAD NETWORK MODELING

by

Jie Wang
B.S. August 2004, Beijing Jiaotong University, China
M.E. March 2008, Institute of Computing Technology, CAS, China

A Dissertation Submitted to the Faculty of
Old Dominion University in Partial Fulfillment of the
Requirements for the Degree of

DOCTOR OF PHILOSOPHY

MODELING AND SIMULATION

OLD DOMINION UNIVERSITY
August 2011

Approved by:

_____
Yuzhong Shen (Director)

_____
Frederic D. McKenzie (Member)

_____
Jiang Li (Member)

_____
Duc T. Nguyen (Member)

ABSTRACT

AUTOMATIC HIGH-FIDELITY 3D ROAD NETWORK MODELING

Jie Wang
Old Dominion University, 2011
Director: Dr. Yuzhong Shen

Many computer applications such as racing games and driving simulations frequently make use of 3D high-fidelity road network models for a variety of purposes. However, there are very few existing methods for automatic generation of 3D realistic road networks, especially for those in the real world. On the other hand, vast road network GIS data have been collected in the past and used by a wide range of applications, such as navigation and evaluation. A method that can automatically produce 3D high-fidelity road network models from 2D real road GIS data will significantly reduce both the labor and time needed to generate these models, and greatly benefit numerous applications involving road networks. Based on a set of selected civil engineering rules for road design, this dissertation research addresses this problem with a novel approach which transforms existing road GIS data that contain only 2D road centerline information into 3D road network models. The proposed method consists of several components, mainly including road GIS data preprocessing, 3D centerline modeling and 3D geometry modeling. During road data preprocessing, topology of the road network is extracted from raw road data as a graph composed of road nodes and road links; road link information is simplified and classified. In the 3D centerline modeling part, the missing height information of the road centerline is inferred based on 2D road GIS data, intersections are extracted from road nodes and the whole road network is represented as road intersections and road segments in parametric forms.

Finally, the 3D road centerline models are converted into various 3D road geometry models consisting of triangles and textures in the 3D geometry modeling phase.

With this approach, basic road elements such as road segments, road intersections and traffic interchanges are generated automatically to compose sophisticated road networks. Results show that this approach provides a rapid and efficient 3D road modeling method for applications that have stringent requirements on high-fidelity road models.

This dissertation is dedicated to my family.

ACKNOWLEDGMENTS

There are many people who have contributed time, knowledge, skill and support to the successful completion of this dissertation. Firstly I extend many, many thanks to my advisor, Dr. Yuzhong Shen, for his patience and guidance on my study and editing of this manuscript. His untiring efforts deserve special recognition. I also really appreciate Dr. Rick McKenzie, Dr. Jiang Li and Dr. Duc T. Nguyen for taking time out of their busy schedule to serve as my dissertation committee members. Their attention, advice and review of this dissertation are extremely valuable for me. Finally I want to thank my family for their unconditional love and support.

TABLE OF CONTENTS

Page

LIST OF TABLES

LIST OF FIGURES

Figure Page

Figure Page

Figure Page

CHAPTER 1

INTRODUCTION

Road networks are critical infrastructures of human civilization and probably the most important means of transportation. This chapter gives an introduction to this research from three aspects: motivation, procedure, and contributions; finally it explains the organization of this dissertation.

1.1 Motivation

With advances in computing technologies, 2D and 3D road models have been employed in many applications, such as computer games and virtual environments. Traditional road models were generated manually by professional artists using modeling software tools such as Maya [1] and 3ds Max [2]. This approach requires both highly specialized and sophisticated skills and enormous labor. Procedural modeling-based automatic road generation methods create road models using specially designed computer algorithms or procedures and they can significantly reduce the amount of manual editing needed for road modeling [3]. However, most existing procedural road modeling methods are aimed at the visual effects of the generated roads, not the geometric or architectural fidelity. Furthermore, the majority of existing road generation methods only model simplified road elements, such as single road segments, ignoring complex ones such as sophisticated road intersections and highway interchanges that are indispensable components of modern road networks.

Geographic information systems (GIS) are computer-based systems widely used to store, manipulate, display, and analyze geographic information in many fields. With

the rapid development and widespread use of GIS techniques, vast GIS data have been collected through various digital data collection methods such as satellite remote sensing, digital scanners and LIDAR (Light Detection and Ranging). Road GIS data which contain information of the real road network have also been used in various fields, such as transportation, homeland security and defense, and automotive navigation systems. Since real road GIS data already contain road network information, it will significantly reduce both time and labor cost if a 3D road network can be generated from road GIS data directly and automatically. However, roads are represented as 2D (latitude and longitude) centerlines in the form of polylines, i.e., connected line segments in existing road GIS data; and there are very few existing methods for GIS based automatic 3D high-fidelity road network generation.

The aforementioned limitations seriously restrict the applicability of the generated road models and new approaches should be developed to address these existing problems. This dissertation research proposes a method for automatically generating a 3D high fidelity road network based on real road GIS data, taking into account civil engineering rules with emphasis on road intersections and highway interchanges. The proposed method is a complex process and contains a series of procedures. A procedural method is put forward to generate realistic high resolution terrain from low resolution terrain using the diamond-square fractal algorithm and Perlin noise, and the generated high resolution terrain is then used to support the road network and provide initial elevation values for road points. The raw road GIS data are preprocessed to obtain the road network topology, merge redundant links and classify road types. The original discrete representation (polylines) of the road network is converted into a parametric representation, which

provides many advantages, such as arbitrary resolution for levels of detail and reduction of memory usage through segmentation and fitting using various criteria and least square methods. To model the most critical component of roads, namely, the road surfaces, a basic set of civil engineering rules for road design is selected in order to produce realistic road surfaces, including cross slope, superelevation, grade, etc. Then the road surfaces are generated in compliance with these civil engineering rules. Traffic interchange modeling is the most critical and challenging component due to its complexity and the lack of (relative) height information (elevation) in existing road GIS data. The proposed method first detects interchanges in a road network using advanced searching algorithms and then determines overlapped road segments. Algorithms are then developed to determine the elevations of the overlapped road segments based on predefined level values, empirical observations of real interchanges, and mathematical formulations.

To further satisfy the needs in high fidelity simulations, the visual aspects of the roadways are generated as well, such as road markings, road surface conditions and environmental objects. Pavement markings, which provide the primary steering information for traffic and are the essential means to maintain transportation safety, are created in this project and placed on the road surface. Various road textures are employed to render the road surfaces with texture mapping and normal mapping to simulate different road conditions. In addition, water areas are detected and their dynamic surfaces are rendered using high quality pixel shaders. Miscellaneous environmental objects such as trees and buildings are added using existing 3D models as needed to enhance the visual effects.

This dissertation research is critical for applications that have stringent requirements on high fidelity road networks, such as driving simulation, homeland security, and military modeling and simulations. With increasing computational capabilities of GPS (global positioning system) navigation devices, it is possible to use the proposed method in these devices to provide more accurate information about road surfaces. With minor modification, the proposed method can be extended for other areas, such as the generation of a subway system based on 2D subway maps.

1.2 Procedure

The major goal of this dissertation research is to automatically generate high-fidelity 3D road models from 2D road network GIS data, based on certain civil engineering requirements. Inputs to the proposed method include road design rules, terrain and road GIS data; outputs are 3D road models that have both high geometrical and visual fidelities. The overall structure of the proposed solution is illustrated in Fig. 1 and each component is discussed briefly as follows.

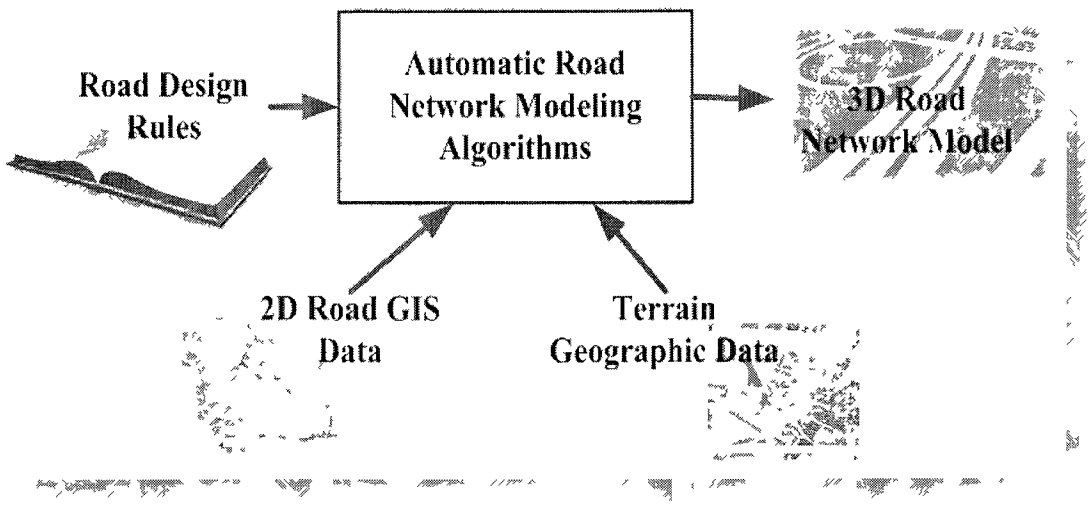

Fig. 1. Structure of the proposed automatic road generation system

1.2.1 Road Design Rules

Road design rules vary with countries and states. Thus, based on the target area for which the roads are generated, appropriate design rules should be applied. For the roads in the U.S., the most relevant industry standard for highway geometric design is *A Policy on Geometric Design of Highways and Streets* (commonly known as the "Green Book"), edited by the American Association of State Highway and Transportation Officials (AASHTO), which provides detailed rules for geometric design of road network [4]. In addition, Departments of Transportation (DOT) of different states also provide road design manuals and guidelines such as [5]. These road design manuals describe every aspect of road design, such as road cross sections, interchanges, maximum and minimum grades, overbridges, underbridges, abutments, merges and diverges, roundabouts, and turn radii. Additionally, the U.S. Department of Transportation Federal

Highway Administration gives detailed requirements for pavement marking in its publications *Standard Highway Signs and Markings (SHSM)* [6] and *Manual on Uniform Traffic Control Devices (MUTCD)* [7]. Clearly it is infeasible, and also not necessary to use all design rules in our automatic road generation system for modeling and simulation applications. As a result, it is necessary to determine a minimum set of design rules for our automatic road generation system according to our requirements. The rules selected in this dissertation research are introduced in Chapter 4 at length.

1.2.2 Geographic Data

Geographic data supply the basic information for the 3D road generation, and two kinds of geographic data are used in this research: road GIS data and terrain geographic data. Road GIS data are the primary data source and provide information about road centerlines, which determine the position of the whole road network as well as some road attributes such as road name and the city and state where the road is. Terrain geographic data provide supplemental information for road modeling, especially for the road elevation determination. As described in [8], real terrain elevation data with different resolutions were used to determine the road elevation, and a similar method is used in this research.

1.2.3 Automatic Road Network Modeling Algorithms

To automatically generate high fidelity roadways from real road and terrain geographic data with special focus on civil engineering principles and complex traffic interchanges, our proposed automatic road generation algorithms mainly consist of the following components:

- Data Preprocessing

  Both road GIS data and terrain geographic data are preprocessed in preparation for further use.

  - Road GIS data preprocessing

    Raw road GIS data are imported and converted into UTM coordinate system from geographic (longitude/latitude) coordinate system. Then explicit road network topology is extracted from road GIS data; road links are combined and classified into different categories based on their functionalities.

  - Digital elevation data-based terrain modeling

    High resolution terrain is generated using diamond-square algorithm and Perlin noise model from low resolution digital elevation data, and used to initialize the elevation of road points.

- 3D Road Centerline Modeling

  Missing elevation information of the road centerline is inferred based on 2D road GIS data and road networks are represented via parametric road segments and road intersection models.

  - Interchange modeling

    Overlapped positions are identified, traffic interchanges are formed, and appropriate elevation values are estimated and assigned to every road centerline point.

  - Representation parameterization

Road polylines are segmented, fitted, parameterized and represented in two analytic forms: straight line and circular curve.

- Intersection modeling

  Road intersections are synthesized from road nodes based on the parametric representation of road network.

- 3D Geometric Modeling

  3D road centerline models, namely the analytic representations of segments and intersections, are converted into various 3D road geometric models consisting of triangles and textures.

  - Road segment modeling

    The main body of road segment is produced from straight line or circular curve. Segment transition is created between two connected road segments as needed. Road pavement is marked and accessorial objects such as lanterns and guard rails are imported and placed.

  - Road intersection modeling

    Two kinds of intersections (normal intersection and merging/diverging intersection) are modeled to fit different situations. Intersection surfaces are marked based on selected road rules using procedural methods.

- Model rendering

  Geometric modeling of the road network only generates the geometry of the roadways. To enhance the visual effects, various shaders are employed in this project to render the resulted models including various road elements and environment objects.

1.2.4 Output Road Model

The output of this research is 3D road network models which have enough fidelity and resolution required by high-end modeling and simulation applications such as racing games and driving simulations.

1.3 Contributions

The contributions of the proposed dissertation research include the following.

- A novel road generation approach which creates high-fidelity road network models automatically from 2D GIS data based on selected civil engineering rules. In particular, this approach consists of the following innovations.
  - An innovative method to generate 3D road centerline models from 2D road centerline data, especially from data containing traffic interchange, which identifies overlapped positions, groups them into interchanges and assigns appropriate height values to all road points.
  - An original method to represent road network via parametric representation, which automatically converts discrete road points into analytic representations of the centerline of road segments (lines & curves) and intersections.
  - A selected civil engineering rule set and a total solution to generate geometry models of various road elements (e.g., road segments and intersections) from centerline models and combine them together to make up road networks seamlessly.

1.4 Organization

The remainder of this dissertation is organized as follows. Section II gives a detailed description of previous work. Section III discusses the preprocessing of road GIS data. Section IV briefly presents the selected civil engineering rules. Section V presents the details of 3D centerline modeling. Section VI describes the 3D geometric modeling. Section VII describes the implementation and results and discusses the problems in the existing road GIS data. Finally Section VIII concludes this dissertation and discusses the future work.

CHAPTER 2

RELATED WORK

This chapter presents an overview of previous work in two areas: automatic road modeling and high fidelity terrain synthesis.

2.1 Road Generation

Roads are a primary component of human civilization and many types of roads exist, e.g., highways, freeways, expressways, arterial streets, and rural roads [4]. With advances in computing technologies, road models have been widely used in many applications such as games and virtual environments. In early computer applications involving road models, almost all 2-dimensional (2D) and 3-dimensional (3D) road models were generated by professional artists manually using modeling software tools such as Maya [1], 3ds Max [2], and Creator [9]. From geometrical modeling of the road segments to texture mapping, good results were achieved through manual road modeling at the expense of extensive labor and time. This low level manual modeling greatly limited the number of roads generated and thus their widespread uses in various applications. In order to facilitate automatic road generation, various road modeling approaches have been proposed, especially for applications that contain 3D environments. In the following, we discuss them respectively.

Road network is an essential component of virtual cities that are used in many applications, such as computer games, movies and historical architecture reconstruction. Parish and Muller utilized the Lindenmayer system (L-system), which is a variant of a formal grammar and best known for modeling natural phenomena such as plant growth

[10], in their procedural modeling software CityEngine for road generation, building construction, and building face creation [11]. Sun et al. extracted four kinds of common road patterns (Population-Based, Raster, Radial, and Mixed) from existing road networks and generated road networks automatically based on these pattern templates [12, 13]. An agent-based technique was proposed by Lechner and his group to generate road network as part of virtual city generation [14, 15]. Various existing procedural techniques including Voronoi diagrams, subdivision, and L-system were combined in by Glass to replicate the identified features of road patterns in south African informal settlements [16]. A tensor field-based procedural method was put forward by Chen et al. to model the street networks of large urban areas interactively [17]. However, all these methods focused on the creation of artificial road networks for virtual environments to achieve visual satisfaction; the detailed road geometry and structure based on civil engineering principles were not taken into account by these methods.

Different from virtual city modeling applications, road modeling in driving simulations placed more emphasis on civil engineering rules-based accurate road geometric design. Artz proposed a database for use in the driving simulator at Ford Motor company in order to support high speed road surface query, such as height, normal direction, coefficient of friction, surface type, etc. [18]. In this system, road network was represented via four analytic segment types (straight section, constant radius curve, planar intersection and transition spiral) and each segment was modeled in a convenient local coordinate system to simplify the road surface definition and segment description. Road parameters were stored as functions of road axis length x and road width y. For instance, basic road height was defined as a parabolic function of x and road crown

height was given by a function of y. Mourant et al. developed a virtual environment editor for driving scenes through three kinds of two-lane road tiles (3-link 90-degree intersection tile, straight section tile and 90-degree curve tile) [19]. The road produced by this editor was not elevated and contained no geometric information. Complex parts of road networks were modeled by Kaussner and his partners using three types of parametric segments: straight lines specified by their start and end points, simple bends defined by their start and end points as well as the tangent angles at these points, and segment of super-curves representing junctions that could not be modeled using straight lines or bends [20, 21]. In a method proposed by Donikian et al., road networks were constructed with a set of eleven different classes: Ordinary Road Sections (basic section, shrinking and widening sections), Connection Sections (parting section, regrouping section, fork section and junction section) and Crossing Sections (T-shaped crossroads, Y-shaped crossroads, X-shaped crossroads and tunnel & bridge) [22, 23]. Each kind of section had its own geometry defined by one to four axial lines and associated coding, which could be used to generate road network using some specified section coding grammars. Wang and his group extended this approach from 2D to 3D and employed ribbon networks to model navigable road networks in virtual environments [24-28]. In contrast to Donikian's approach of dividing road network into various detailed specimens, their method introduced a definition of "corridor" and developed generic representations of road networks, including intersections. Ribbon based road network generation, terrain modeling, vegetation modeling and autonomous traffic modeling were integrated into a comprehensive program to create flexible virtual environments in the work by Achal and Ronald [29]. In general, analytical representations of road segment produce more

accurate road surfaces because there are no inaccuracies due to interpolation and discontinuities. However, since local coordinate systems are generally used to facilitate modeling of road segments, there is heavy computational overhead for mapping between a global coordinate system and a local coordinate system. For instance, as mentioned in [28], 20.2% of computational time were spent on mapping from Cartesian to ribbon coordinate that was used to model road segments.

Existing landscape visualization software utilized different methods to create 3D environment models from GIS data for various purposes [30-33]. Some of them generated city environment models based on GIS data in order to help users make informed decisions about urban planning, land-use planning and resource management. For example, CommunityViz [33] provides tools for making interactive 3D models of real places as they are now and as they could be in future based on GIS data. Some of them focused on vegetation and rural landscape visualization [30-32]. For instance, Biosphere3D [31] combines satellite images, orthographic photos (.ecw and jp2), digital elevation models (DEM, "stretched" .jp2), vegetation plots from ESRI multipoint shapes, 3D plants (.flora3d), 3D objects (Collada/.dae), and atmosphere to create photorealistic views. Usually for all of these software applications, a 3D environment which can be flown through and walked around is generated; however, these software applications paid little attention to generation of the road network in the environment. In general, road models used in these environments were just simple texture mapped flat surfaces with no specific information about the intersection and road geometry.

Professional software packages have been developed for real road design and construction. Bentley [34] is a company that offers software solutions for the entire

construction process of infrastructure assets, including building, road, bridge, tunnel and so on. Bentley InRoads, MxRoad and Geopak are a series of software packages geared to the needs of major civil engineering and transportation projects. Accurate design of all road types in 3D can be achieved using those software packages. Due to their professional orientation toward civil engineering, these software packages are very complex and difficult to use and thus not appropriate for modeling and simulation applications, similar to that automobile design software used by General Motors is not appropriate for video game companies to model the vehicles in the games. Creator Road Tools [35], an add-on module for Creator from Presagis company [9], was developed in conjunction with the University of Iowa [36], for high-fidelity real-time 3D graphics applications. It generates realistic roadways based on engineering standards, mainly from AASHTO standards [4]. However, although this tool utilizes civil engineering standards, it is not based on real GIS data and it is still mainly a manual process.

As discussed above, road modeling and generation have gone a long way and many useful methods and tools have been developed. However, existing road generation methods still have limitations that should be improved. First, existing road generation methods involve significant manual operations and require frequent user intervention and interactions. It is desired to reduce manual operations and increase the degree and extent of automatic road generation. Second, none of the existing methods-generated road network is based on real GIS information, which is useful in many modeling and simulation applications, such as homeland security and defense. Third, few existing approaches considered carefully modeling of road geometry based on civil engineering principles such as superelevation, grade and so on. For instance, few existing road models

have superelevation, which is a very important feature reflecting the road surface condition and has great impact on the driving experience, especially driving at a high speed. This Ph.D. dissertation research aims to address these limitations in existing road modeling methods and tools by automatically generating a geometrically accurate road network based on real GIS information, taking into account civil engineering rules and with emphasis on road intersections and highway interchanges.

2.2 High Resolution Terrain Synthesis

Road networks cannot exist by themselves in any environment, real or virtual, and they must be constructed on top of terrain or through terrain (in the case of tunnels). Also, most road GIS data contain no elevation information and the elevation of terrain can be a very important approximation of the height of road centerline. Thus, accurate road modeling and generation require high resolution terrain. However, for many modeling and simulation applications, the terrain data at hand do not have sufficient resolution and it is necessary to model high-resolution terrain from the existing data. Among various terrain synthesis methods, diamond-square fractal algorithm and Perlin Noise are two common ways employed to create high-resolution terrains.

Many things in nature are fractal. Fractals were discovered by mathematicians around the beginning of the 20th century [37]. In [37], fractal was defined as a complex object, the complexity of which grew from the repetition of a given shape at a variety of scales. The repetition of form over a variety of scales is called self-similarity: a fractal looks similar to itself on a variety of scales. There are many self-similar things in nature, such as snowflakes, clouds and mountains. Terrain also falls into the "self-similar" category. Since Benoit Mandelbrot, the inventor of fractals and fractal geometry,

introduced the fractal landscape models and made beautiful images of them in 1982 [38], many fractal-based subdivision methods have been introduced for terrain synthesis. These methods include random midpoint displacement, diamond-square algorithm, the stochastic subdivision method and so on [39]. The diamond-square algorithm [40, 41] named after the order in which midpoint values are calculated, was utilized in our solution to model high-resolution terrain.

Random numbers are commonly used to model variations for different purposes. However, if random numbers are used directly in terrain synthesis, the resulting synthetic terrain is noisy due to the uncorrelated nature of random noise. Perlin Noise [42] produces more realistic results by interpolating random noise. Perlin noise first generates a set of pseudorandom gradient vectors at all lattice points and then interpolates the gradient vectors to produce the desired noise. Various methods can be used to generate the random gradient vectors and there are different interpolations of these gradient vectors. For example, any existing pseudo-random number generator (PRNG) is suitable for random gradient vector generation and the *smoothstep* function (cubic function) $y = 3x^2 - 2x^3$ referred to in [3] is widely used for the interpolation.

CHAPTER 3

DATA PREPROCESSING

In this chapter, methods employed to handle the raw input data are introduced at length. Through these methods, the raw input data are refined, organized and prepared for further use. A detailed flow chart is given in Fig. 2.

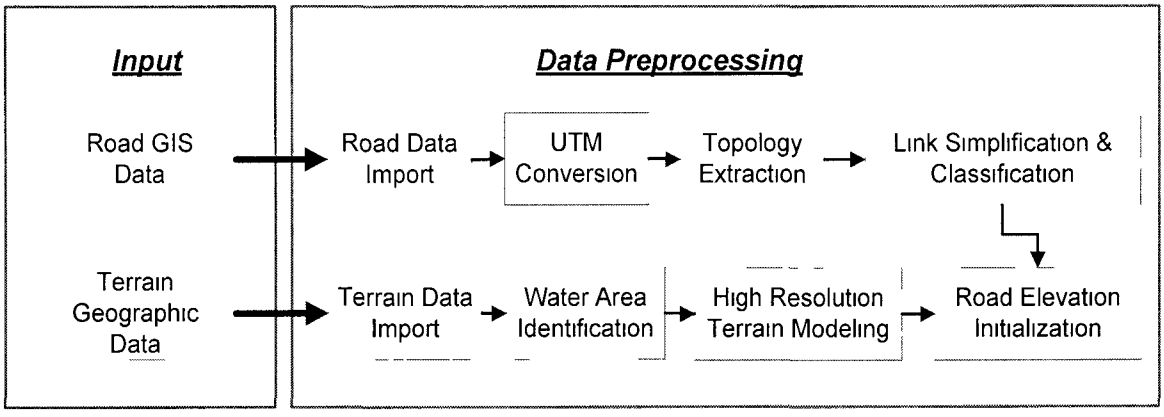

Fig. 2. Detailed flow chart of data preprocessing

3.1 Road Data Preprocessing

During road data preprocessing, road data are imported from GIS data files and converted from a geographic (longitude/latitude) coordinate system to the Universal Transverse Mercator (UTM) coordinate system; topology of the road network is extracted and link information is simplified and classified. Each step of the road data preprocessing is described in detail as follows.

3.1.1 GIS Data Import

Although various data formats have been developed for GIS applications, such as GML (geographic markup language) and TIGER (reference file format), shapefile format is the most widely used format. Road GIS data used in this research were obtained from the Virginia Department of Transportation in the form of shapefile format (.shp). A typical shapefile consists of a main file, an index file, a dBase file and a projection file. The first three files define the geometry and attributes contained in a shapefile and in total three kinds of shape types are used to represent geometric shape features, which are Point, Polyline and Polygon [43]. In general, the main file contains the primary reference data with one record per shape feature; the index file stores the position and content length for each record in the main file; the dBase file contains the feature attribute for each record in the main file. The raw road GIS data used in this research mainly contain the centerline information of the road network recorded as Polyline, which is composed of line segments determined by road points, and some complementary information stored as feature attributes. Fig. 3 shows an example of raw road GIS data in ArcGIS [44], the industry standard for GIS applications and Fig. 4 shows the attributes provided by raw road GIS data for every road record with detailed explanations in Table 1. A library named shapelib [45] is used in this project to read data from shapefile.

(a) (b)

Fig. 3. An example of raw road GIS data. (a) Road GIS data containing all Norfolk street information displayed in ArcGIS. (b) An enlarged view of streets around Old Dominion University is denoted by the red rectangle in (a).

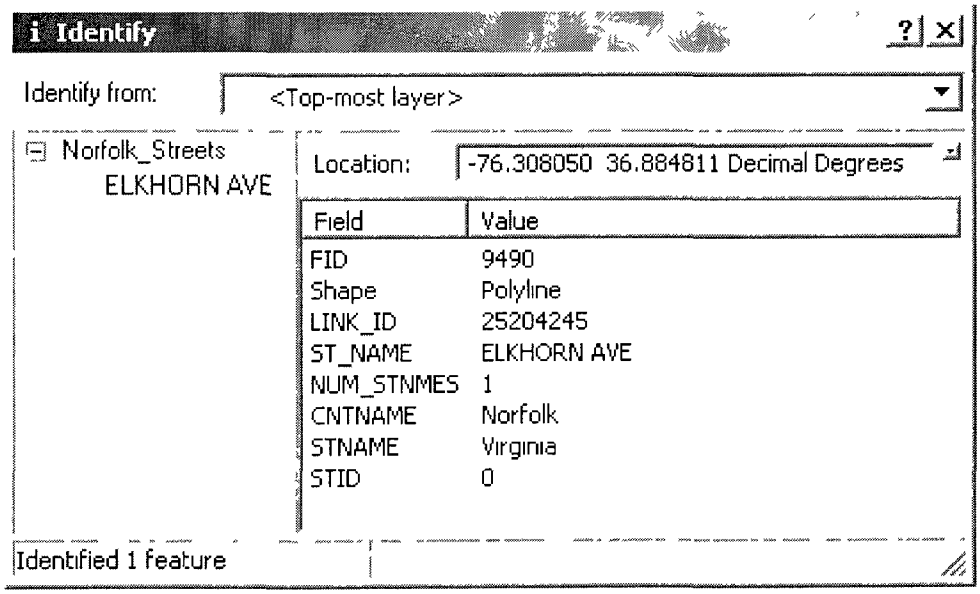

Fig. 4. An example of attributes provided by raw road GIS data for road record

Table 1. Attributes for raw road GIS data

Field	Description
FID	Feature ID number, unique identifier for this road record numbered by GIS system; cannot be changed after generation.
Shape	The shape type of this road record. It is Polyline in our data for road record.
LINK_ID	Link ID number, unique identifier for this road record given by data provider.
ST_NAME	The name of this road
NUM_STNMES	The number of road names contained in this road. In this research, it is used to represent the number of lanes.
CITNAME	The name of the city to which this road belongs
STNAME	The name of the state to which this road belongs
STID	The state ID (not used)

3.1.2 Coordinate System Conversion

In the raw road GIS data, the positions of road centerline points are recorded in geographic (longitude and latitude) coordinate system. This coordinate system is based on a spherical surface and is not convenient for road network modeling. In this research, the latitude and longitude of road link points are first converted to another 2D horizontal Cartesian coordinate system, the Universal Transverse Mercator (UTM) geographic coordinate system.

The UTM system is a grid-based method of specifying locations on the surface of the Earth. Unlike latitude and longitude, there is no physical frame of reference for UTM grids. In other words, UTM grids are created by laying a square grid on the earth and projecting the 3D earth surface onto a 2D plane as shown in Fig. 5. Since the earth isn't perfectly round, and it isn't even a perfect ellipsoid, slightly different shapes work better for some regions than for the earth as a whole. Different grids will be generated for different maps depending on the datum used (model of the shape of the earth), and the most modern data are North American 1983 Datum (NAD83) and WGS84 [46]. Both of them are based on worldwide data and are truly global. Differences between these two systems derive mostly from redetermination of station locations rather than differences in the datum, so they can probably be regarded as essentially identical. WGS stands for the World Geodetic System which defines a reference system describing the size and shape of the earth and WGS84 is the latest revision. WGS is used as a standard in cartography, geodesy, and navigation. For example, WGS84 is the reference coordinate system used by the Global Positioning System. Considering this, our project uses WGS84 to do the conversion and detailed steps can be found in [47]. With this reference coordinate system, for example, a position with longitude = -76.20283 and latitude = 36.87427 is converted to UTM zone 18S with x = 392798.73487 and y = 4081600.16053.

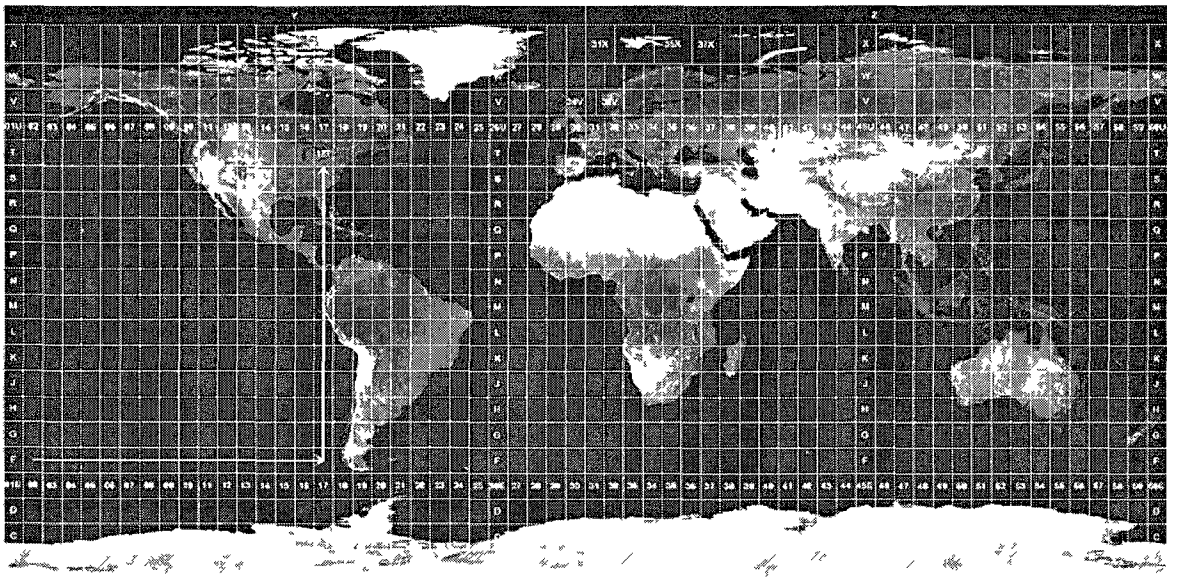

Fig. 5. An illustration of UTM grid [48]

3.1.3 Road Network Topology Extraction

Road links and intersections are essential elements of a road network. However, in existing road GIS data, the road link is represented as 2D centerlines in the form of polylines, i.e., connected line segments that consist of consecutive but discrete road centerline points as shown in Fig. 6(b), and the road networks are stored as a group of polylines at different locations of the shapefile. Road network topology or connectivity information is not explicitly represented in the raw GIS road data, so it is difficult to determine whether two polylines are connected or not without explicitly comparing the points that compose the polylines. To expedite the automatic road generation process and to facilitate road navigation, an explicit representation of the road network or topology is necessary. In this research, a method proposed in [49] is employed to extract the topology information of the road network from raw road GIS data. Detailed steps are listed as follows.

1. Import Polylines from the shapefile and number each Polyline with a unique link ID between 0 and $N - 1$, where N is the number of the link.
2. Number two nodes of each link i with node IDs $2i$ and $2i + 1$.
3. Group identical nodes which have the same physical locations and replace their IDs with the smallest one for each group.
4. Renumber all the nodes consecutively.

The output of this method is a road network represented as a graph consisting of road nodes and road links as shown in Fig. 6(c).

3.1.4 Link Simplification and Classification

The raw road GIS data contain redundant representations for road links that have multiple names. That is, the same road with two or more different names is stored as two or more independent roads in the raw road GIS data. While this redundancy might be useful for other purposes, the same physical road should have only one 3D representation in this project. Hence road links with the same physical positions but different names are combined into one road link with multiple names, eliminating the redundancy of the network representation. And then short road links are combined into a long road link if they have the same name and are connected by a two-leg node, i.e., a node which just has two connected road links. The numbers of both the road links and road nodes are reduced after this step since the two-leg nodes between combined road links are deleted from the road node list.

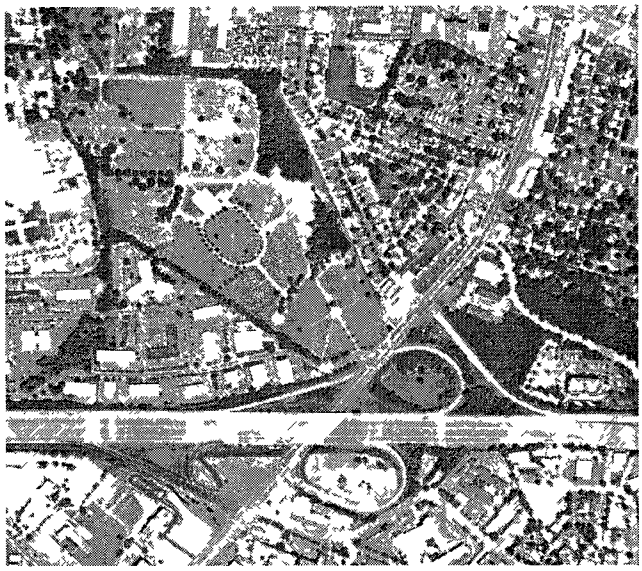

(a)

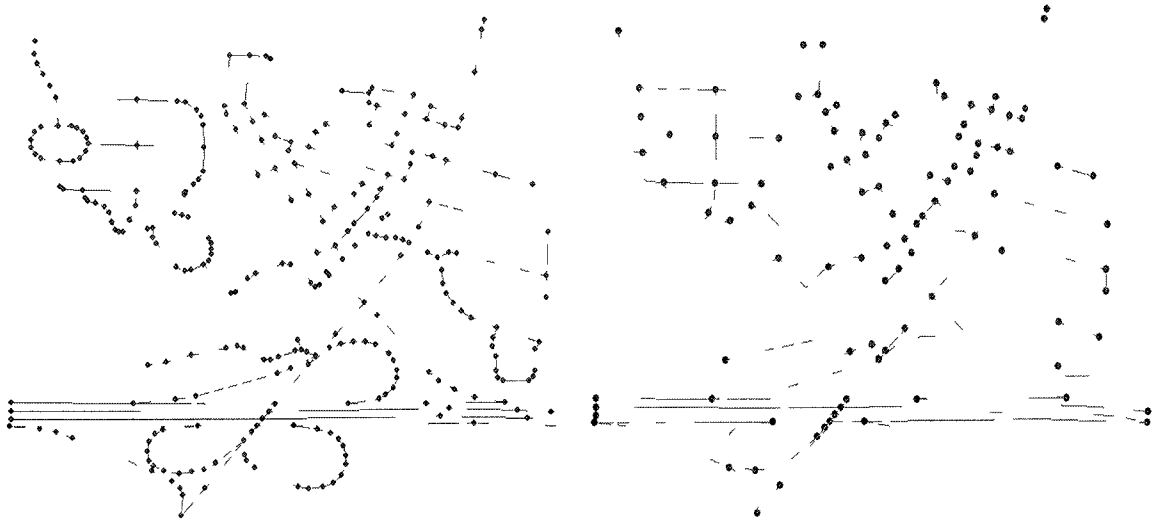

(b) (c)

Fig. 6. A road network example containing several road segments, road intersections and a traffic interchange. (a) Satellite photo around VA-403 Norfolk, VA, from USGS [50]. (b) Road centerline and discrete road centerline points from road GIS data displayed in ArcGIS for the same area. (c) Road network after topology extraction with extracted road nodes indicated by red points and road links denoted by green lines.

In order to obtain more information about road network, road links are classified into different categories according to their names. Some keywords are identified for the purpose of classification and totally six road categories are defined in this research, which are highway, local, ramp, bridge, tunnel, and unknown. For instance, keywords used to identify local roads are a set including "LN," "ST," "RD," "DR," "AVE," "BLVD" and "PKWY." Keywords used for the road classification in this project are listed as follows:

- Highway: "I-" (e.g. I-64), "HWY, "
- Local: " LN," " ST," " RD," " DR," "AVE," "BLVD," "PKWY,"
- Ramp, " RAMP," 0-9+A-Z (e.g. 14B), begin with 0-9 (e.g. 14),
- Bridge: "BRIDGE,"
- Tunnel: "TUNNEL,"
- Unknown: "NULL."

3.2 Terrain Data Preprocessing

As discussed before, road networks must be constructed on top of terrain or through terrain (in the case of tunnels). At the same time, most road GIS data contain no elevation information, so the elevation of terrain can be a very important approximation of the height of road centerline. Data downloaded from U.S. Geological Survey (USGS) [50] are used in this research. These terrain data are free but they do not have sufficient resolution. It is necessary to synthesize high-resolution terrain from the existing data. In this step, besides the datum import and water area identification, attentions are mainly paid to how to synthesize a high resolution terrain grid from existing low resolution grid and make it more realistic. A two-step procedure was utilized in this research. In the first

step, the diamond-square fractal algorithm [40, 41] is utilized to interpolate new points between existing points and produce a finer terrain grid. In the second step, Perlin noise is inserted into the high-resolution terrain so that it exhibited natural variations.

3.2.1 Terrain Elevation Data Import

USGS provides a vast array of biologic, geographic, geologic, and hydrologic scientific data that was collected or created by USGS scientists and partners. Among them, the National Elevation Dataset (NED) is its primary elevation data product, which is a seamless dataset with the best available raster elevation data of the conterminous United States, Alaska, Hawaii, and territorial islands. The NED data can be downloaded freely from USGS [50], and for every downloaded zip file, mainly two types of files are used in our research. They are .HDR files that contain the header information (e.g., number of columns and rows, cell size and longitude & latitude values for the left bottom corner) and .flt files which contain the elevation data ordered from south to north in profiles that are ordered from west to east. Hence after the data import a terrain grid storing the elevation of every point is formed.

3.2.2 Water Area Identification

Water areas surrounding bridges and tunnels are an important part of the environment, and they must be treated differently than the regular terrain to reflect the dynamic nature of the water surfaces. Thus, it is necessary to identify the water areas in the environment. The elevations for water areas in the elevation data file provided by USGS are zeros, as shown in Fig. 7. Of course, we cannot ignore the fact that the elevations of some land points are zero or less. However, based on our observation, elevations for land points are rarely exactly zero, although they can be very close to zero.

Based on this observation, zero-elevation points with at least one adjacent zero-elevation point will be marked as water points.

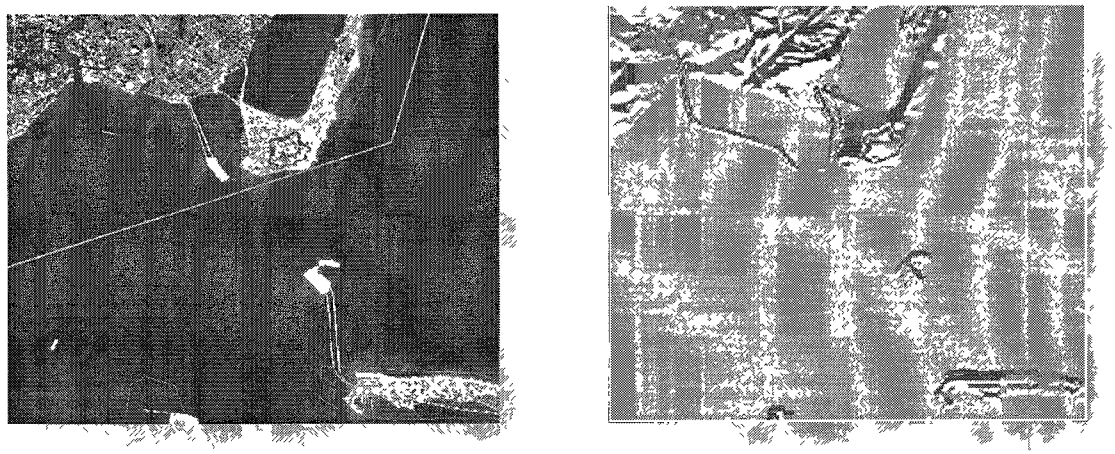

(a) Satellite image (b) Elevation image

Fig. 7. An example of the water area in Norfolk, Virginia. (a) Satellite image from USGS. (b) Corresponding terrain data.

3.2.3 Diamond-Square Fractal Algorithm

The diamond-square algorithm originally proposed by Fournier et al. [40] and then improved by Miller [41] is utilized in this research to synthesize high-resolution terrain. This method is a two-step iterative subdivision routine as follows.

1. The diamond step: Take a square of four points represented by white circles in Fig. 8(a); then calculate the midpoint by averaging the four corner values. The new midpoints are represented by gray circles in Fig. 8(b).
2. The square step: Take each diamond of four points (white or gray circles); then calculate the midpoint by averaging the four corner values. If the

midpoint is on the edges of the grid, average the three corner values to compute the midpoint. The new midpoints are represented by black circles in Fig. 8(c).

Random noise can be added to the calculated midpoints to increase the visual realism of the synthesized terrain in both the diamond step and the square step, or in just one of them. In addition, the magnitude of the random noise should decrease with the progress of the fractal iteration in order to avoid abrupt variations in the synthesized terrain. Correlated Perlin noise is utilized to introduce controlled variations into the terrain surface.

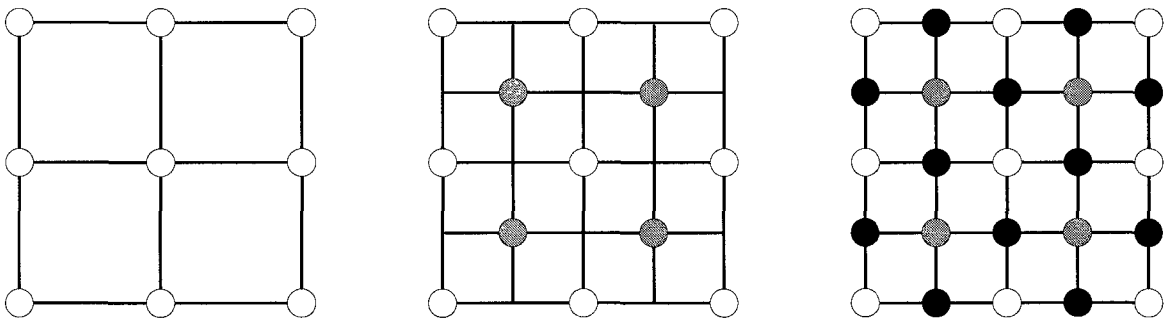

(a) (b) (c)

Fig. 8. An illustration of diamond-square algorithm. (a) Original data before applying the diamond-square fractal algorithm. (b) The diamond step: the gray points are the new generated midpoints. (c) The square step: the black points are the new generated midpoints.

3.2.4 Perlin Noise

Perlin noise first generates a set of pseudorandom gradient vectors at all lattice points and then interpolates the gradient vectors to generate the desired noise. In this

research, to obtain richer stochastic characteristics in the synthesized terrain, a random number generator is used to generate the gradient vectors with components between −1 and 1, and a cubic function $3x^2 - 2x^3$ is employed to interpolate the gradient vectors [3]. Also spectral synthesis with Perlin noise is used as the primitive. A number of Perlin noise components with different frequencies are generated and their amplitudes are adjusted so that they are inversely proportional to their frequencies. The different Perlin noise components are then added together as follows.

$$N_I(x,y) = \sum_{f=1}^{N} \frac{1}{2^f} N_s\left(x2^f, y2^f\right), \tag{1}$$

where N_s represents Perlin noise, f represents frequency, and N_T is the final noise after spectral synthesis. The final noise N_T is then added to the high-resolution terrain generated by the diamond-square fractal algorithm. However, we need to retain the elevations of the points in the original coarse terrain so that they are not changed by Perlin noise. One special property of Perlin noise is that its value is zero for points with integer coordinates as shown in Fig. 9. Thus, in the Perlin noise spectral synthesis, the coordinates of the grid points are scaled so that the original coarse terrain points have integer coordinates. As a result, only the new points are affected by the Perlin noise. Fig. 10(a) shows a very coarse terrain with only 2 × 2 grid points and Fig. 10(b) shows the resulting high-resolution (65×65) terrain using the diamond-square algorithm and spectral synthesis of Perlin noise.

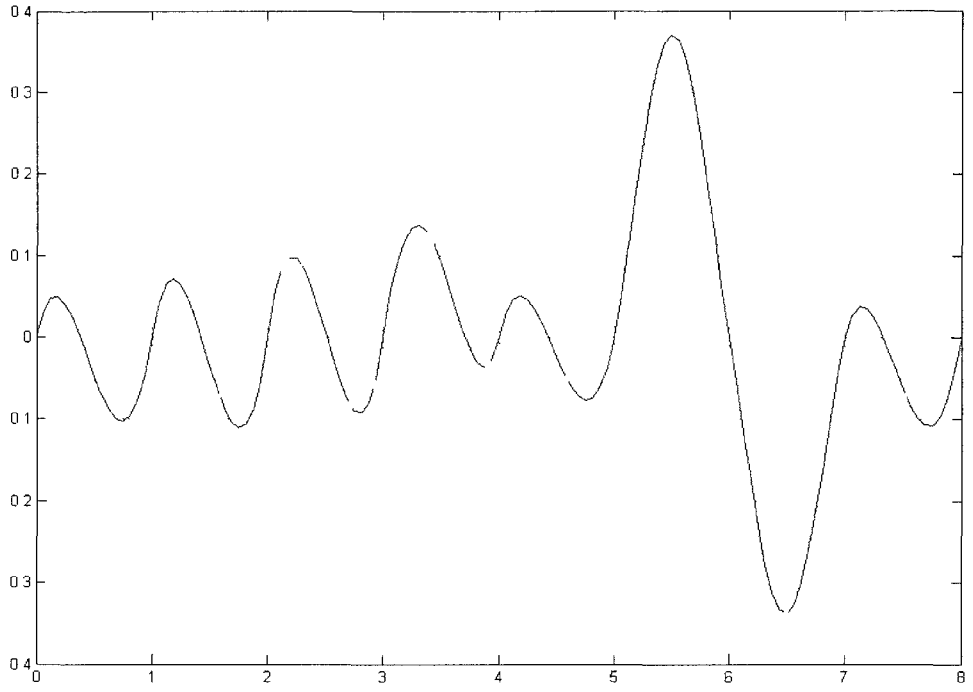

Fig. 9. Perlin noise function. Perlin noise is zero for points with integer coordinates.

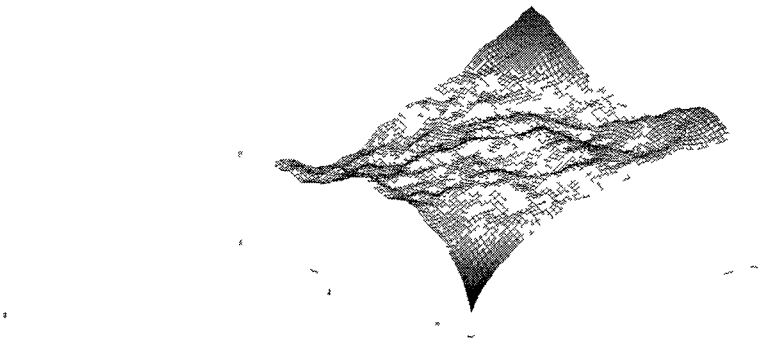

(a) (b)

Fig. 10. High-resolution terrain synthesis. (a) The original coarse terrain (2 × 2). (b) The synthesized high-resolution terrain (65×65) using the diamond-square fractal algorithm and spectral synthesis of Perlin noise.

3.3 Road Elevation Initialization

Note that exiting road GIS data contain no elevation information of the road centerline. Initial elevation value is assigned to every road point to obtain the first 3D road network which is refined by the following process. For a road network, in some cases if related terrain data are not available or we do not want to use them, the initial elevation value for every road point is set to zero; otherwise, the preprocessed terrain data are used to initialize elevation of road points. In [8], the road elevation data was extracted from digital terrain elevation data (both 30-meter and 5-meter DEMs) to support emergency evacuation during the Hurricanes Katrina and Rita. We utilize similar approach and obtain road elevation from our synthesized high resolution terrain model. Given the 2D position of any road point, its elevation value is calculated via bilinear interpolation from the high resolution terrain elevation grid. This method provides every road point an appropriate elevation value from its corresponding terrain elevation. However, traffic interchanges, including overpasses and underpasses, contain several or many overlapping points that have the same positions cannot be handled by this method and they still have the same initial elevation values. A solution for such situations is proposed in Chapter 5 on interchange modeling.

CHAPTER 4

SELECTED CIVIL ENGINEERING RULES

Since the goal of this research is to generate high-fidelity road models, how roads are designed according to civil engineering rules in real road construction activities should be taken into account carefully and the final result ought to be consistent with basic civil engineering requirements. In civil engineering, road design is the determination and arrangement of various elements of a road, including vertical and horizontal alignment, grades, sight distance, widths, slopes, etc. Since the centerlines of the road network are determined by the existing GIS data, some rules such as horizontal alignment of the road centerline are already enforced and thus are not considered in this research. We mainly focus on elements related to the elevation change, such as grades and road surface modeling such as superelevation. The reason for putting more emphases on road surface modeling is that road surface is the most important element of roads and its quality completely determines the driving experience. Besides the geometric modeling of the road surface, road markings that provide regulations, warnings, and guidance information are also very important for road users to facilitate their travel. In this chapter, a basic set of civil engineering rules (e.g., cross slope and superelevation) that have significant impact on the geometry of the road surface are selected and utilized to generate realistic road geometry models, and several pavement marking standards are also adopted to mark road surfaces correctly.

4.1 Selected Road Design Rules

Based on previous discussion, civil engineering rules about five primary design elements that have the most relevance to road geometry are selected from the AASHTO

standard [4] and the highway design guide [5], which are lane width, design speed, normal cross section, superelevation and grade. These five design elements and pertinent modeling methods will be discussed in detail in this section. Besides these five basic design elements, advanced rules for road intersection design are introduced at the end of this section.

4.1.1 Road Width

Lane widths of 2.7 to 3.6 m are generally used with 3.6 m lanes predominant on most highways, which provide desirable clearances between large commercial vehicles traveling in opposite directions on two-lane, two-way rural highways. In [4], 3.6 m has been adopted as the standard basic lane width for new constructions of two-lane and multilane highways, ramps, collector roads, and other appurtenant roadways. In this research, the default lane width is set to 3.6 m, and it can be changed in order to meet special requirements. A road contains at least one lane and usually more than one lane. Given the lane width, the road width can be roughly determined by the product of two parameters, the lane width and the number of lanes. Also the road width can be further refined by taking more road features into account such as curb width and shoulder width.

4.1.2 Design Speed

Design speed is defined as "a speed selected to establish specific minimum geometric design elements for a particular section of highway" [5]. The design speed should be a reasonable one which respects the topography, anticipated operating speed, the adjacent land use and the functional classification of road and will be used as an overall design control. Once the design speed is fixed, all pertinent road geometric design elements should be determined correspondingly to satisfy it and to achieve a balanced

design. These design elements include vertical alignment, horizontal alignment, superelevation and sight distance.

If the design speed is contained in the road GIS data, it can be directly used. Otherwise, the design speed will be determined mainly based on road types and conditions (Table 2). The relationship between the design speed and curve radius is shown in Table .

Table 2. Relationship between road types, conditions and design speed [5]

Road Types and Conditions	Design Speed (km/h)
Freeways & expressways in mountainous terrain	80-130
Freeways in urban areas	90-130
Freeways and expressways in rural areas	110-130
Expressways in urban areas	80-110
Conventional highways in rural flat terrain	90-110
Conventional highways in rural rolling terrain	80-100
Conventional highways in rural mountainous terrain	60-80
Conventional highways for urban arterial streets	60-100
Conventional highways for urban arterial streets with extensive development	50-70

Table 3. Relationship between design speed and curve radius [5]

Design Speed (km/h)	30	40	50	60	70	80	90	100	110	120	130
Minimum Radius of Curve (m)	40	70	100	150	200	260	320	400	600	900	1200

It is worth noting that the design speed is not the speed limit posted by the road. The speed limit is dependent on the design speed. It is commonly set at or below the 85th percentile speed, the speed at which 85% of the traffic is travelling, and in the U.S. it is typically set 13 to 19 km/h below that 85th percentile speed.

4.1.3 Normal Cross Slope

Undesired accumulations of water on the surface of roads will cause inconvenience to road users and increase accident potential. Sloping on roadway cross sections is employed to meet the drainage needs and direct water off the traveled way. Usually the minimum values for cross slope are between 1.5% to 2.5% in order to consist with the type of highway and amount of rainfall, snow and ice [4]. According to [5], the standard cross slope to be used for new constructions on the traveled way for all types of surface should be 2%. In civil engineering, two kinds of downward cross slope models are commonly used: plane model and rounded model. In the plane model, the cross slope has a peak in the middle and then uniformly slopes on each side; in the rounded model, usually a parabolic function is used to generate a road surface that is slightly round in the middle and increasingly slanted toward the edges of the road. The rounded model is advantageous for facilitating drainage but disadvantageous for construction, especially

for warping of pavement areas at intersections. A plane model with a peak in the middle and a 2% cross slope downward toward both edges is utilized in this research for normal road surface modeling.

4.1.4 Superelevation

According to the laws of mechanics, a vehicle traveling on a curve undergoes a centrifugal force which moves it outward. If this force is not resisted well, the vehicle will skid outward, imposing danger to the vehicle and driver. The superelevation of a curve road segment is used to balance this force with gravity and side friction. To reach equilibrium of these forces, the following equation should be satisfied

$$Centriugal\ Factor = e + f = \frac{0.0079V^2}{R} = \frac{V^2}{127R} = \frac{v^2}{gR}, \quad (2)$$

where

e = Superelevation slope rate,

f = Side friction factor which varies from 0.4 for design speed at 15 km/h to about 0.15 for 70 km/h,

v = vehicle speed (m/s),

V = Velocity (km/h),

g = gravitational constant (9.98m/s^2), and

R = Curve radius (m).

Thus, the superelevation rate can be determined based on the side friction factor, road radius and vehicle speed. In this research, the standard superelevation rate will be used [5] for various situations with different range of curve radius, road types and surface

conditions. Except for short radius curves, this standard superelevation rate results in very little side thrust at speeds less than 75 km/h and provides maximum comfort for most drivers. Furthermore, superelevation is unnecessary for horizontal curve with a radius of more than 3000 m. The centerline of the roadbed will be used as the axis of rotation for superelevation. An illustration of a superelevation transition from normal crown to full superelevation is given in Fig. 11. In this figure, two primary processes for the transition are indicated:

1. Crown Runoff: From 1 to 2, the cross slope of the high side of the section surface increases from −2% to 0%.
2. Superelevation Runoff: From 2 to 4, the cross slope of the high side of the section surfaces increases from 0% to the full superelevation rate. Two-thirds of the superelevation runoff should be on the tangent and one-third within the curve as indicated by 3.

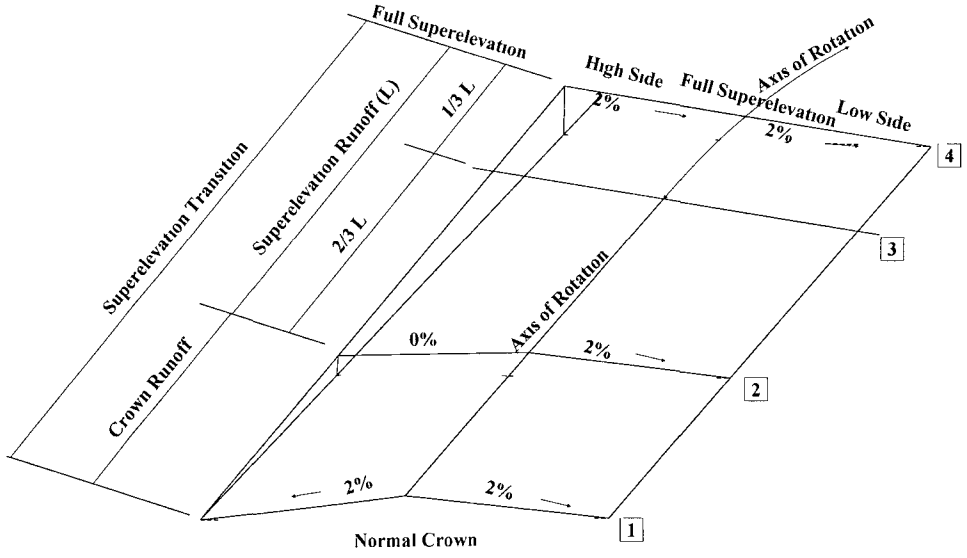

Fig. 11. An illustration of a superelevation transition

The length of the superelevation runoff L can be calculated using formulas given in Table 4 where the parameter e is the superelevation rate and D is the distance from the axis of rotation to the outside edge of lane in meters. Note that superelevation transitions on bridges should be avoided whenever possible [5].

Table 4. Length calculation of the superelevation runoff [5]

2 Lane Roads	$L = 750\ e$
Multilane Roads & Branch Connections	$L = 150\ De$
Multilane Ramps	$L = 750\ e$ if possible
Single Lane Ramps	$L = 600\ e$

4.1.5 Grade

The elevation of the road changes according to the terrain surface due to the construction economy, especially for mountainous and rolling terrain. The grade line is a reference line by which the elevation of the road is established and must meet requirements of sight distance, which is the continuous length of highway ahead visible to the driver for the designed speed. It provides safety, comfortable driving, good drainage and pleasing appearance. Steep grades affect traffic speed and cause operational problems at intersections. Thereby in general the flattest practicable grade is desirable, or at least the maximum grades given for terrain conditions in Table 5 shall not be exceeded.

Table 5. Maximum grades for types of highway and terrain conditions [5]

Type of Terrain	Freeways and Expressways	Rural Highways	Urban Highways
Level	3%	4%	6%
Rolling	4%	5%	7%
Mountainous	6%	7%	9%

A parabolic vertical curve is commonly used to represent the grade line as shown in Fig. 12, either at crests or sags. The shape of the grade line can be determined using the following set of equations.

$$A = G - G', \qquad K = \frac{L}{A}, \qquad m = \frac{(G'-G)L}{800}, \; d = \frac{4mD^2}{L^2} = \frac{(G'-G)D^2}{200L}, \tag{3}$$

where

L is the length of curve in meters. Its minimum value L_{min} can be determined according to the following rules:

- $L_{min} = 2V$, V = design speed for grade >= 2% and V >= 60 km/h,
- L_{min} = 60 m for grade < 2% or V < 60 km/h,

G and G': grade rates in percent (a rising grade carries a plus sign, while a falling grade carries a minus sign),

m = the middle ordinate in meters,

d = the correction from grade line to curve,

D = the distance from the beginning of the vertical curve (B.V.C) or the end of the vertical curve (E.V.C) to any point on curve, and

K = the distance required to achieve a 1% change in grade.

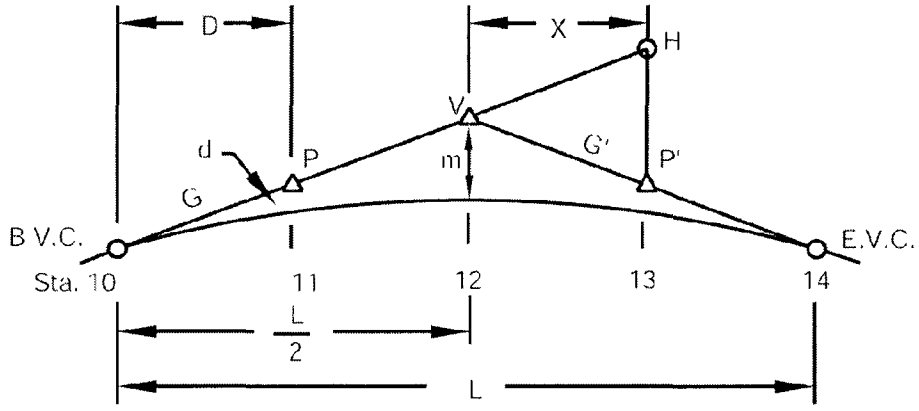

(a)

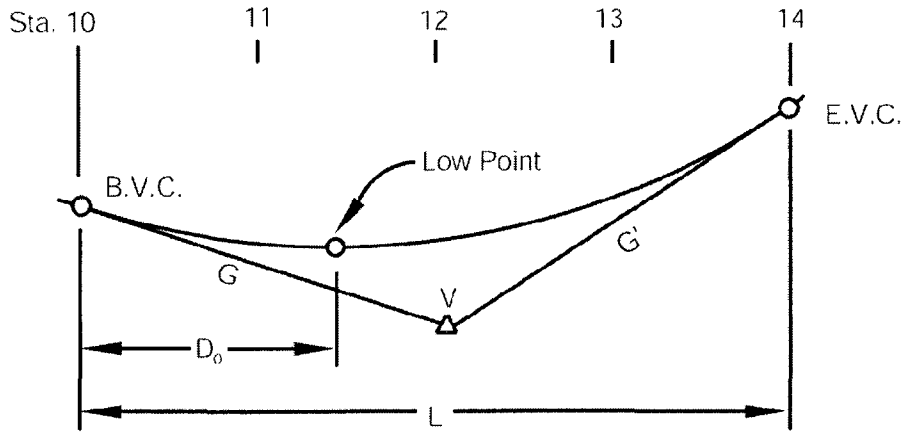

(b)

Fig. 12. Vertical grades [5]

In this research, this grade rule will be used to smooth the connection of two road segments which have different grades. Note that if the grade is 0.5% or less, a vertical curve is not required. Also, for two lane roads, vertical curves with a crest longer than 1 km should be avoided.

4.1.6 Intersection Design

A road intersection is the junction where three or more road legs join. Several rules are chosen from AASHTO standards [4] in this research to guide the intersection modeling. According to the number of connected road legs, intersections can be classified into three basic types: three-leg or T type, four-leg type, and multileg type. An intersection with more than 4 legs is not recommended. Also generally the angle of intersection is not more than 30 degrees from perpendicular (i.e., from approximately 60 to 120 degrees). With a fixed intersection angle, edges connecting two adjacent road legs mainly determine the shape and function of intersections; therefore the edge design is a critical part of intersection design. According to [4], the corner radii should be based on minimum turning path of the selected design vehicles in order to provide turning vehicles, especially right-turning vehicles enough space. Three minimum designs for the inner edge of the traveled way are provided as simple curve, simple curve with taper, and three centered compound curves with different radii [4]. Taking the effect of curb radii on pedestrians into consideration, radii of 7.5m or more should be provided at minor cross streets, on new construction and on reconstruction projects where space permits while curb radii ranging from 1.5 to 9m and most being between 3 and 4.5 m have been used in urban areas, usually because of space limitations.

Different from the normal intersection, the merging/diverging intersection where a ramp merges into or diverges from a highway has more complicated design requirements. The continuity in basic number of lanes and the principle of lane balance are two fundamentals which should be complied with during the design of a merging/diverging intersection. The basic number of lanes is a constant number of lanes assigned to a route and should be maintained over a significant length of route, irrespective of changes in traffic volume and lane-balance needs. The lane balance requires that the traveled way of the highway should be reduced or increased by no more than one traffic lane at a time. These two fundamentals work together to reduce confusion and erratic operations for through traffic on the freeway and lower difficulty in diverging from or merging with the main line flow. When the principle of lane balance seems to conflict with the concept of continuity in the basic number of lanes, arrangements should be made to bring these two into harmony by means of auxiliary lanes as shown in Fig. 13. For intersections with a changing number of lanes, the end of the lane drop should be tapered into the highway. Two general models provided by AASHTO standards [4] for the merging or diverging process are tapered design and parallel design as shown in Fig. 14. The taper design provides a direct entry or exit at a flat angle with a long, uniform taper whose desirable rate is about 50:1 to 70:1 (longitudinal to lateral), whereas the parallel design has an auxiliary lane of sufficient length for merging or diverging and a taper at the end of the lane. The parallel design is preferred generally and length requirements for the auxiliary lane and taper can be found in [4] for different situations. For instance, a taper length of approximately 90 m is suitable for design speeds up to 70 mph for parallel-type entrances.

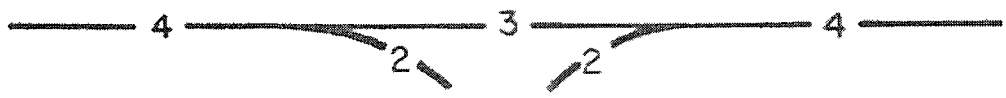

LANE BALANCE BUT NO COMPLIANCE WITH BASIC NUMBER OF LANES

- A -

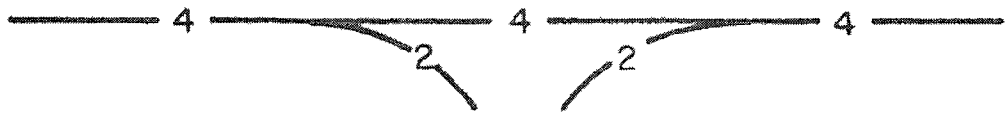

NO LANE BALANCE BUT COMPLIANCE WITH BASIC NUMBER OF LANES

- B -

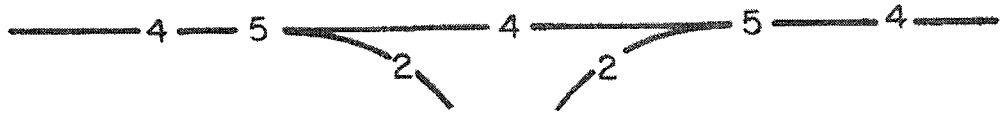

COMPLIANCE WITH BOTH LANE BALANCE AND BASIC NUMBER OF LANES

- C -

Fig. 13. Coordination of lane balance and basic number of lanes [4]

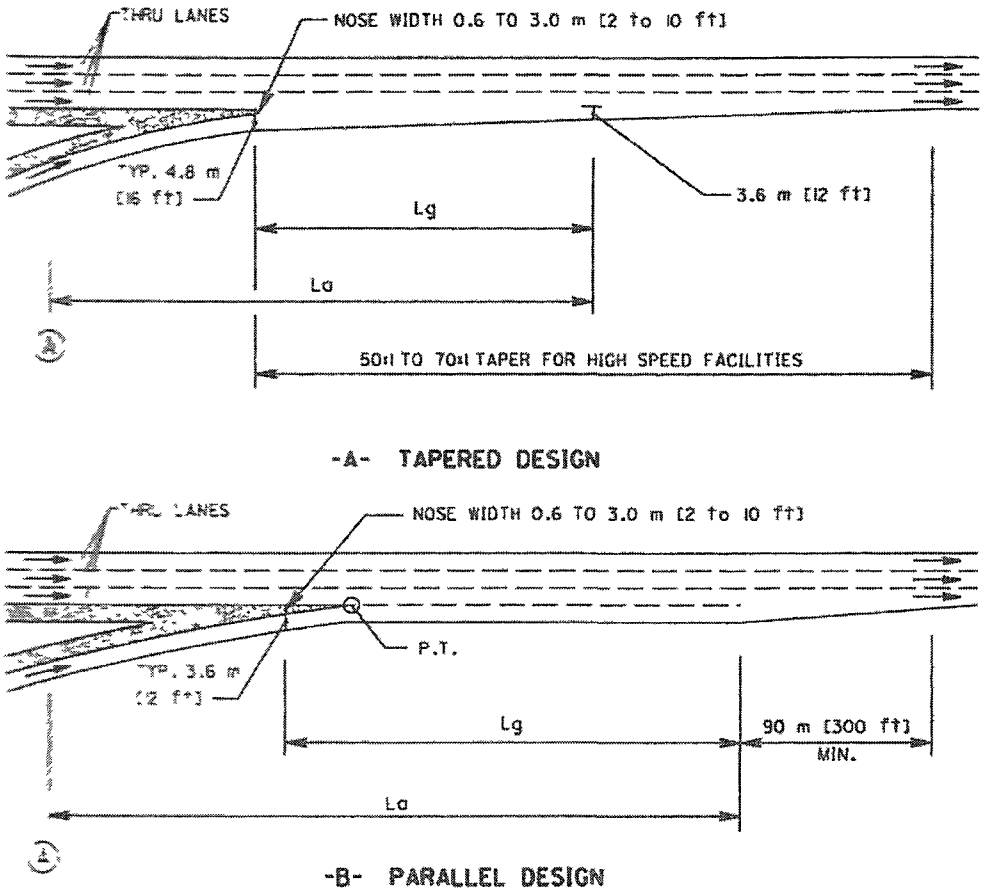

NOTES:

1. La IS THE REQUIRED ACCELERATION LENGTH AS SHOWN IN EXHIBIT 10-70 OR AS ADJUSTED BY EXHIBIT 10-71
2. POINT (A) CONTROLS SPEED ON THE RAMP. La SHOULD NOT START BACK ON THE CURVATURE OF THE RAMP UNLESS THE RADIUS EQUALS 300 m [1000 ft] OR MORE.
3. Lg IS REQUIRED GAP ACCEPTANCE LENGTH. Lg SHOULD BE A MINIMUM OF 90 TO 150 m [300 to 500 ft] DEPENDING ON THE NOSE WIDTH.
4. THE VALUE OF La OR Lg, WHICHEVER PRODUCES THE GREATER DISTANCE DOWNSTREAM FROM WHERE THE NOSE EQUAL 0.6 m [2 ft], IS SUGGESTED FOR USE IN THE DESIGN OF THE RAMP ENTRANCE.

Fig. 14. Typical tapered design and parallel design for single-lane entrance ramp [4]

4.2 Selected Road Marking Rules

There are many types of traffic markings on the surface of roads or along the roads [5], including pavement and curb markings, object markers, delineators, colored pavements, barricades, channelizing devices and islands. All of these markings provide regulations, guidance or warning information to road users. Standards for markings on highways and on private roads are described at length in [7] while detailed sizes for various markings are given in [6]. The development of road markings in this research is also based on these two documents and all generated markings should be consistent with them.

The major road markings to be generated in this research are pavement markings which provide the primary steering information for traffic and are the essential means to maintain transportation safety and facilitate a smooth traffic flow. Common examples of pavement markings include yellow or white, solid or broken center lines. While seemingly simple, it is not feasible in this research to generate these pavement markings automatically and procedurally due to the lack of complete marking information and other practical issues. For example, because of the lack of road direction information, it is impossible to generate the yellow center line pavement marking delineating the separation of traffic lanes that have opposite directions of travel on a roadway. Hence, the pavement markings to be generated in this research mainly consist of three kinds of line markings: solid white lane line pavement marking, broken white line marking and dotted white line marking. The standards for these three kinds of line markings from [7] are listed as follows:

1) Solid white lane line pavement marking discourages or prohibits crossing. The width of this normal line on the surface of pavement should be 4 to 6 inches and this line is used to delineate the right or left edge of a roadway.
2) Broken white line marking indicates a permissive condition where crossing the lane-line marking with care is permitted. This marking is normal line segments separated by gaps; usually broken lines should consist of 10-foot line segments and 30-foot gaps, or dimensions in a similar ratio of line segments to gaps as appropriate for traffic speeds and need for delineation. This marking is used to delineate the separation of traffic lanes that have the same direction of travel, such as centerline markings of a two-lane roadway.
3) Dotted white line-marking provides guidance or warning of a downstream change in lane function. This marking has noticeably shorter line segments separated by shorter gaps than those used for a broken line. Patterns for dotted lines depend on the application. A dotted line for line extensions within an intersection or taper area should consist of 2-foot line segments and 2- to 6-foot gaps; a dotted line used as a lane line should consist of 3-foot line segments and 9-foot gaps.

Pavement markings become more complicated at normal intersections where road segments with different numbers of lanes meet, or merging/diverging intersections where a ramp merges or diverges. Fig. 15 gives an illustration of road marking for two types of merging/diverging intersection designs from MUTCD [7]. In this research, these pavement markings are modeled as 2D textures and laid on the road surface automatically with a procedural modeling method.

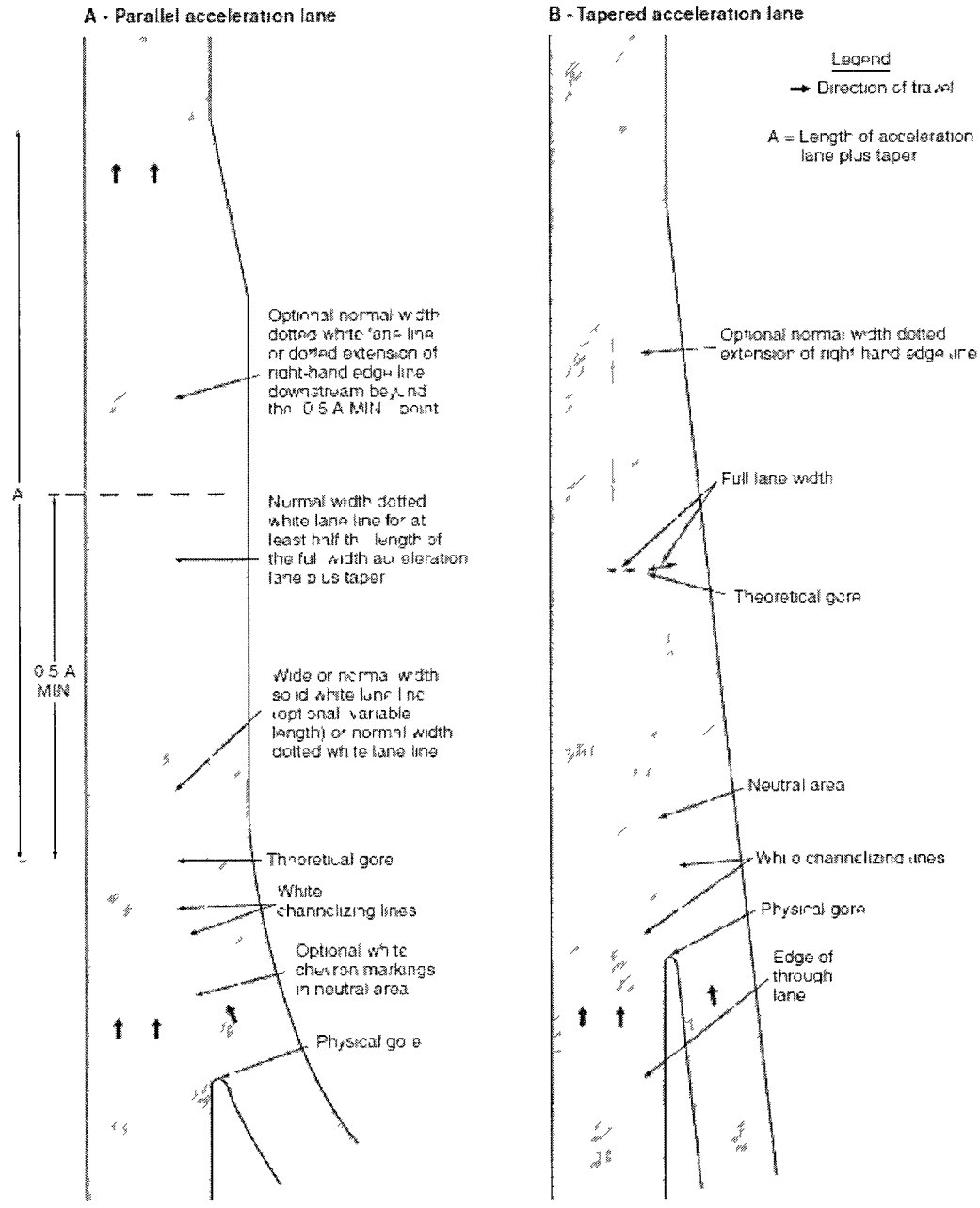

Fig. 15. An illustration of road marking for two types of merging/diverging intersection designs from MUTCD [7]

CHAPTER 5

3D ROAD CENTERLINE MODELING

3D road centerline modeling is the most important component of the whole road network modeling process because during this phase the missing height information of the road centerline is inferred based on 2D road GIS data. In particular, overlapped positions are identified, traffic interchanges are formed, appropriate elevation values are assigned to every road centerline points, road network are parameterized and represented in analytic forms and finally road intersections are synthesized from road nodes. The parametric 3D centerline models are generated for the whole road network and will be used as inputs for generating geometric models. Fig. 16 shows the detailed flow chart of this process.

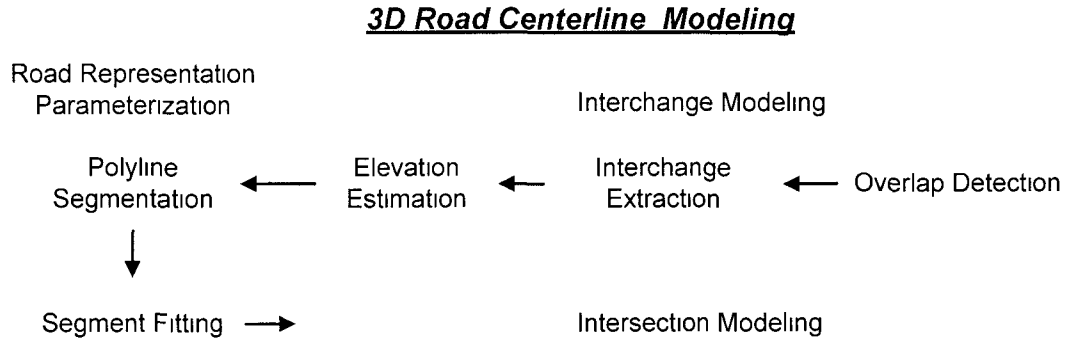

Fig. 16. Detailed flow chart of 3D road centerline modeling

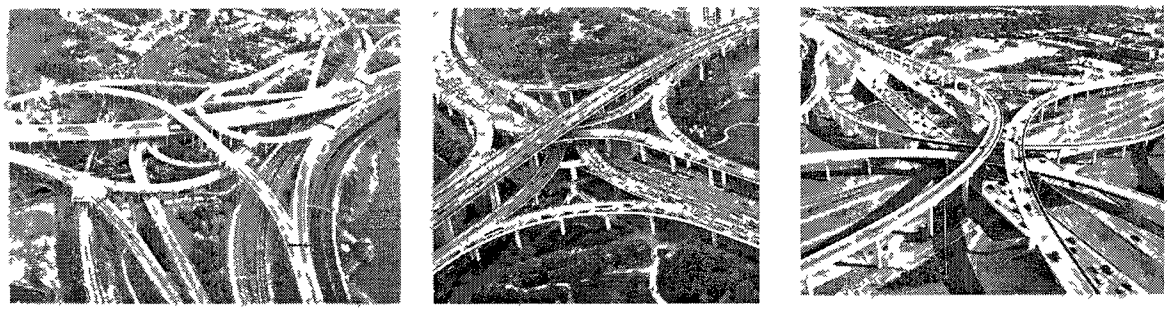

Fig. 17. Real complex interchanges

5.1 Interchange Modeling

Road interchanges are special road intersections that combine ramps and grade separations at the junction of two or more highways in order to reduce or eliminate traffic conflicts, improve driving safety and increase traffic capacity. Complex interchanges such as the ones shown in Fig. 17 are large scale civil architectures, and they are the hallmark of advanced urban development. As can be seen from these examples, automatic generation of interchanges from road GIS data is a challenging problem, as existing road GIS data do not contain height information (vertical position) about interchanges. This can be illustrated further by two popular mapping software packages: Google Maps and Bing Maps. Fig. 18 shows the interchange between I-64 and I-264 in Norfolk, Virginia. While the relative positions of different road segments in the interchange are visible in the satellite images shown in Fig. 18 (a) and (b), they become unavailable in the Bing Maps shown in Fig. 18 (c) and (d); that is, we do not know whether two road segments intersect or overlap in Fig. 18 (c) and (d). Google maps (Fig. 18 (e) and (f)) does a better job, as it displays correctly the relative positions of different

road segments. However, only relative positions are not sufficient for interchange modeling and their absolute positions must be determined completely. The road GIS data used in this research does not contain relative positions of overlapping road segments. This can be illustrated by the example in Fig. 19, which displays polylines from the GIS data, corresponding to the interchange shown in Fig. 18. The roads in the area indicated by the red circle are just represented as individual road segments consisting of consecutive 2D discrete points (Fig. 19(b)), without any information pertinent to the interchange. Also, more than one interchange may be included in a road network at the same time. Hence in order to generate the 3D models of interchanges contained in a road network, first of all, the overlapped road points contained must be identified and grouped into interchanges correctly, and then elevations are estimated and assigned to road points so that these road links do not intersect or collide with each other. In this research, traffic interchange modeling can be divided into three steps as follows.

1) Overlap detection: Identify overlapped positions and find road links containing overlapped positions.
2) Interchange extraction: Group the overlapped positions into one or more interchanges and add the related road links as part of the interchange (interchange links).
3) Elevation estimation: Assign elevation level to every overlapped road point based on predefined elevation level values and selected rules. Calculate their absolute elevations and then compute the elevations of road points located between them using linear interpolation.

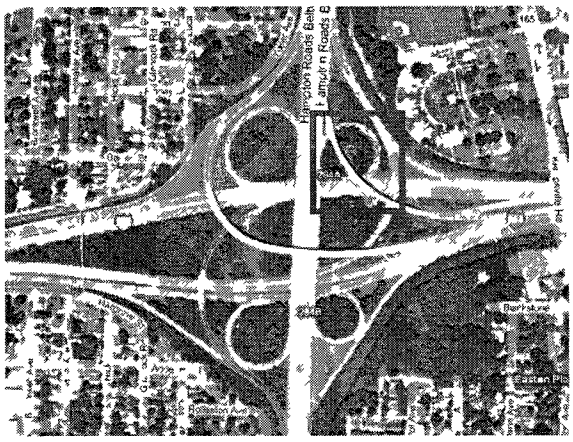

(a)

(b)

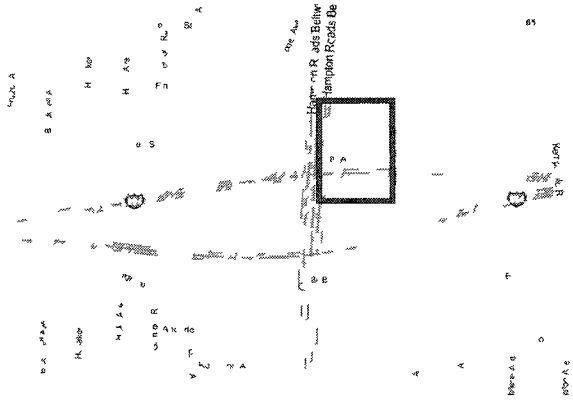

(c)

(d)

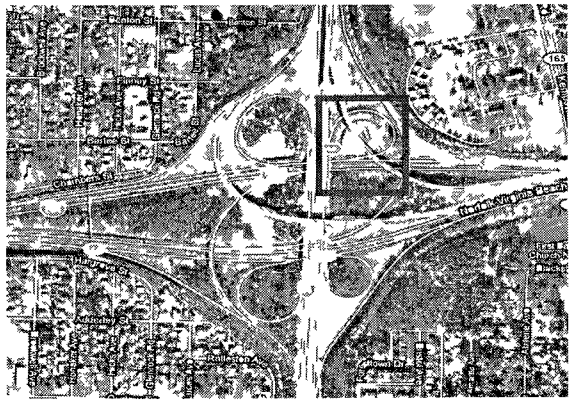

(e)

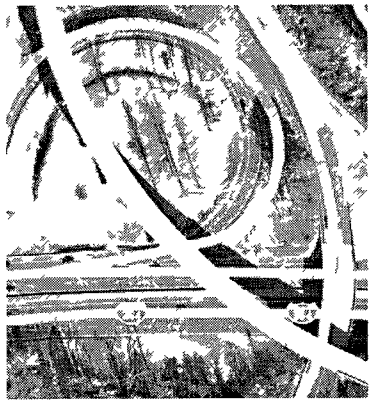

(f)

Fig. 18 The interchange between I-64 and I-264 from Bing Maps [51] and Google Maps [52]. (a)(c)(e) Satellite image from USGS, Bing maps and Google maps respectively (b)(d)(f) Corresponding enlarged results of the areas indicated by red rectangles in their left images

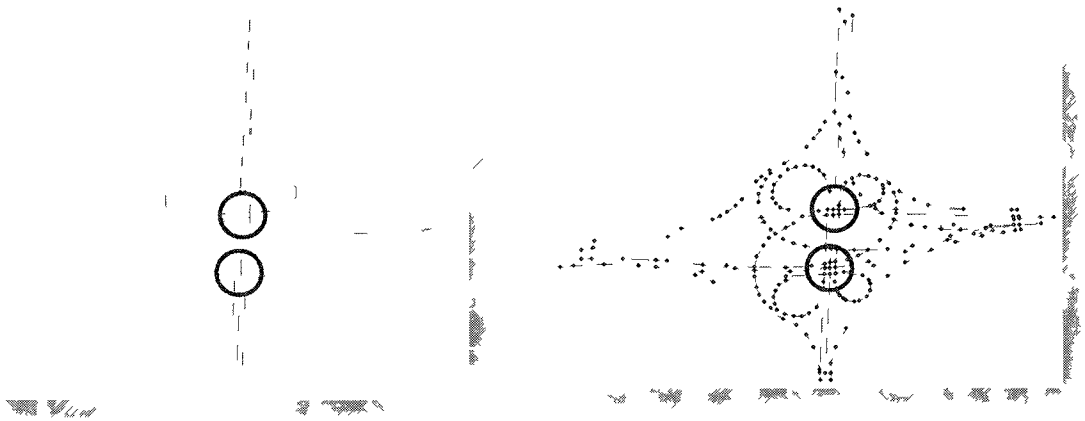

(a) (b)

Fig. 19. GIS data for the interchange shown in Fig. 18. (a) Polylines. (b) Polylines with discrete points

5.1.1 Overlap Detection

In the road GIS data, road intersections only occur at the end points of road polylines. Thus, if two road polylines contain the same point that is not the endpoint of either polyline, this point is the location where these two road polylines overlap. This characteristic of the road GIS data is used to find the overlapped positions of two or more road polylines, and this procedure is repeated to find all overlapped positions contained in the road GIS data as shown in Fig. 20(a). Also related road links containing the overlapped positions can be identified as shown in Fig. 20(b).

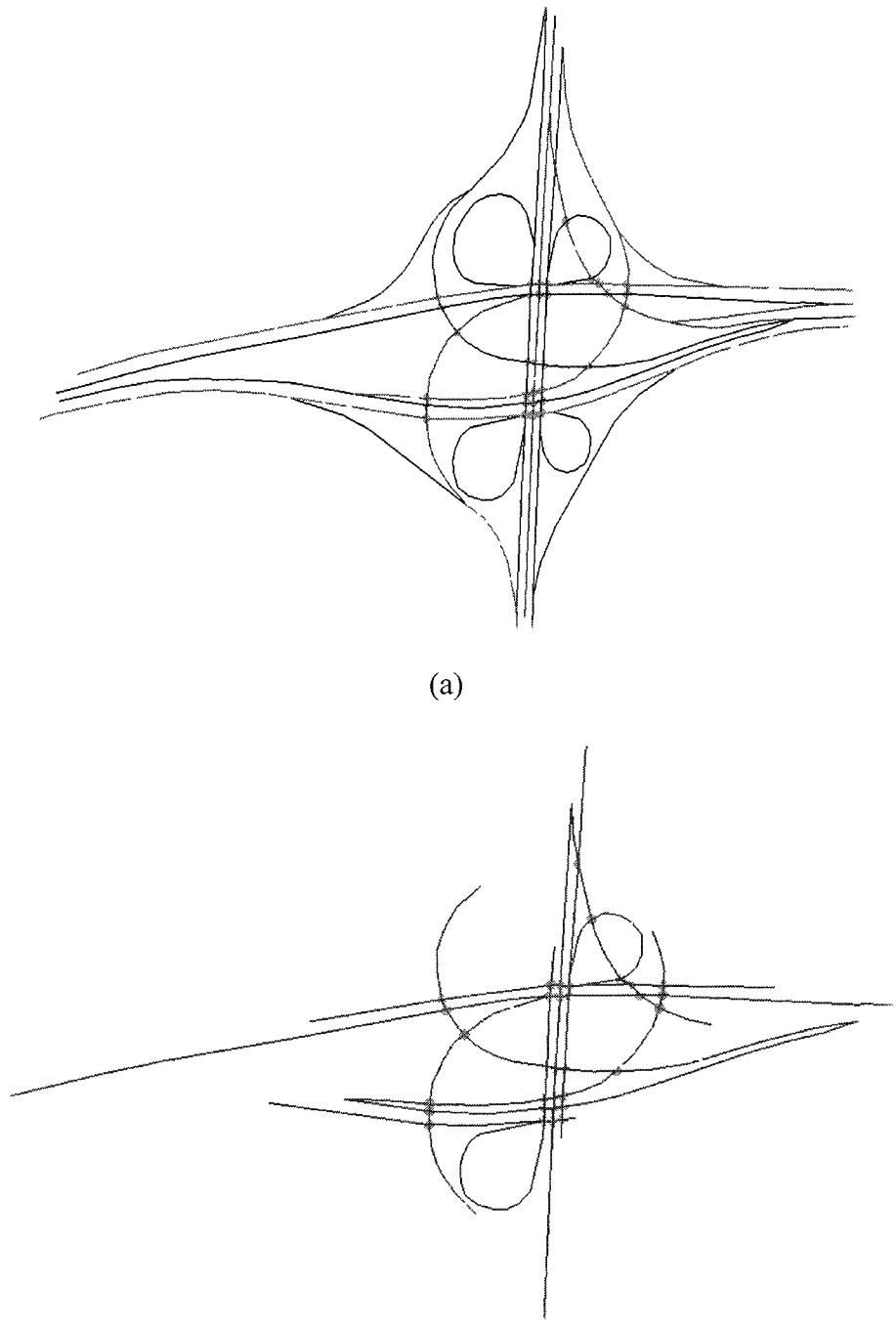

(a)

(b)

Fig. 20. Results from the interchange detection procedure. (a) Overlapped positions (green points) contained in the interchange. (b) Overlapped positions and related road links.

5.1.2 Interchange Extraction

Since more than one interchange may be contained in a road network as shown in Fig. 21(a), it is necessary to first group the identified overlapped positions into interchanges and then process each interchange independently. Based on the position of every identified overlap point, a simplified clustering algorithm similar to the k-means clustering is used in this project. Different from the k-means clustering method, this simplified clustering algorithm does not need to determine the number of groups at the very beginning and starts with only one group; a new group is generated during iteration when an observation is out of the range of every existing group defined by the centroid and distance threshold. A central position is employed for each interchange to record the average position of all overlapped points belonging to this interchange and used as the centroid; a distance threshold is set to determine whether a new overlapped position belongs to an interchange by comparing this value with the distance between this new overlapped position and the central position of the interchange. Whenever a new overlapped position is added to an interchange, the central position of this interchange is updated immediately. Based on the grouping information of overlapped positions, related interchange road links can also be divided into different interchange groups. Finally an interchange is composed of two kinds of elements: overlapped positions (interchange points) and related road links (interchange links). Fig. 21 shows an example of the interchange extraction where all overlapped positions contained in this road network are identified and grouped into two interchanges that are denoted by red and green, respectively.

(a)

(b)

Fig. 21. An example of the interchange extraction where all the overlapped positions are grouped into two interchanges automatically. (a) Satellite image of the interchange connecting I-64, I-264 and I-664 in Chesapeake, Virginia. (b) GIS data shown in ArcGIS for the interchange in (a). (c) Overlapped positions are identified and grouped into two interchanges: the red one and the green one. (d) Related interchange road links are also divided into two different interchange groups based on the grouping information of overlapped position.

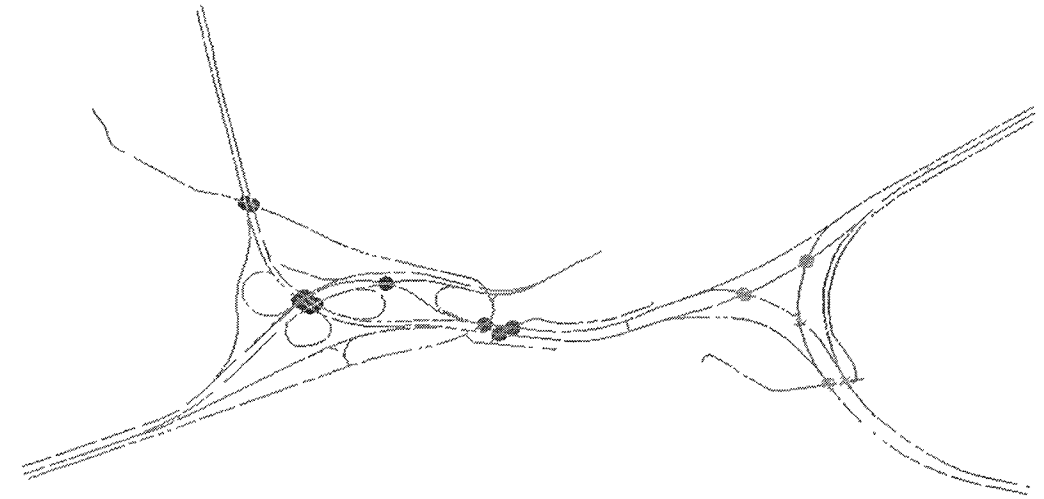

(c)

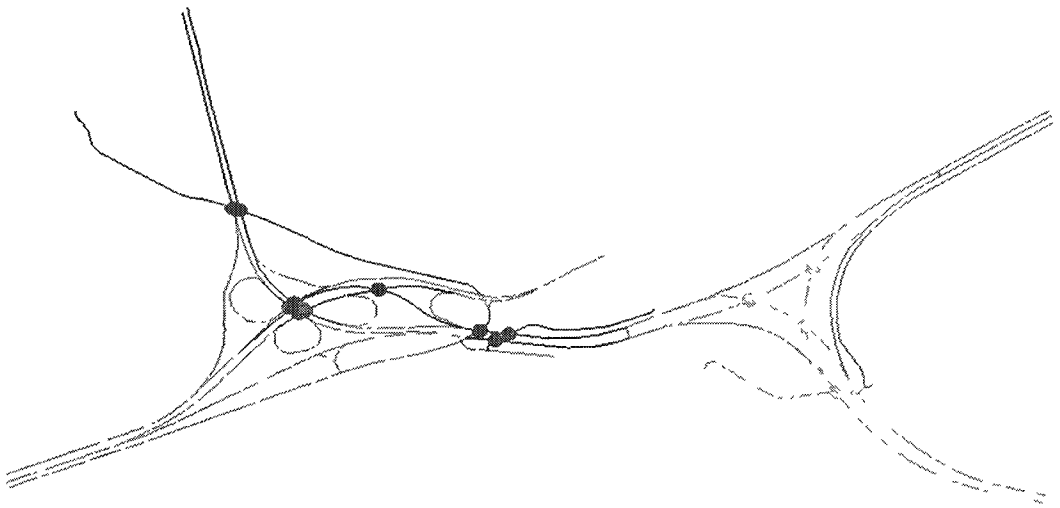

(d)

Fig. 21. Continued

5.1.3 Elevation Estimation

To generate 3D models of traffic interchanges, the elevation of each road link must be determined correctly, especially the elevation of overlapped positions. The elevation estimation process includes two steps: elevation level determination and absolute elevation calculation.

a) Elevation Level Determination

In this research, we use the concept of "elevation level" to roughly represent different heights of road points. Larger level values correspond to higher elevations. In particular, Level 1 indicates that these road points are directly placed on the terrain surface and Level 2 means that these road points are over the Level 1 road points and a layer higher than them. Levels 3, 4, and so on can be determined in the same manner. Elevation level is assigned to every overlapped road point contained by road links in the interchange mainly based on the following rules:

- Grade: The grade of any road link should be less than the maximal rate given by standard design rules to avoid a sharp drop or rise in road elevation. This means two close overlapped road points belonging to the same road link should have the same elevation level.
- Crest/sag: One road link can contain only one crest or sag in a certain distance (150m in this research) to reduce road users' discomfort caused by driving up and down frequently.
- Overlapped position: The more overlap positions a road link contains, the more likely this road link has higher level road points.

The road link elevation level for each interchange can be determined using the following procedure.

- Basic level determination (Level 1 or Level 2): roughly divide the overlapped road points into Level 1 points and Level 2 points. This approach is utilized because most existing road interchanges are two level interchanges except

some complicated ones which have a few of Level 3 or higher road links. Two steps listed below are executed iteratively until all overlapped road points are determined. A flowchart of this procedure is shown in Fig. 22 and a result of this procedure is demonstrated in Fig. 23.

- Step 1: Find the interchange road link containing the most conflicting continuous overlapped positions and assign these continuous road points a predefined elevation level (Level 1 or Level 2). At the same time assign their corresponding (overlapped) road points on other road links the other elevation level (Level 2 or Level 1), so for each overlapped position, two road points will have different elevation levels and will not intersect or collide with each other.
- Step 2: Overlapped road points close to the determined overlapped road points are assigned the same elevation level as their neighbors according to the grade rule mentioned before.

- Collision avoidance: Collisions may happen since adjacent overlapped road points belonging to the same road link are forced to have the same elevation level. To address this problem, elevation levels for the collided road points are adjusted based on the procedure shown in Fig. 24. Road points with Level 3 or higher elevation height levels are generated in this procedure if necessary.

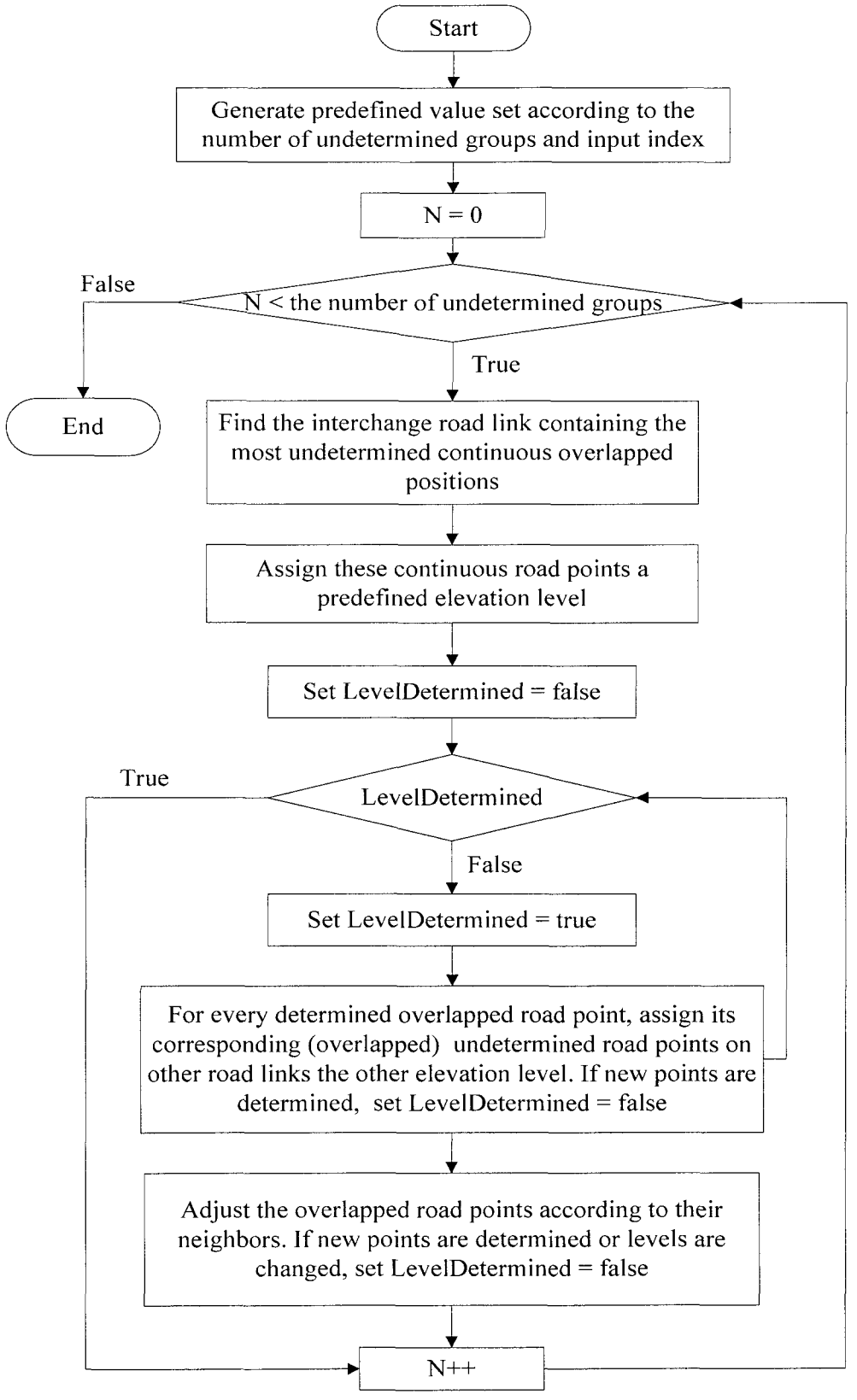

Fig. 22. Flowchart of basic level determination procedure

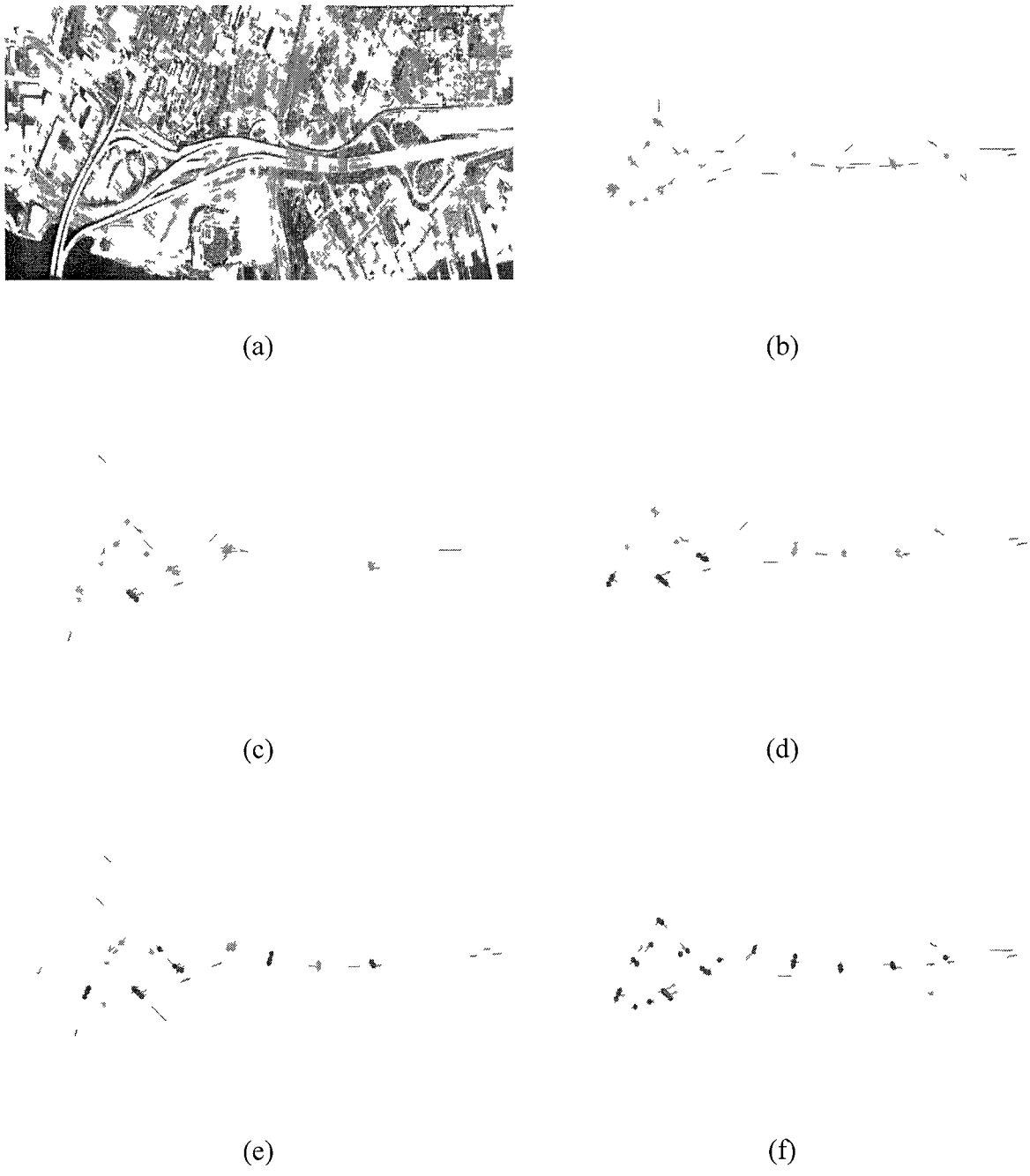

(a) (b)

(c) (d)

(e) (f)

Fig. 23. An illustration of the basic level determination procedure, using an interchange in Norfolk, Virginia, as an example. Green points indicate the undetermined overlapped points, red points present the determined overlapped points that are assigned values in step 1, and orange points show the determined overlapped points assigned values in step 2. (a) Satellite image of an interchange in Norfolk, Virginia. (b) All Overlapped positions are identified (c) After the 1st iteration of basic level determination. (d) After the 3rd iteration of basic level determination. (e) After the 6th iteration of basic level determination (f) Finally all overlapped positions are determined.

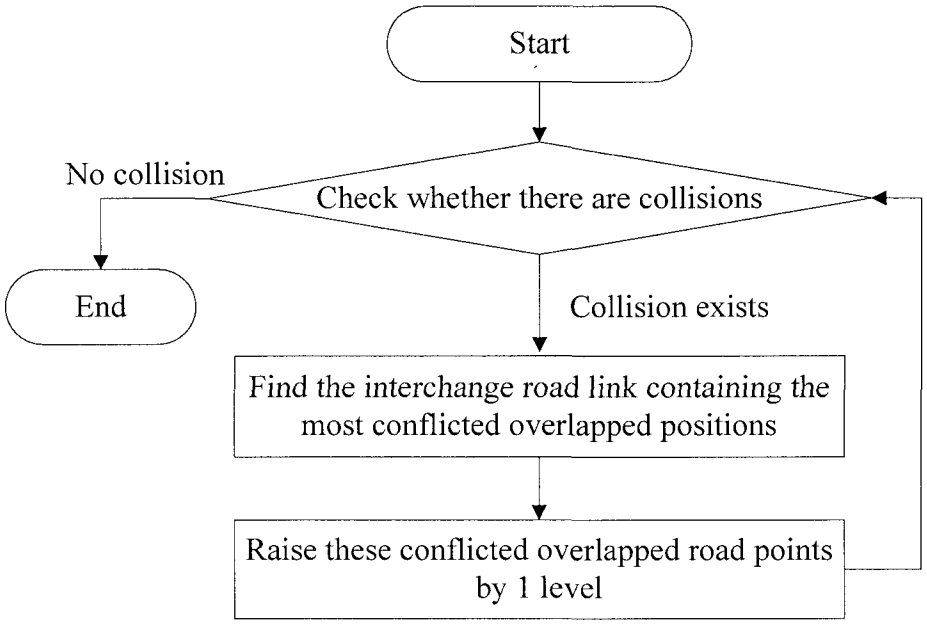

Fig. 24. Flowchart of collision avoidance procedure

The final model of the interchange is mainly decided by the value of the predefined elevation level assigned in Step 1, and diverse interchange models can be obtained by adjusting the value of the predefined elevation level to meet different requirements. In this research, all possible sets of predefined elevation level values are generated in advance and the predefined elevation level values used for an interchange generation can be determined by an input index number. For example, if 3 predefined elevation level values are used in an interchange generation, in total there are eight possible sets of these predefined elevation level values listed as follows:

- (1, 1, 1), (1, 1, 2), (1, 2, 1), (2, 1, 1), (2, 1, 2), (2, 2, 1), (1, 2, 2), (2, 2, 2).

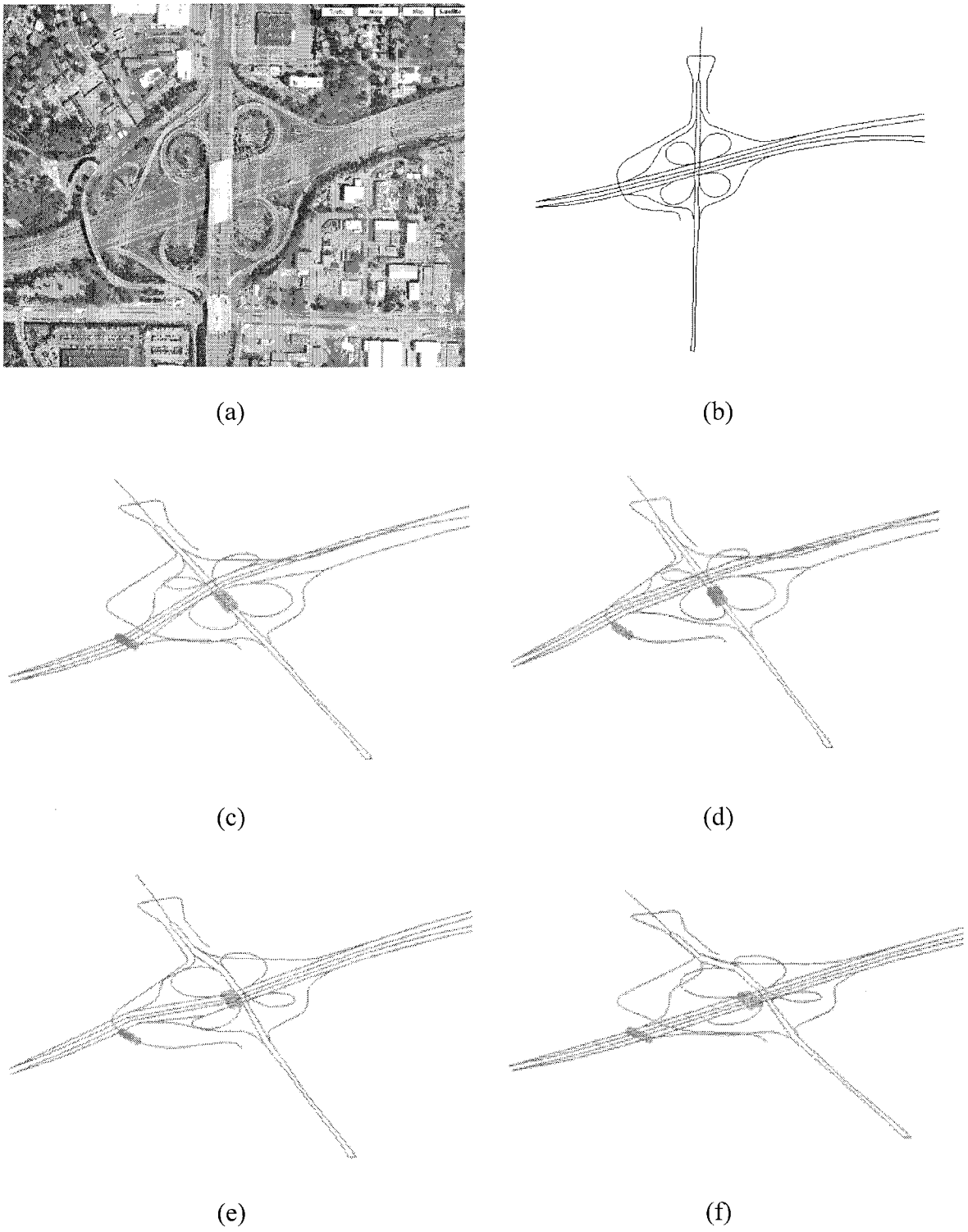

(a) (b)

(c) (d)

(e) (f)

Fig. 25. An example of the interchange modeling with different predefined level values. (a) Satellite image of a traffic interchange in Norfolk, Virginia. (b) Road GIS data for previous traffic interchange display in ArcGIS. (c)(d)(e)(f) Four different interchange models from interchange modeling with the same road GIS data. The green points indicate the overlapped road points located at the first level.

So if the predefined elevation level values used for an interchange generation are supposed to be determined by an input index number of 2, the value set (1, 2, 1) will be used during the execution. Fig. 25 gives an example of the interchange modeling with different predefined level values and a total of 4 different interchange models are generated from the same road GIS data.

b) Absolute Elevation Calculation

After determining the elevation level of each overlapped road point, absolute elevations are calculated based on the terrain elevation and level height, and linear interpolation is used to compute the elevations for road points located between two overlapped positions. Grade rule should be complied with during the linear interpolation processing, especially for handling the junction between the interchange road link and normal road link which does not have any overlapped position yet connects to the interchange road link. Fig. 26 gives a simple example of road network after absolute elevation calculation.

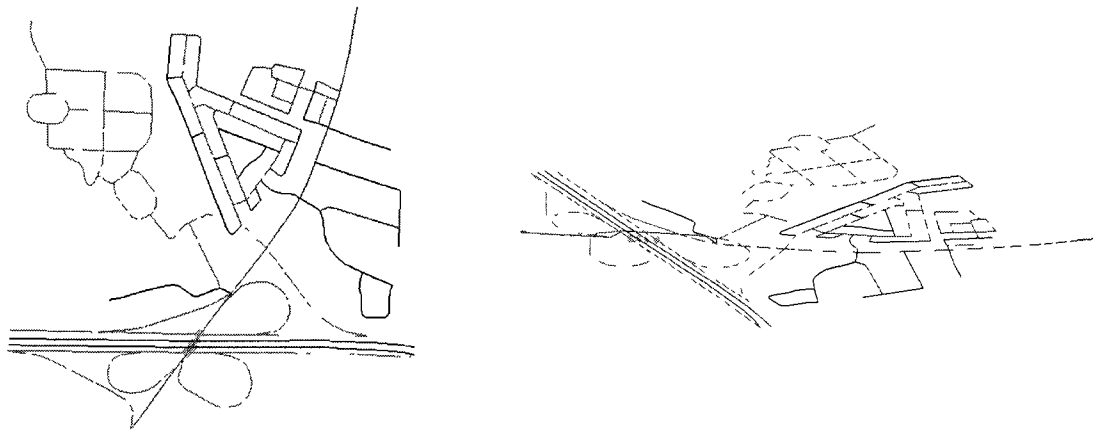

(a) (b)

Fig. 26. An example of road network after absolute elevation calculation based on GIS data shown in Fig. 6 (overlapped positions are indicated by green points). (a) Top view. (b) Side view.

5.1.4 Interchange Evaluation

As mentioned before, various interchange models can be generated from the same road GIS data with different predefined level values. Because the predefined elevation level values used in this research are 1 and 2 representing level 1 and level 2, respectively, this method can generate exactly the same model for any existing two-level road interchange. As shown in Fig. 25, among four generated interchange models, the one displayed in Fig. 25(f) has exactly the same structure as the real one shown in Fig. 25(a). However, for an interchange containing three or more levels, the proposed algorithm does not guarantee results that are exactly the same as the real interchange, due to the complexity of interchange structure. To evaluate the quality of the different interchanges produced by the proposed method, we calculate several metrics for every interchange. These metrics include the highest elevation level, the number of crests and sags, maximal grade, average grade and the total length. Using the interchange between I-64 and I-264

shown in Fig. 18 as an example, values of these metrics for 32 generated interchange models are calculated and listed in Table 6 with the smallest value of each highlighted in yellow. At the same time, some selected centerline models are shown in Fig. 27.

Based on intuitive knowledge, the lower the highest elevation level is, the fewer the number of crests and sags, the smaller the grade, and the better the generated interchange. According to Table 6, it is easily to find that generated model with input index 31 is the optimal result which has smallest length, smallest maximal grade, fewest crests and sags and small average grade. Comparing the generated models with the real interchange, it is really delightful to find that among all of them the generated model with input index 31 provides the closest match to the real one. The difference between them is that a ramp part which is located in Level 3 in the real situation is placed in Level 1 in the generated model. Considering that the maximal grade of this generated model is 4%, meaning that it complies with the grade rules strictly, this generated model offers another good choice for the construction of this interchange.

Table 6. Values of metrics for interchange evaluation

Input Index	Predefined Level values	Maximal Grade	Average Grade	Length	Highest Level	Crest & Sag
0	1 1 1 1 1	0.046587	0.00812474	5907.88	3	18
1	1 1 1 1 2	0.046587	0.00935301	5559.71	3	21
2	1 1 1 2 1	0.046587	0.00943954	5084.99	3	18
3	1 1 1 2 2	0.046587	0.0123272	4867.28	3	24
4	1 1 2 1 1	0.056011	0.00919174	5222.08	3	17
5	1 1 2 1 2	0.056011	0.010669	4873.91	3	20
6	1 1 2 2 1	0.056011	0.0109111	4399.19	3	17
7	1 1 2 2 2	0.056011	0.014349	4181.48	3	23
8	1 2 1 1 1	0.056011	0.0139841	6864.95	3	32
9	1 2 1 1 2	0.056011	0.015345	6516.78	3	36
10	1 2 1 2 1	0.056011	0.0129565	5557.08	3	24
11	1 2 1 2 2	0.056011	0.0157322	5339.36	3	31
12	1 2 2 1 1	0.046587	0.0121953	5903.93	3	25
13	1 2 2 1 2	0.046587	0.0136795	5555.76	3	29
14	1 2 2 2 1	0.046587	0.0104437	4596.05	3	17
15	1 2 2 2 2	0.046587	0.0137038	4378.34	3	24
16	2 1 1 1 1	0.040952	0.0112842	6026.12	3	25
17	2 1 1 1 2	0.040952	0.00939886	5107	3	17
18	2 1 1 2 1	0.040952	0.0142001	5352.09	3	29
19	2 1 1 2 2	0.040952	0.0140245	4563.44	3	24
20	2 1 2 1 1	0.056011	0.0127333	5340.32	3	26
21	2 1 2 1 2	0.056011	0.0108568	4421.21	3	18
22	2 1 2 2 1	0.056011	0.016287	4666.29	3	30
23	2 1 2 2 2	0.056011	0.0165049	3877.64	3	25
24	2 2 1 1 1	0.056011	0.0138706	6632.72	3	27
25	2 2 1 1 2	0.056011	0.0126015	5713.61	3	20
26	2 2 1 2 1	0.056011	0.0138846	5473.7	3	23
27	2 2 1 2 2	0.056011	0.0136605	4685.05	3	19
28	2 2 2 1 1	0.040952	0.0119894	5671.7	3	22
29	2 2 2 1 2	0.040952	0.0100998	4752.58	3	15
30	2 2 2 2 1	0.040952	0.0115231	4512.68	3	18
31	2 2 2 2 2	0.040952	0.0107411	3724.03	3	14

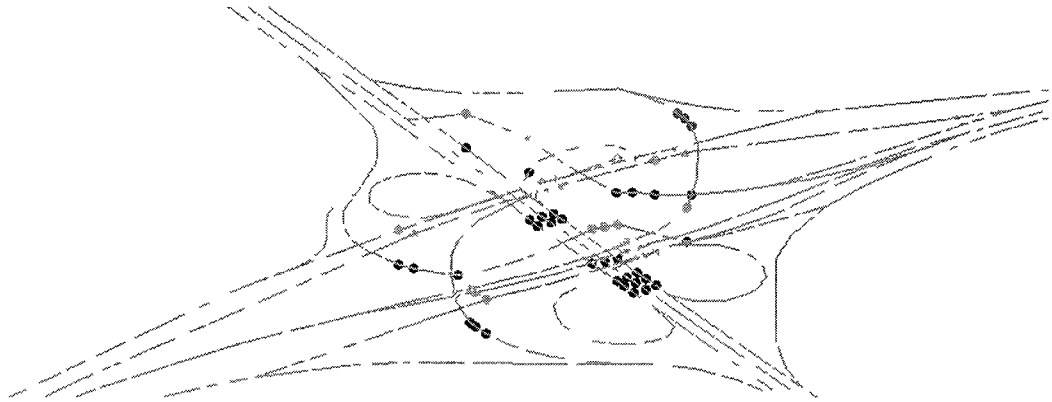

(a) Input index = 0

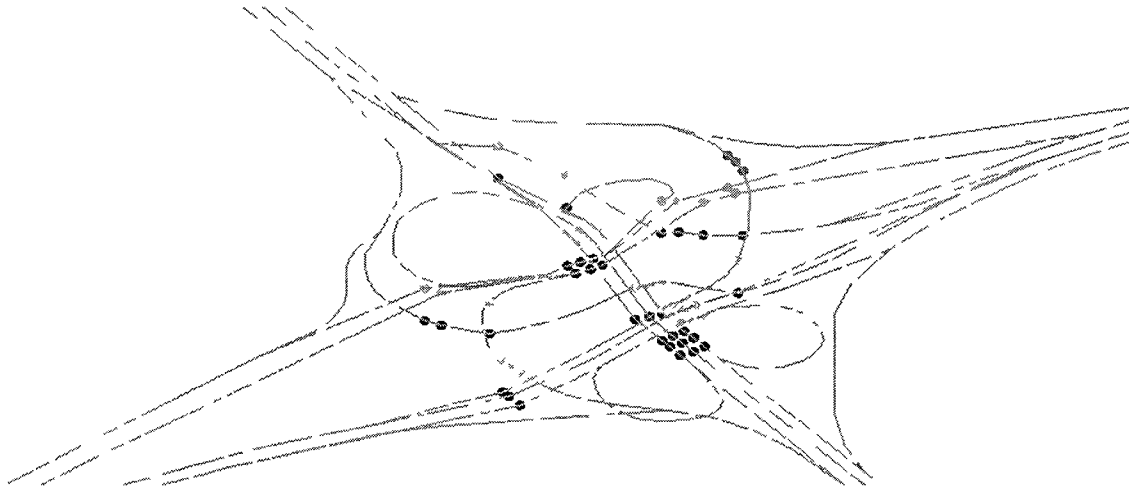

(b) Input index = 9

Fig. 27. Selected generated models for interchange containing more than 2 levels. Overlapped road points are indicated by points with different colors: Level 1 road points by blue points, Level 2 road points by green points and other road points by red points.

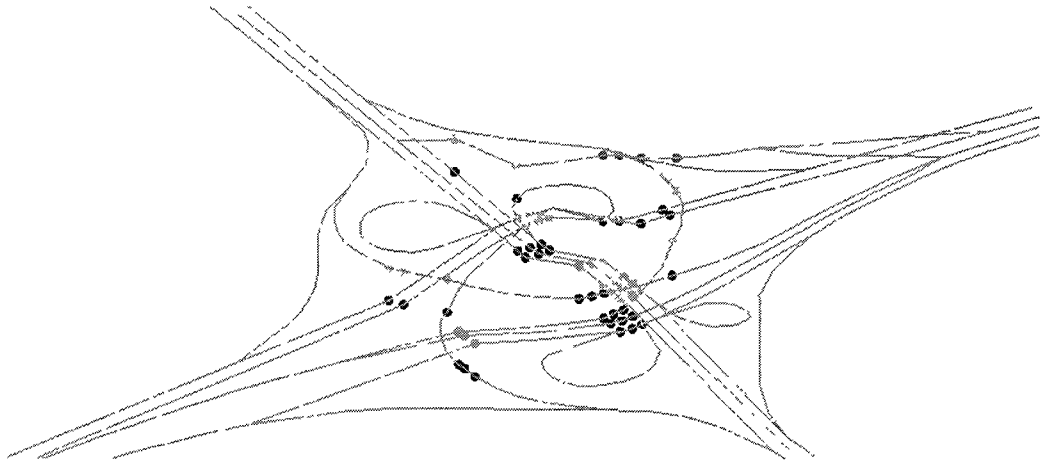

(c) Input index = 22

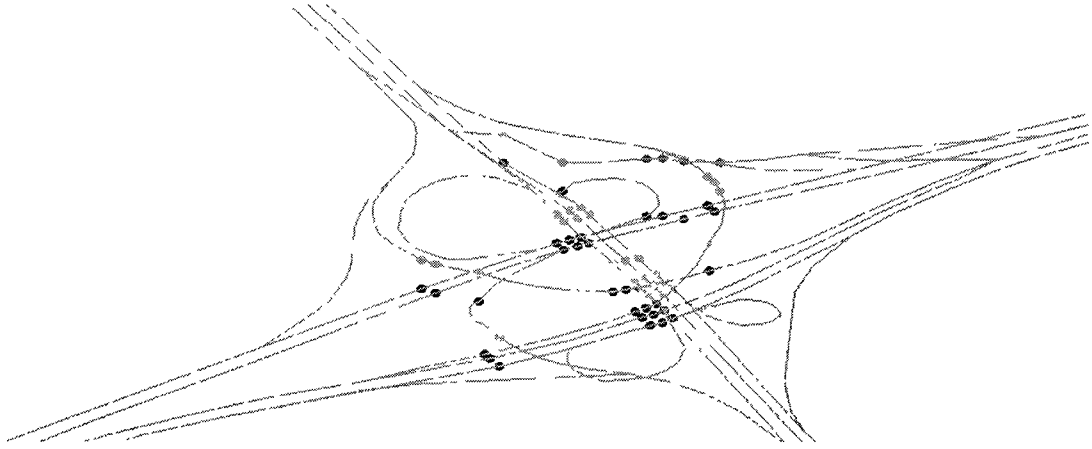

(d) Input index = 31

Fig. 27. Continued

5.2 Road Representation Parameterization

Converting discrete road points into analytic representations of road segment centerlines is a challenging task. In our research, this procedure is divided into two subtasks: polyline segmentation, which partitions the polyline into segments according to some criteria through a segmentation process; and segment fitting, which fits the

segments into two standard forms using the least square method. The two standard forms used to represent the segment units are:

- Straight Line (Line): A straight line connecting two points and specified by its ID, start point, end point, start side vector and end side vector.
- Circular Curve (Curve): Part of a circle and specified by its ID, position of center point, radius, start point, end point, start side vector, end side vector, start angle, end angle and direction (clockwise / anticlockwise).

Among these parameters, side vectors indicate the extension direction of road surface. This representation method of road segment has several advantages. First, it is relatively simple and easy to understand and implement. More importantly, it is well-suited to apply civil engineering principles, especially for superelevation generation for which the center point and radius are required.

5.2.1 Polyline Segmentation

In order to divide the road polylines into different segments that can be represented in standard segment forms, four types of critical points are identified to segment the road polylines: acute turn, S-turn, turn start/end and elevation change. The first three are defined based on their 2D geometric features [53] and the last one is just for overlapped road points contained in traffic interchanges to reflect the elevation change of road links. A detailed description of them is given as follows and an illustration is given in Fig. 28.

- Acute turn: The angle between the adjacent line segments of this point less than a predefined threshold, resulting in a sharp turn when passing through

this point. In this research, if the angle is smaller than 150°, this point is considered an acute turn point.

- S-turn: A signed curvature is calculated for each point of the polyline. S-turn is such a point after which the signed curvature changes sign.
- Turn start/end: The polyline representations of roads tend to have dense points for road segments with large curvature and sparse points for relatively straight road segments. Thus the lengths of two line segments at a point can be used to indicate a transition from a straight line to a curve, or vice versa. The proposed method calculates the ratio of the lengths of the two adjacent line segments at a point and compares it with a predefined threshold to determine whether it is the turn start/end point. In this research, if the ratio is less than 0.4 or greater than 2.5, that point is the start or end of curved road segments.
- Elevation change: For an overlapped road point, if its elevation is greater than or equal to those of its two adjacent overlapped road points which belong to the same road link but do not have the same elevations, it is considered an elevation change critical point; if its elevation is less than or equal to its two adjacent overlapped road points which belong to the same road link but do not have the same elevations, it is also an elevation change critical point.

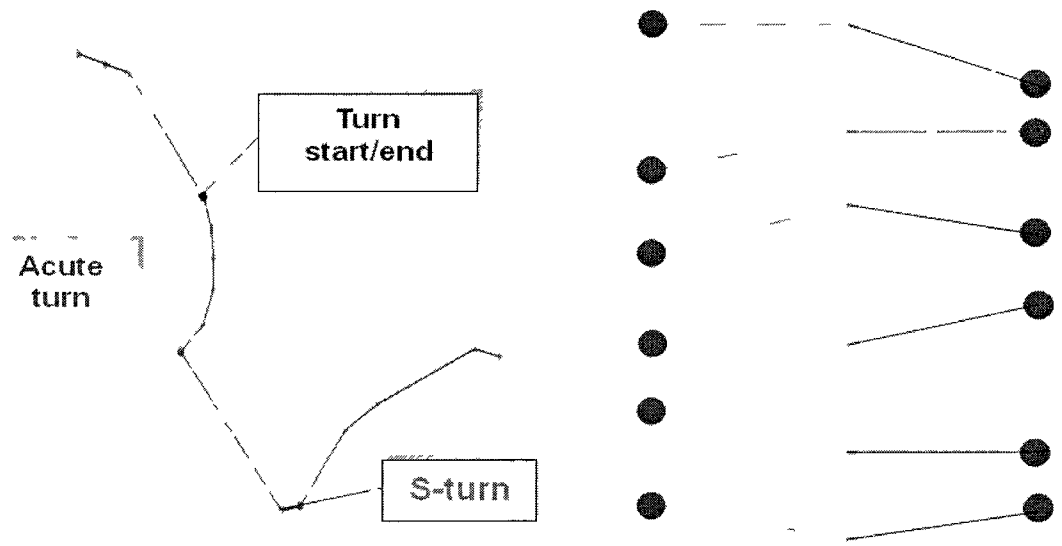

(a) (b)

Fig. 28. An illustration of critical points. (a) First three types of critical points. (b) Elevation change critical point indicated by the yellow point.

After the critical points are identified, road polyline links are partitioned into a set of segments that are groups of discrete points ready for segment fitting to obtain their appropriate analytic representations. Then least square methods [53] are employed to fit these road segments into straight lines and circular curves.

5.2.2 Segment Fitting

In this section, we focus on fitting a set of points (x_i, y_i), $i = 1, \ldots, N$ into a straight line or circular curve using the least square method.

- Straight Line Fitting

A line can be represented by the equation $y = ax + b$ and the parameters a and b completely determine the line. To fit N points to a line, the sum of squared residuals is computed first in (4),

$$s = \sum[y_i - f(x_i)]^2 = \sum[y_i - (a + bx_i)]^2. \quad (4)$$

In order to obtain the line that best fits the N points, the value of s should be minimized by computing its partial derivatives with respect to a and b as (5) and (6)

$$\frac{\partial s}{\partial a} = -2\sum(y_i - a - bx_i) = 0, \quad (5)$$

$$\frac{\partial s}{\partial b} = -2\sum(y_i - a - bx_i)x_i = 0. \quad (6)$$

Solving the above system of equations, we obtain

$$a = \frac{\sum x_i y_i \sum x_i - \sum y_i \sum x_i^2}{(\sum x_i)^2 - n\sum x_i^2}, \quad (7)$$

$$b = \frac{\sum x_i \sum y_i - n\sum x_i y_i}{(\sum x_i)^2 - n\sum x_i^2}, \quad (8)$$

and the correlation coefficient [54] r as (9):

$$r = \frac{\sum(x_i - \bar{x})(y_i - \bar{y})}{\sqrt{\sum(x_i - \bar{x})^2}\sqrt{\sum(y_i - \bar{y})^2}}, \quad (9)$$

where

$$\bar{x} = \frac{\sum x_i}{n}, \ \bar{y} = \frac{\sum y_i}{n}. \quad (10)$$

The value of r is in the range $[-1, 1]$. The closer the absolute value of r is to 1, the more likely this set of points becomes a straight line.

- Circular Curve Fitting

Based on different measurement criteria and representation forms, Gander et al. [55] proposed three methods for circles fitting using least square method: minimizing the algebraic distance, minimizing the geometric distance, and geometric fit in parametric form. In these three methods, different representations are used to represent the circle. According to the discussion in [55], method 1 is simple but does not always minimize the geometric distance; method 2 and method 3 generate the "best" circle; however, both of them have high computational complexity since they use the iterative Gauss-Newton method. Furthermore a good initial vector is needed by both methods 2 and 3. Because the circle fitting is executed numerous times during the whole road fitting procedure with high accuracy requirement, none of these methods meets our demand. Instead we minimize the squared geometric distance rather than the real geometric distance used in methods 2 and 3, greatly reducing computational complexity. A circle can be determined by its center (A, B) and its radius R as shown in Fig. 29 and it can be expressed as

$$R^2 = (x - A)^2 + (y - B)^2. \tag{11}$$

That is

$$R^2 = x^2 - 2Ax + A^2 + y^2 - 2By + B^2. \tag{12}$$

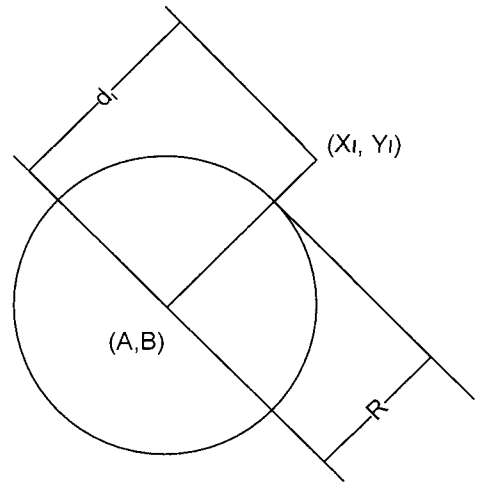

Fig. 29. An illustration of parameters used for circular curve fitting

Let a = -2A, b = -2B and $c = A^2 + B^2 - R^2$, we have $x^2 + y^2 + ax + by + c = 0$ and if values of a, b and c are known, the values of A, B, R can also be computed as follows

$$A = \frac{a}{-2}, B = \frac{b}{-2} \text{ and } R = \frac{1}{2}\sqrt{a^2 + b^2 - 4c}\,. \tag{13}$$

The squared geometric distance can be expressed by

$$d_i{}^2 = (X_i - A)^2 + (Y_i - B)^2\,. \tag{14}$$

So the difference δ_i for point i is

$$\delta_i = d_i{}^2 - R^2 = (X_i - A)^2 + (Y_i - B)^2 - R^2 = X_i{}^2 + Y_i{}^2 + aX_i + bY_i + c, \tag{15}$$

and the total difference of squared geometric distances of the whole point set is

$$Q(a,b,c) = \sum \delta_i{}^2 = \sum\left(X_i{}^2 + Y_i{}^2 + aX_i + bY_i + c\right)^2\,. \tag{16}$$

To minimize the value of Q(a, b, c), its partial derivatives are computed with respect to a, b and c,

$$\frac{\partial Q(a,b,c)}{\partial a} = \sum 2\left(X_i^2 + Y_i^2 + aX_i + bY_i + c\right)X_i = 0\,, \tag{17}$$

$$\frac{\partial Q(a,b,c)}{\partial b} = \sum 2\left(X_i^2 + Y_i^2 + aX_i + bY_i + c\right)Y_i = 0\,, \tag{18}$$

$$\frac{\partial Q(a,b,c)}{\partial c} = \sum 2\left(X_i^2 + Y_i^2 + aX_i + bY_i + c\right) = 0. \tag{19}$$

Solving this system of equations, we have

$$a = \frac{HD-EG}{CG-D^2},\ b = \frac{HC-ED}{D^2-GC} \text{ and } c = -\frac{\sum(X_i^2+Y_i^2)+a\sum X_i+b\sum Y_i}{N}, \tag{20}$$

where

$$C = \left(N\sum X_i^2 - \sum X_i \sum Y_i\right), \tag{21}$$

$$D = \left(N\sum X_i Y_i - \sum X_i \sum Y_i\right), \tag{22}$$

$$E = \left(N\sum X_i^3 + N\sum X_i Y_i^2 - \sum(X_i^2 + Y_i^2)\sum X_i\right), \tag{23}$$

$$G = \left(N\sum Y_i^2 - \sum Y_i \sum Y_i\right), \tag{24}$$

$$H = N\sum X_i^2 Y_i + N\sum Y_i^3 - \sum(X_i^2 + Y_i^2)\sum Y_i \tag{25}$$

Based on these two fitting methods for straight line and circular curve, an iterated method is used in this research to implement the segment fitting. Also two threshold values are used to control the accuracy of the fitting result, one for the correlation coefficient during the straight line fitting and one for the total difference of squared geometric distances of the whole point set during the circular curve fitting. The detailed fitting procedure is as follows:

Variables: Two parameters sIndex and eIndex are used to record the positions of the start point and end point of the road segment to be fitted. Variable newEIndex represents the position of the end of the extended road segment. Variable resL is the correlation coefficient for the line fitting process and variable resC the total difference of

squared geometric distances of the whole point set divided by the size of fitted road points for the curve fitting process. Variables lineRes and circleRes are employed to control the accuracy of the fitting results for straight line and circular curve, respectively. In this research, usually lineRes = 0.998 and circleRes = 1.0. A Boolean variable breakNeed indicates whether a road segment should be generated immediately or after more iteration to reflect the elevation change of road link. Function abs(x) returns the absolute value of x.

Procedure: Fig. 30 gives the flowchart of this procedure for every road link and N is the number of road points contained in this link.

Fig. 31 shows an example of road segmentation and fitting using part of I-64. Fig. 31(a) displays the original polylines imported from a shape file. Fig. 31(b) shows the results after segmentation. Polylines are divided into several segments separated by critical points: red points for curved segment and black points for line segments. Fig. 31(c) shows the resulting line and circle fitting using the least square method. Two circles with radii of 1433.1m and 686.7m are extracted from points on the curved parts and three straight lines are extracted from points on the line segments. It can be seen that the proposed segmentation and fitting methods are very effective, producing parametric representations of the road segments that fit very well the original polyline representations. Besides this, Table 7 gives a detailed analysis of the memory storage required before and after the segment generation, which shows that almost half of memory usage is saved.

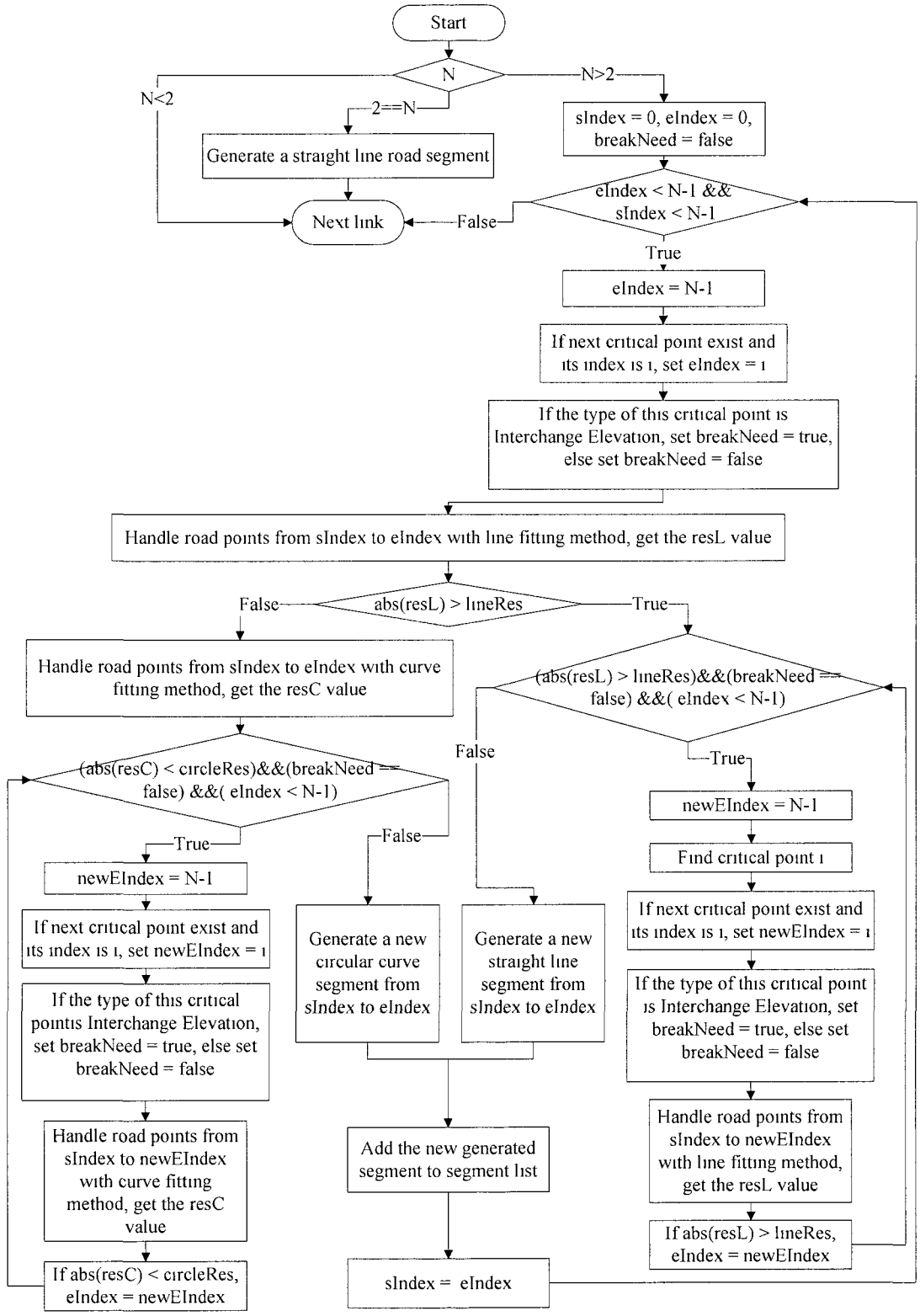

Fig. 30. The flowchart of the fitting procedure

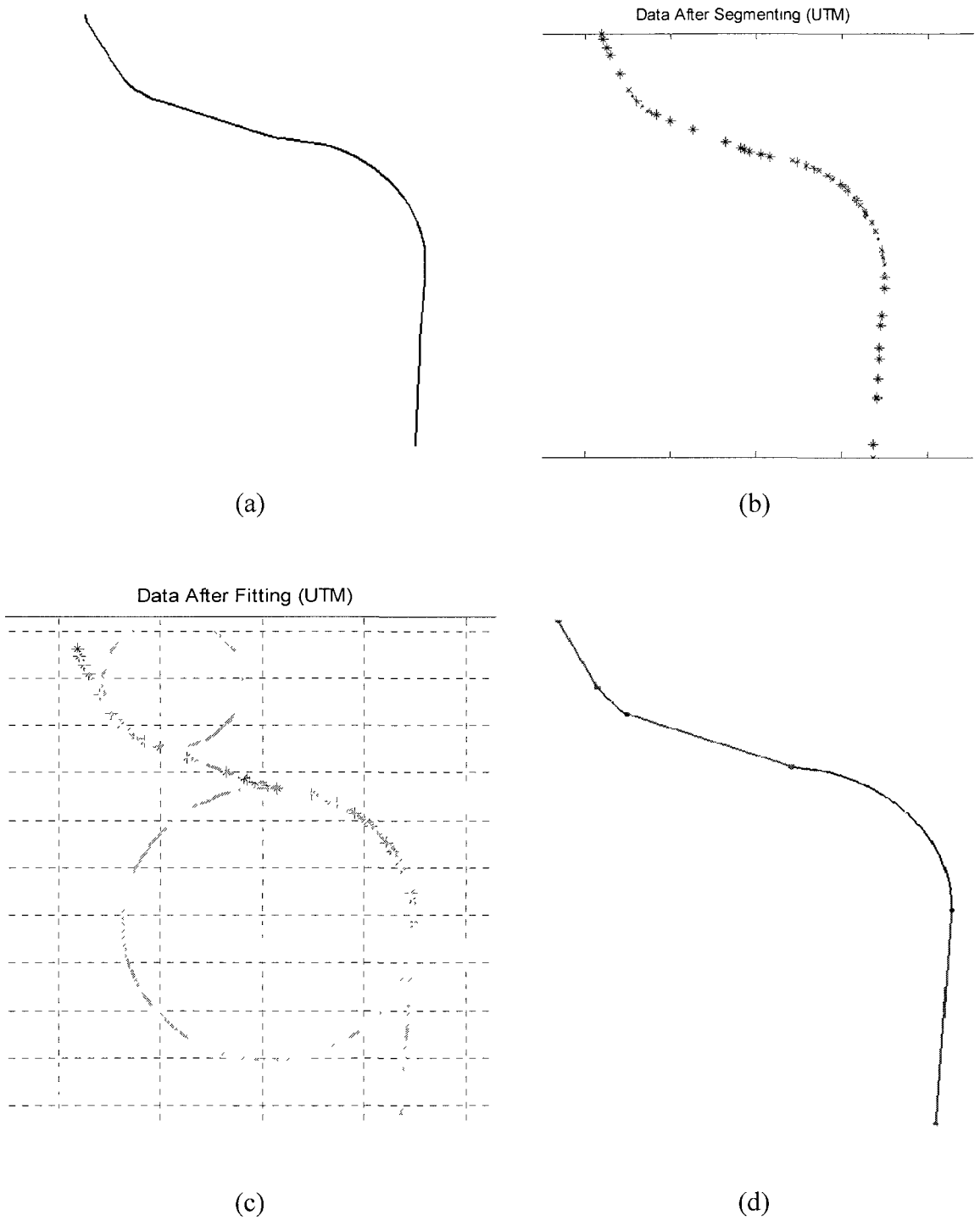

Fig. 31. Results from link segmentation and fitting. (a) Road links for part of I-64 HOV lane imported from a shape file. (b) Segmentation results. Polylines are divided into several segments: red points for curved segment and black points for line segment. (c) Data after curve and line fitting. Two circles with radii of 1433.1m and 686.7m are extracted from discrete point data. (d) Final result (red: straight line; blue: circular curve).

Table 7. Memory usage analysis for the example in Fig. 31

	Original Data	**After Extraction**
Shape	53 road points	3 lines, 2 curves
Memory	159 floating point number	72 floating point number, 12 integers
Almost half of storage space is saved		

Fig. 32 illustrates the results of the proposed method for a more complex road network in the Larchmont neighborhood of Norfolk, Virginia. We can see that all roads are well represented by straight lines or circular curves.

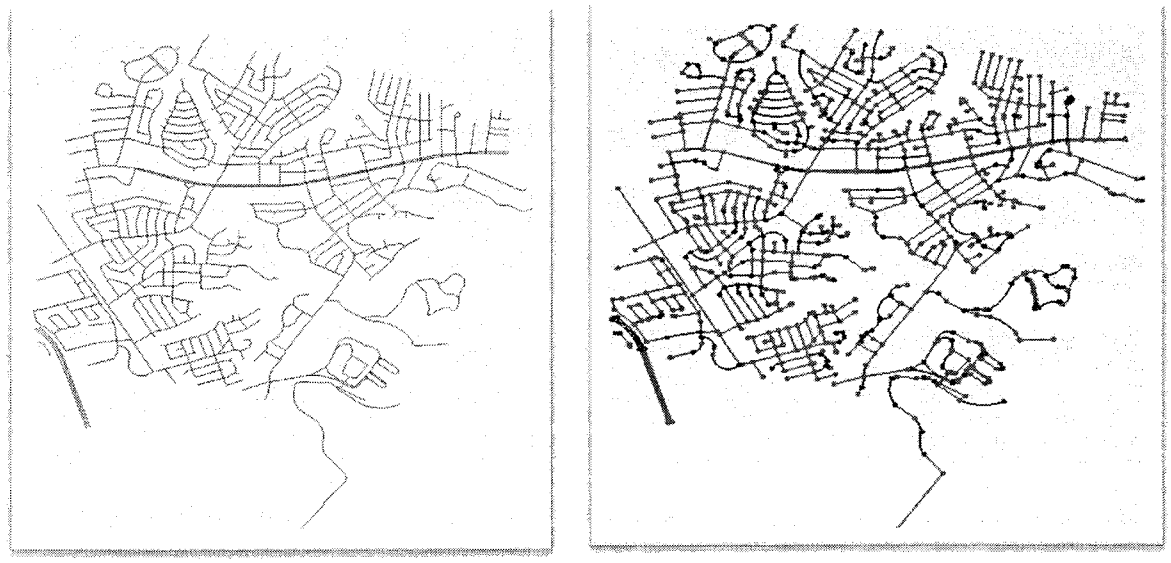

(a) (b)

Fig. 32. Result of the proposed method on the road network of the Larchmont neighborhood in Norfolk, Virginia. (a) GIS data shown in ArcGIS. (b) Same road network after extraction (red: straight line; blue: curve).

5.3 Intersection Modeling

Basic types of intersections are three-leg or T, four-leg, and multileg and it is not recommended that an intersection has more than 4 legs [4]. In this research, according to the shape and function, intersections are divided into two types: normal intersection and merging/diverging intersection. If an intersection has just 3 legs and one of the angles between its adjacent intersection legs is less than 30°, it is considered a merging/diverging intersection; otherwise, it is a normal intersection. For a normal intersection, the effect of curb radii should be taken into consideration and for a merging/diverging intersection, the merging or diverging of the ramp leg must be handled correctly. The main task of the centerline modeling of intersection is to determine the end position of every intersection leg and separate it from the connected road segment. In order to achieve this goal, the method proposed in [13] for junction synthesis was adopted, expanded and finally integrated into this research to generate the road intersection. Compared with the original method that just considered synthesizing junctions from connected straight line road segments with the same road width, our expanded method not only produces smooth junctions from both line and curved road segments with the help of side vectors that indicate the extending direction of road surface, but also handles road segments with different road widths correctly. Assuming the road width for each road segment is known, the road segment can be approximated as a plane with fixed boundary. Using Fig. 33 which shows two adjacent road segments connecting to the same road node, the main steps for intersection generation are listed as follows:

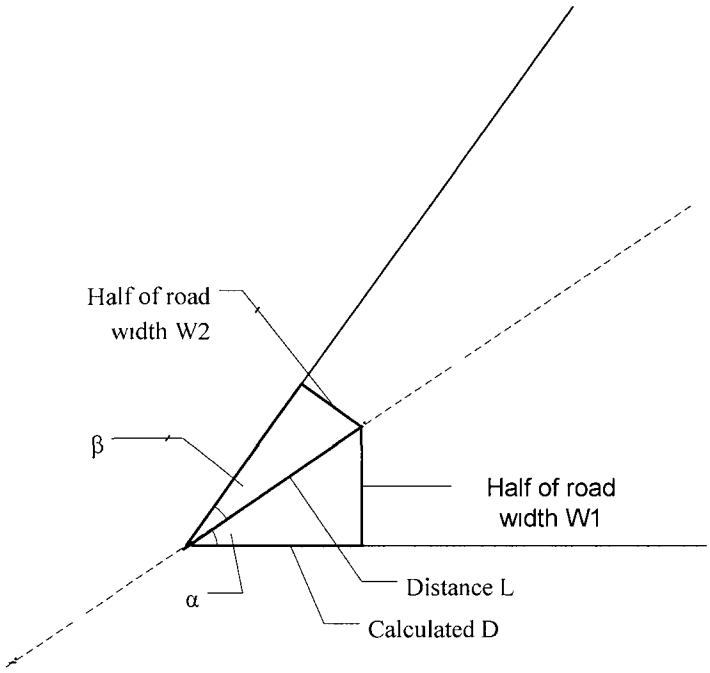

Fig. 33. An illustration of road intersection generation

1. For each intersection node connected to 2 or 2+ links, find the nearest segment for each connected link since each link may contain several segments.

2. According to the type of the segment (straight line or circular curve) find the direction of the centerline.

3. Based on the direction of the centerline, calculate the angle θ between every two legs. As shown in Fig. 33, we have that

$$\begin{cases} \theta = \alpha + \beta \\ \frac{sin\alpha}{sin\beta} = \frac{W1}{W2} \end{cases}, \tag{26}$$

where W1 and W2 are road widths of these two road segments. Since for small angle, $sin\theta \approx \theta$, we assume that

$$\begin{cases} \theta = \alpha + \beta \\ \frac{\alpha}{\beta} = \frac{W1}{W2} \end{cases}. \tag{27}$$

Solving this system of equation, we have

$$\alpha = \frac{\theta}{W1+W2} \times W1 \text{ and } \beta = \frac{\theta}{W1+W2} \times W2. \tag{28}$$

So for every two links, the distance L between the node and the intersecting point of the link boundaries can be calculated as

$$L = \frac{W1}{2 \times sin\alpha} \text{ or } L = \frac{W2}{2 \times sin\beta}. \tag{29}$$

4. Then for every two adjacent road segments, calculate the length, denoted as D, which is the distance from the intersection center point to the end point along the centerline for each connected segment and will be considered part of the intersection. The formula is

$$D = \sqrt{L^2 - W^2}. \tag{30}$$

5. For every connected road segment, choose the maximum value of D, denoted as D_{max}. Use it as the final length of center line for this segment contained in the intersection as an intersection leg and adjust the start point or end point of this connected segment according to this D_{max}.

The intersections generated using the above method have the smallest leg length since this method just considers the overlapped part. Taking the edge design discussed in chapter 4 into consideration, additional length should be added to L to reserve some space for the circular edge generation that will be discussed in the next chapter. The resulting road intersection is represented by several parameters, including the position of

the intersection center (node), the end point of the centerline and side vector for each leg (connected road link). This process produces smooth transitions between road segments and an example of the intersection centerline modeling is given in Fig. 34. To conclude this chapter, Fig. 35 illustrates the whole 3D road centerline modeling process.

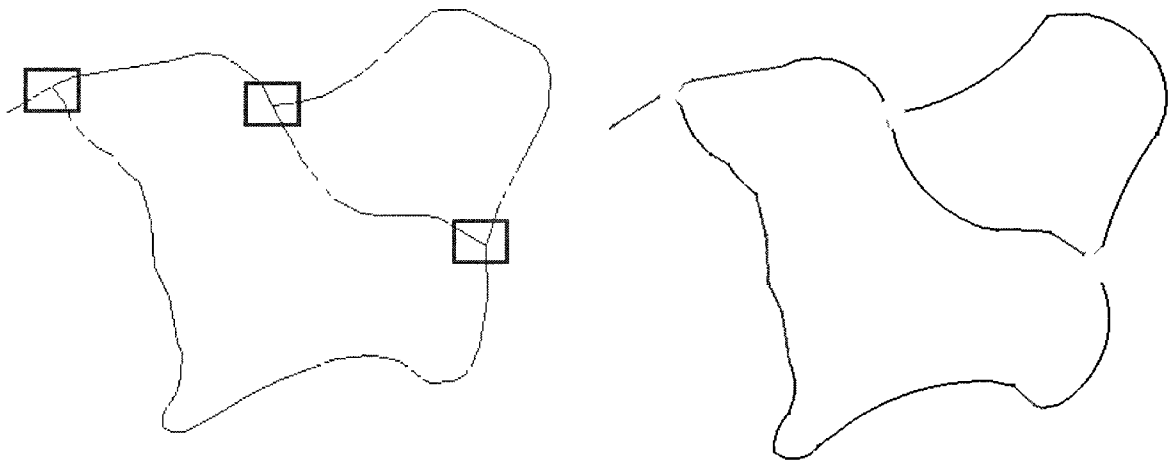

(a) (b)

Fig. 34. Road intersection modeling. (a) GIS data of a road network in VA. (b) The centerline model of previous road network with three road intersections indicated by red rectangles and parametric road segments (red for straight line and blue for circular curve).

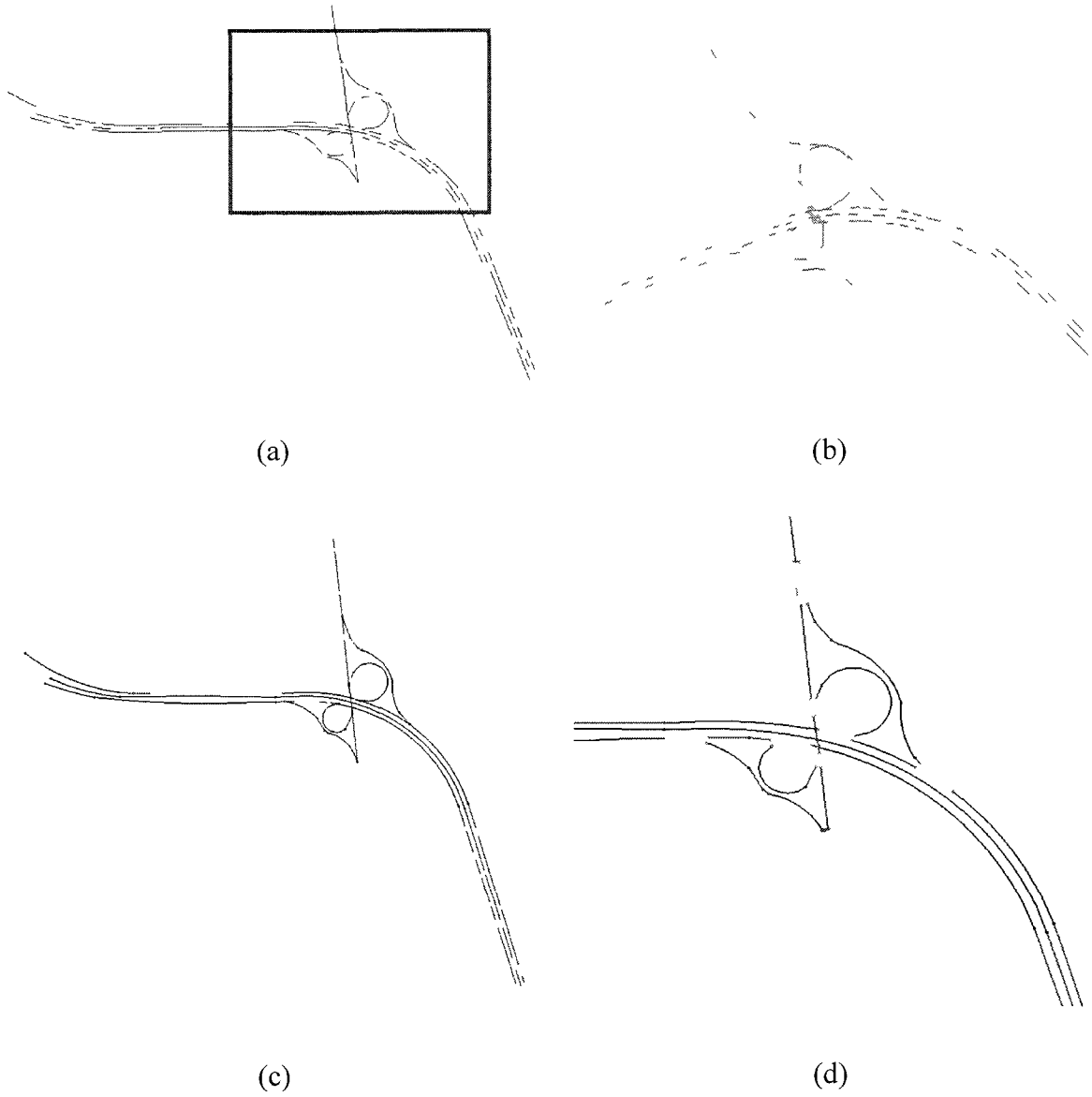

Fig. 35. An illustration of the 3D road centerline modeling. (a) GIS data of a traffic interchange in Virginia. (b) The 3D model of traffic interchange area indicated in a red rectangle after interchange modeling. The overlapped positions are marked with green points. (c) The whole traffic interchange represented by parametric road segments (red for straight line and blue for circular curve) after parameterization. (d) The final centerline model of the traffic interchange with intersections extracted from previous parameterized road network.

CHAPTER 6

3D ROAD GEOMETRY MODELING

In this chapter, 3D road centerline models, namely the analytic representations of intersections and segments, are converted into various 3D road geometric models consisting of triangles and textures. The final 3D road geometric models are generated using two methods. All road surfaces, including surfaces of regular road segments and road intersections, are tessellated directly from road analytic representations through triangulation, while some accessorial parts of the road network such as lights, guard rails and abutments are created in 3D modeling software such as Maya and 3DMax, imported into the system, duplicated and placed at the right locations. The geometric modeling of road surface is a critical component of the proposed method and is discussed in this chapter in detail. Fig. 36 gives a detailed flow chart of this process.

6.1 Road Segment Modeling

Road segment geometric modeling is based on several road attributes, including road centerline positions, normal cross slope, superelevation, number of lanes, and side vectors. The more information is available and used, the better resulting road geometric segment model is. For example, if there is information about curb and shoulder of the road, the width and edge of the road can be modeled more precisely. This section discusses modeling methods for roadbed, superelevation, accessorial objects and road markings in detail.

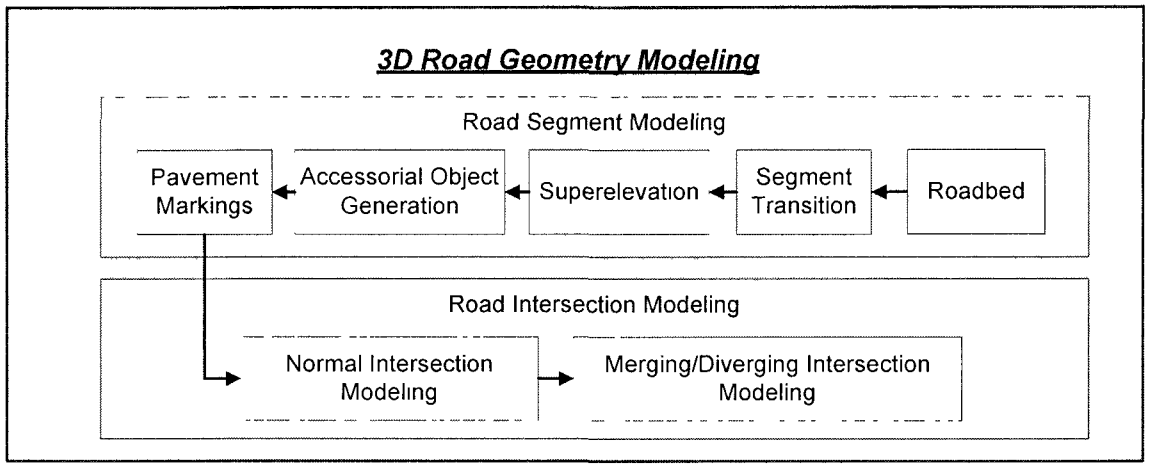

Fig. 36. Detailed flow chart of 3D road geometry modeling

6.1.1 Roadbed

Road width is determined by the number of lanes and lane width. After the road width is determined, road surface is extended from the road centerline along the side vectors in both right and left directions. Discrete road centerline points are generated from the analytic road segment representation and the number of road points contained by every 100 meters can be adjusted based on the resolution specification. Usually the number of road points per 100 meters used in this research is 41, which means the distance between two sequential discrete road centerline points is about 2.5 meters. As shown in Fig. 37, two sequential road centerline points N and N+1 marked with yellow points are used as the middle point and four other road points (right point, right middle point, left middle point and left point) indicated by black points are generated from both of them with the help of the side vector. And then eight triangles are created based on these road surface points and finally form the road surface.

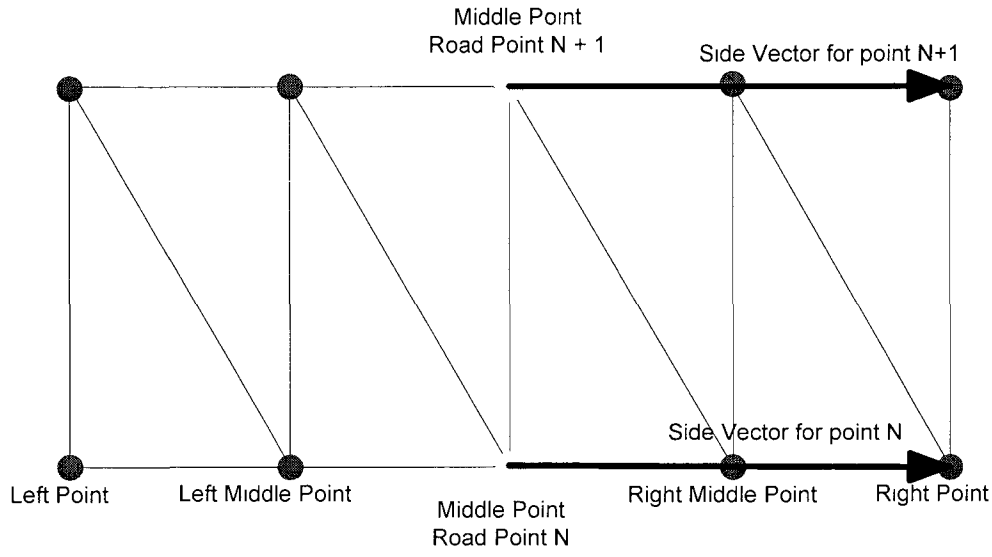

Fig. 37. An illustration of the triangulation of normal road segment surface

For some roads that have auxiliary lanes at their end connecting to a parallel design merging/diverging intersection, the numbers of lanes change and the left road surface and right road surface may have different widths. Given this situation, the numbers of lanes for the left road surface and right road surface should be represented respectively; the additional number of auxiliary lanes is taken into account and added to the corresponding road side. Different numbers of lanes are used to reflect the change of road width, especially for the taper part included at the end of the auxiliary lane to implement the lane merging. An illustration of this process is shown in Fig. 38.

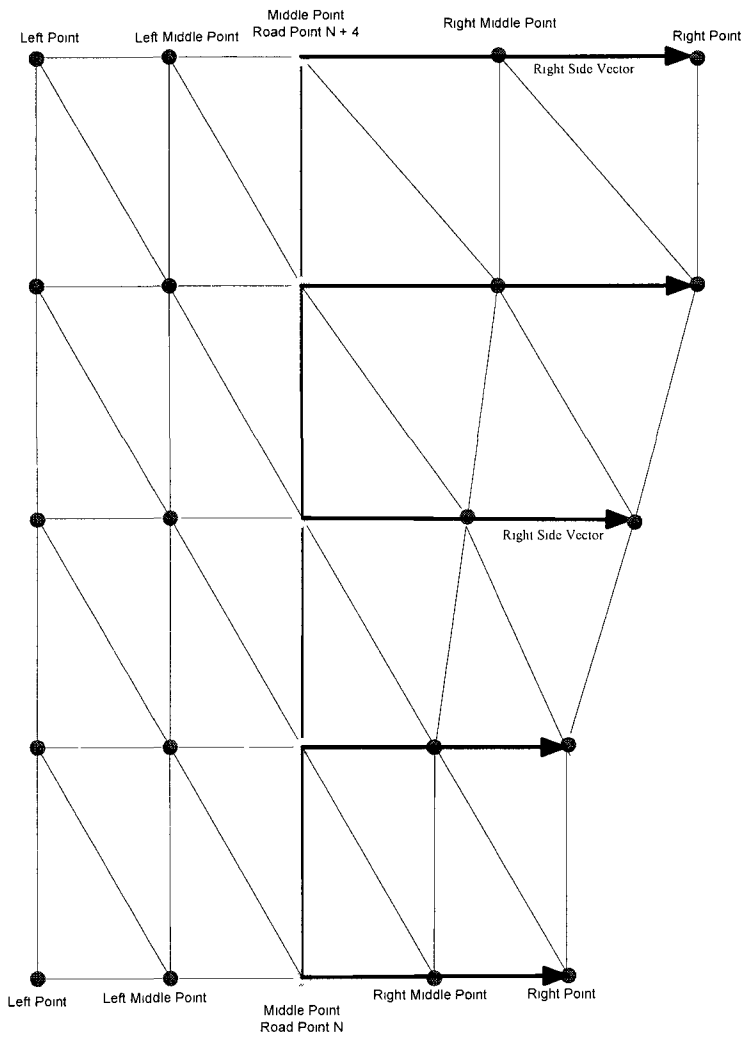

Fig. 38. An illustration of the triangulation of road segment surface with one auxiliary lane on the right side and a taper at its end

6.1.2 Segment Transition

Because the geometric model of road segments is generated from road centerlines via extension along the side vector as described before, two connected road segments which are not collinear have certain overlap, gap or distortion at the junction. The smaller the angle between these two segments is, the more severe the overlap, gap or distortion is. Segment transition is proposed to smooth the junction for such situation. As shown in Fig.

39, using the inside point of intersection of road edges as the center and the road width as the radius, sectorial segment transitions are created to smooth these two connected road segments no matter if the angle is an obtuse angle, a right angle or an acute angle.

6.1.3 Superelevation

Normal cross slope for most road surfaces and superelevation for curved road surfaces are two key factors directly determining the main shape of road surfaces, such as the superelevation transition from normal crown to full superelevation. Considering the civil engineering rule of using the centerline of the roadbed as the axis of rotation for superelevation during road construction, two parameters named lRate and rRate are used to represent the slope rate of the left road side and right road side. For an instance, for normal cross slope, both the lRate and rRate are −2%, which means a 2% cross slope downward toward both edges. Since all road segments are represented as straight line segments or circular curve segments and full superelevations are used for some curved road surfaces only, there are two kinds of superelevation transitions in this approach: transitions between a straight line segment and a curve segment and transitions between two curve segments. For each situation, the parameters lRate and rRate of related road vertexes are adjusted to implement proper superelevation transition as required in [4].

The slope of the road surface is implemented in the road geometric model through rotation transformation. For example, for a road point with an rRate of 2%, using the centerline of the roadbed as the axis of rotation, its right side road surface will be rotated by arctg(0.02) degrees in counter of clockwise direction. Some results of the geometric models of road segments are shown in Fig. 40, and the surface slope rates are exaggerated to clearly demonstrate their impact on road surfaces.

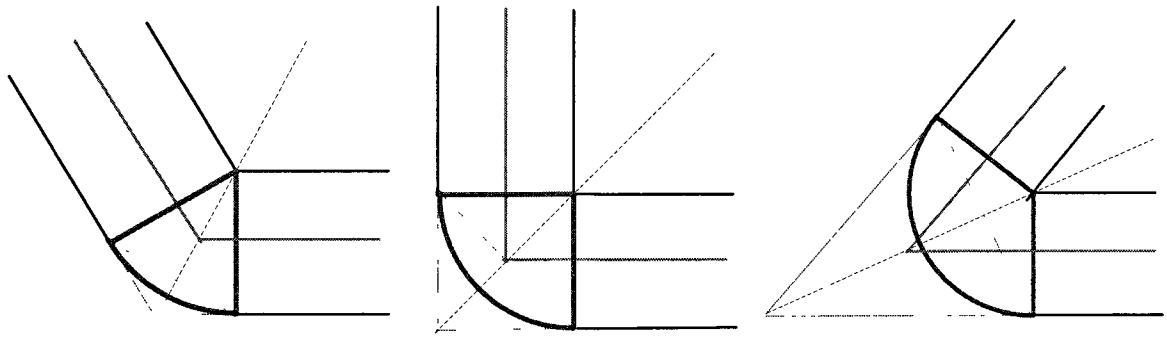

(a) (b) (c)

Fig. 39. Illustration of the generation of segment transition for two connected road segments with obtuse angle, right angle or acute angle. The segment transition is surrounded by red lines and road centerlines are denoted by blue lines. (a) Obtuse angle. (b) Right angle. (c) Acute angle.

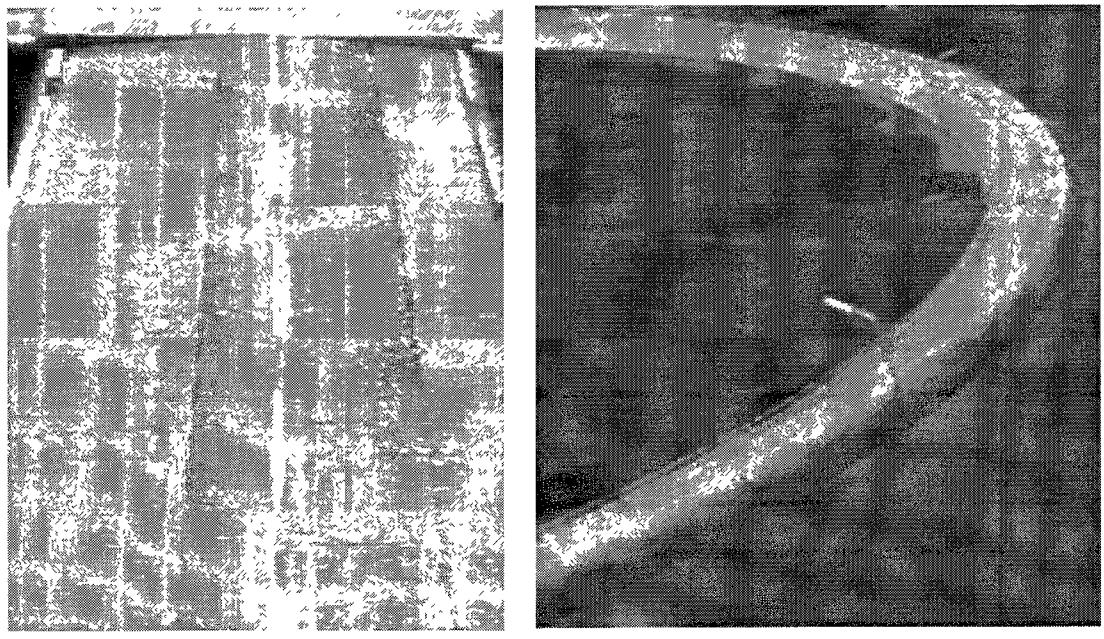

(a) (b)

Fig. 40. Geometric models of road segment. (a) Straight road segment with normal cross slope. (b) Curve road segment with full superelevation.

6.1.4 Accessorial Objects

Via procedural methods, existing 3D models, guard rail, lantern, even some common objects around the road networks such as cars, trees and billboards can be easily integrated into the final road network models according to requirements. An example of road network models with some accessorial objects is shown in Fig. 41. Besides these objects, bridges and tunnels can be modeled in this way too, and Fig. 42 gives some detailed views of generated bridge and tunnel segments.

6.1.5 Road Marking

Lane marking such as normal lines and broken lines are generated automatically based on the number of lanes using procedural modeling methods, and they are added to the road surface as textures. As shown in Fig. 43, the position and type of the lane marking are totally determined by the centerline (yellow line and point) and the number of lanes. For example, the road segment in Fig. 43(a) has two lanes, so a broken line is located on the centerline and two normal lines are placed a lane width away from the centerline. Road markings are generated with roadbed and every marking segment is represented by a rectangle consisting of two triangles in the same way the road body is represented. Moreover, all markings are lifted 0.01 meter above the road surface to prevent them from colliding with the road surface.

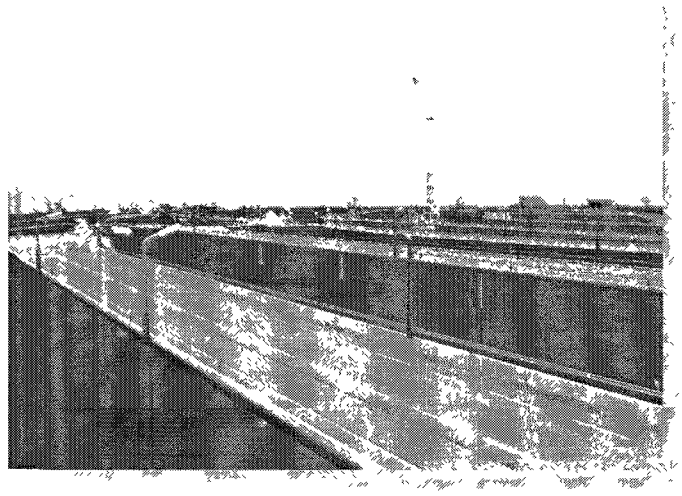

Fig. 41. Road network generated with several accessorial objects

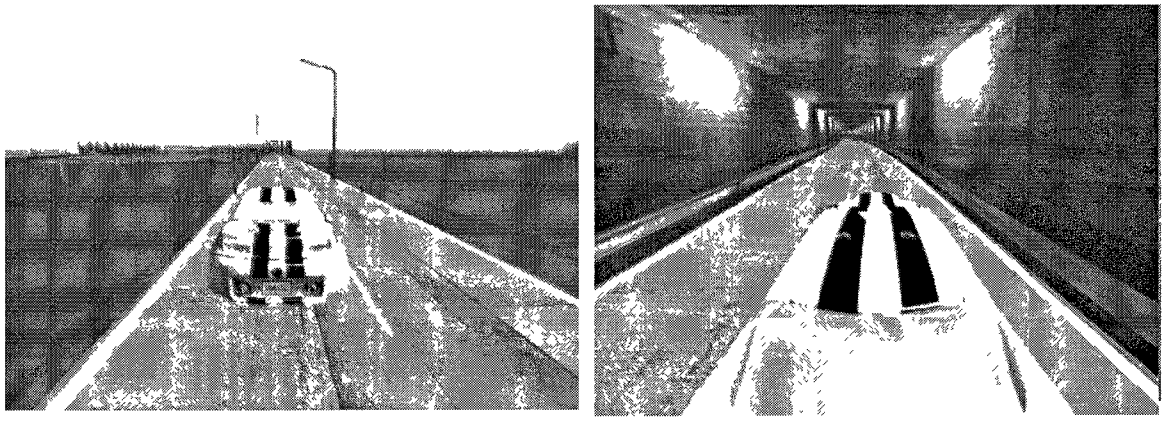

(a) (b)

Fig. 42. Detailed views of generated bridge and tunnel segments. (a) Bridge. (b) Tunnel.

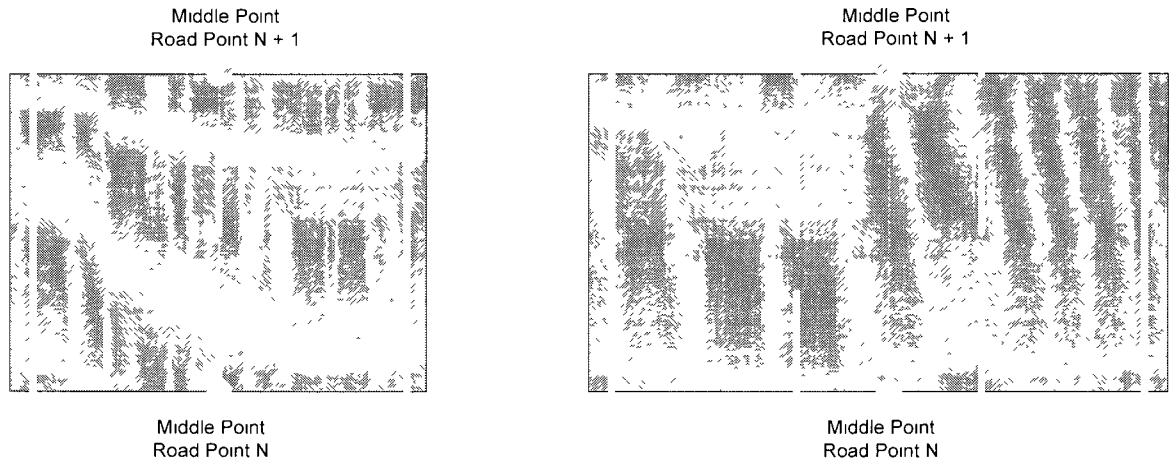

(a) (b)

Fig. 43. An illustration of the road pavement marking. (a) Two-lane road. (b) Three-lane road.

6.2 Road Intersection

The geometric models of intersections are more complex than those of road segments because of various distributions of intersection legs, i.e., different numbers and directions of connected road segments. The outline of the road intersection is composed of two parts: legs and edges between any two adjacent legs. Similar to the road segments, the shape of the leg is determined by its centerline, end position, end width, and side vector. However, to model edges between two adjacent legs, different approaches should be employed to account for different situations.

6.2.1 Normal Intersection

For normal intersections, circular curves are good enough to simulate these edges with suitable curb radii as discussed in Chapter 4. In this research, the corner radius is set

as a modifiable parameter used to generate smooth transitions between adjacent road edges in different situations. For example, as suggested by [4], radii of 7.5m or more should be provided at minor cross streets, on new construction and on reconstruction projects where space permits. Fig. 44 gives an illustration of the generation of edge curve between two adjacent intersection legs. P1 and P2 are two edge points of the ends of two adjacent intersection legs and P0 is the midpoint of the line segment connecting P1 and P2. Line segments L1 and L2 are perpendicular to their corresponding edges at P1 and P2, respectively, and intersect with the line segment L3, which is perpendicular to the line segment P1P2 at P0. The longer one of L1 and L2 is used as radius and its point of intersection with L3 is used as the center. With this result, a circular curve is produced between P1 and P2 eventually.

After the outline of the road intersection is determined, the surface of the road intersection is triangulated to represent this surface with several triangles. In this research, each intersection leg is composed by one triangle and each edge between two legs consists of ten triangles. The number of triangles is not fixed and can be changed according to the requirement of resolution.

Fig. 45 gives an illustration of the triangulation of the road intersection leg and edge. The central point where the original road node is placed is used as the common point of every triangle. Fig. 46 displays three geometric models of normal road intersections indicated by red rectangles in Fig. 34(a) and a comparison between generated results and real satellite images of the same road intersections from Google Maps is given in Fig. 47.

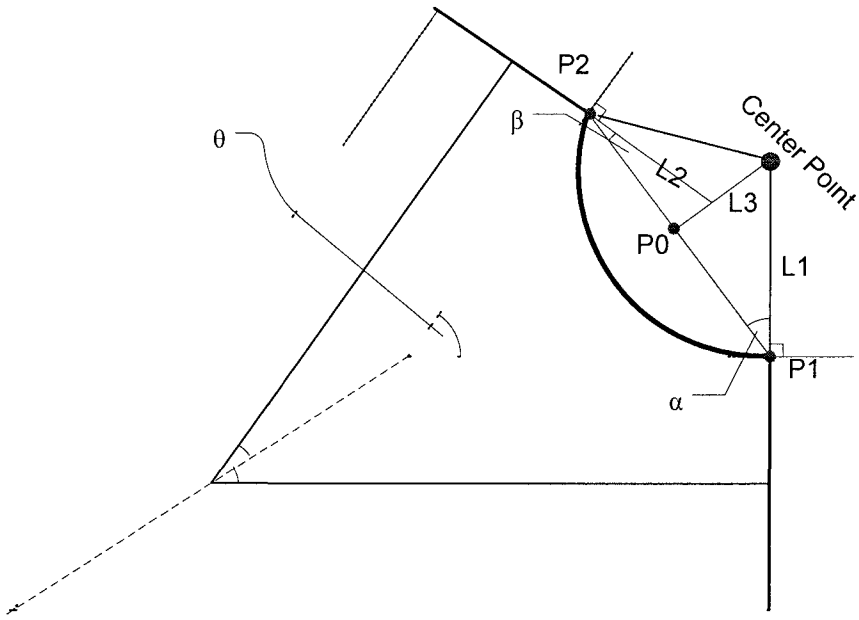

Fig. 44. An illustration of the generation of edge curve between two adjacent intersection legs

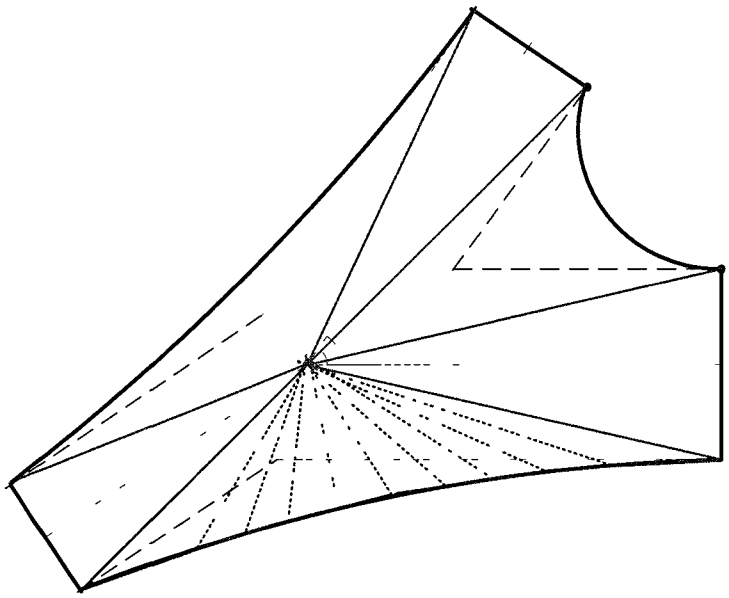

Fig. 45. An illustration of the triangulation of road intersection

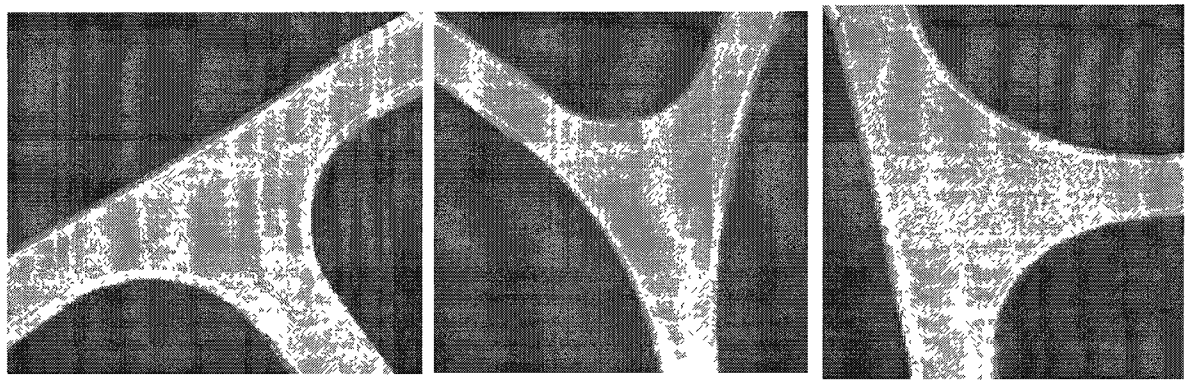

(a) (b) (c)

Fig. 46. Geometric models of normal road intersection indicated by red rectangle in Fig. 34(a)

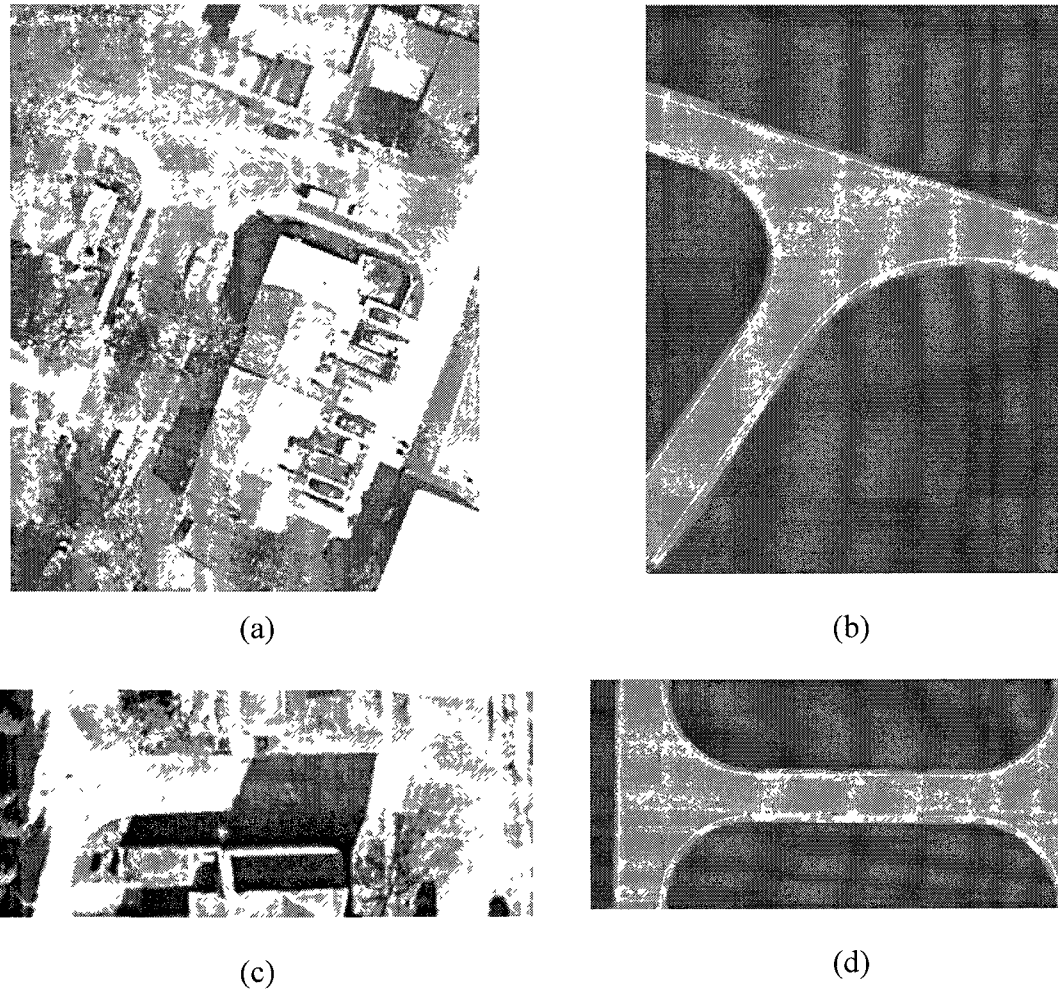

(a) (b)

(c) (d)

Fig. 47. Comparison between generated result (right) and real satellite image (left) of the same road intersections from Google Maps

6.2.2 Merging/Diverging Intersection

As discussed before, two design models are provided for modeling a merging/diverging intersection: Parallel design and tapered design [4]. The parallel design includes additional auxiliary lanes in the merged legs while straight lines are used to represent the taper in the tapered design. Also normal white lines are used to mark the outline of the road intersection and two kinds of broken white lines are utilized to reflect lane channelization. Fig. 48 shows results for each kind of merging/diverging intersection designs and more results are shown in Fig. 49.

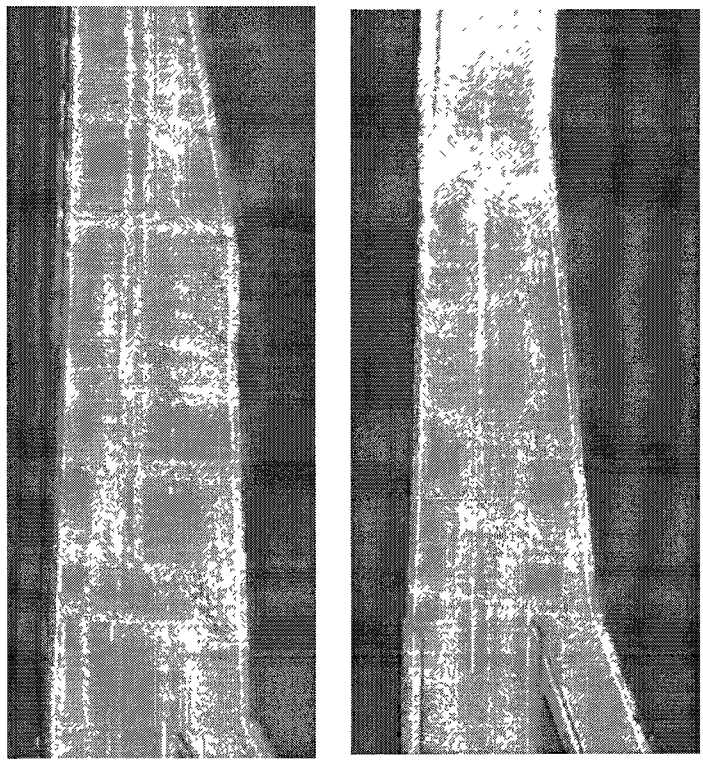

(a) (b)

Fig. 48. Modeling results of these two kinds of merging/diverging intersection designs as shown in Fig. 15. (a) Parallel design (b) tapered design

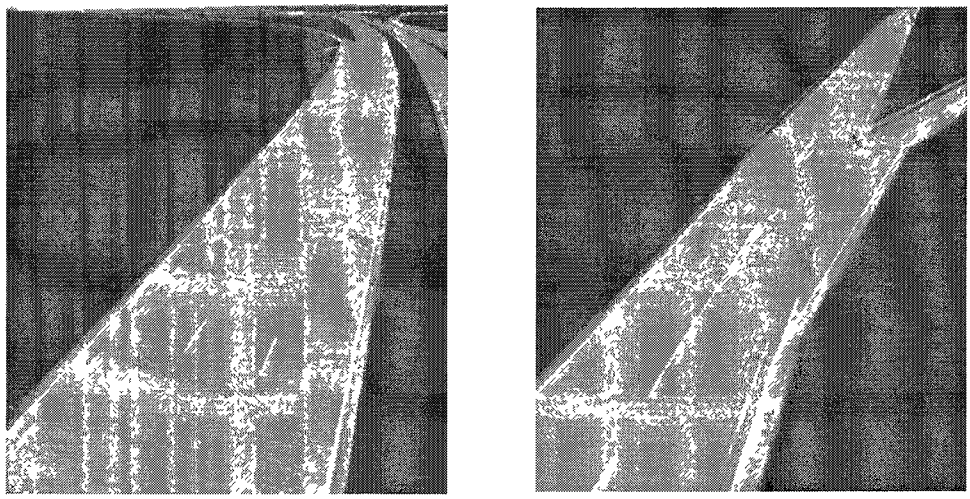

(a) (b)

Fig. 49. More results of road intersection modeling

6.3 Road Surface Rendering

Geometric modeling of the road network only generates the geometry of the roadways. To satisfy the needs of high fidelity simulations, the visual aspects of the roadways must be generated as well.

Road surfaces contain different types of pavements such as asphalt and concrete. Several methods can be used to render the road surface (pavements), which are texture mapping, programmable pixel shaders, and programmable vertex shaders. Texture mapping makes use of a large set of pre-collected textures that are images of different types of road surfaces with varied conditions, and it maps the textures to road surfaces. As shown in Fig. 50, different textures can be used conveniently to render varied road surfaces. Normal textures are also used in texture mapping to further enhance the 3D realism of the road surface by artificially modifying the normals (orientations) of the road surface.

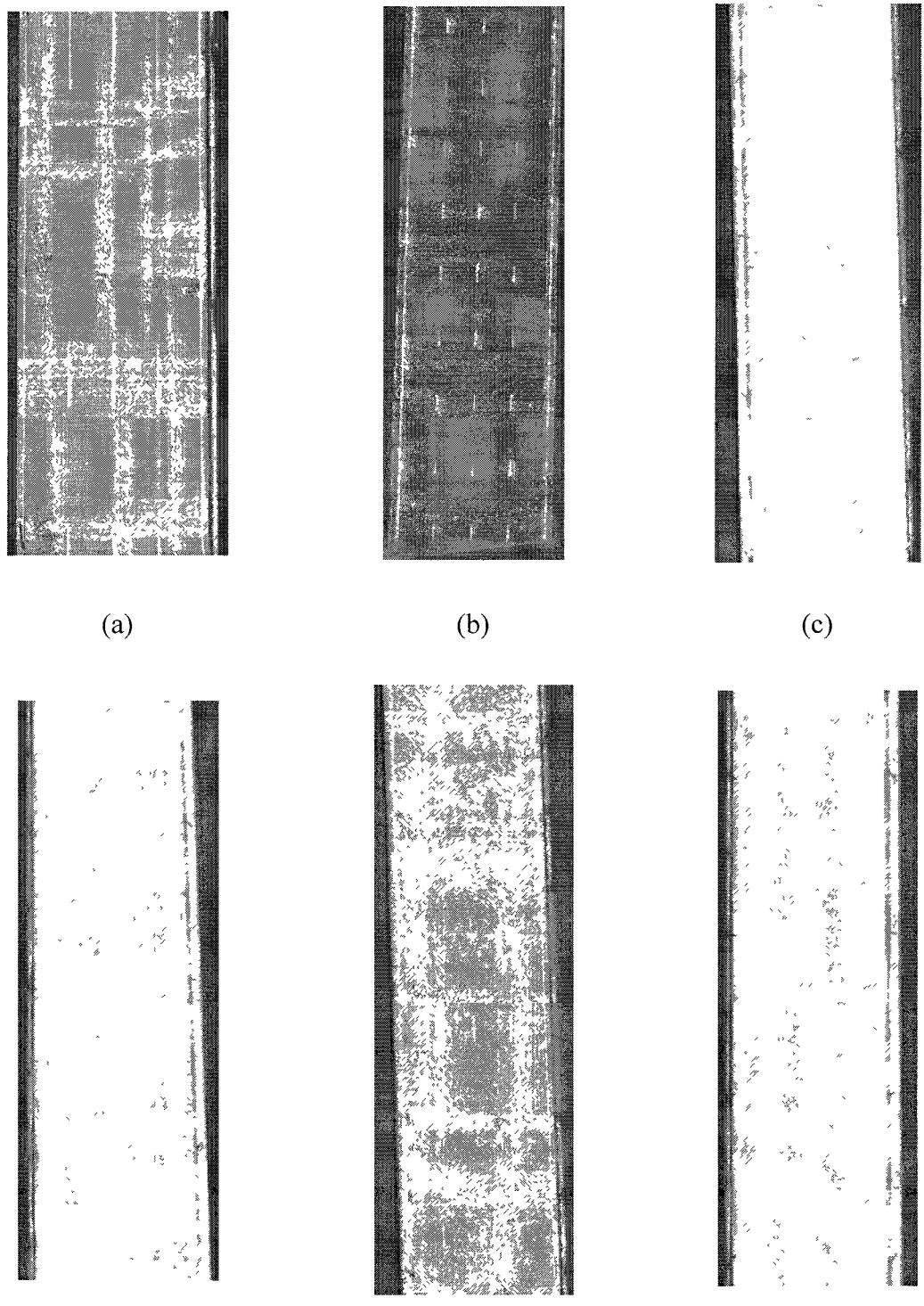

(a) (b) (c)

(d) (e) (f)

Fig. 50. Road segment rendered with different textures

CHAPTER 7

IMPLEMENTATION, RESULTS AND DISCUSSIONS

This chapter describes the implementation of the whole system, gives some experimental results and discusses some existing problems.

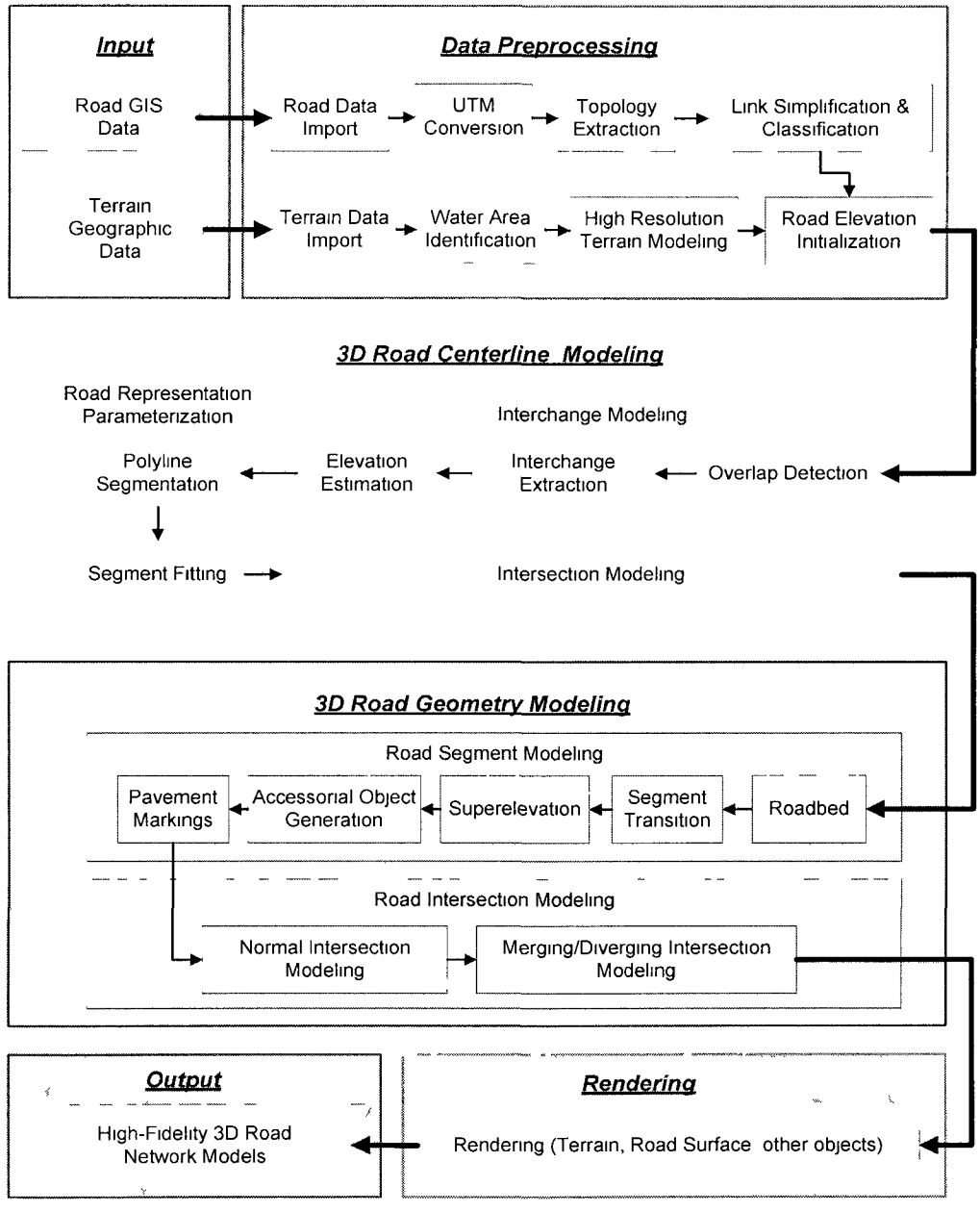

Fig. 51. System architecture

7.1 Implementation and Results

The overall system architecture of the proposed method in this dissertation research is summarized in Fig. 51. Through data preprocessing, 3D road centerline modeling and 3D road geometry modeling, high-fidelity 3D road network models are synthesized from the input 2D road GIS data and terrain geographic data.

For each phase shown in Fig. 51, the representation of the road network changes and adapts to facilitate data processing and synthesis. Fig. 52 shows the evolution of road network data structure. In the original raw road GIS data, the centerline of the road network consists of several polylines, and discrete road points are stored in these polylines sequentially. After data preprocessing, the topology of the road network is extracted and the whole road network is organized in the form of a graph composed of two new road structures: road links and road nodes. Road links are evolved from road polylines and road nodes represent the junction of two or more road links. During 3D road centerline modeling, road links are segmented and fitted into two analytic forms: straight lines and circular curves, and road nodes are extended into road intersections made of an intersection center point and several intersection legs. Then in the 3D road geometry modeling phase, road segments and road intersections are further processed and more complex data structures are used to represent them. For each road segment, a roadbed is generated from parametric road segment centerline; segment transition is synthesized between two segments if needed; accessory road parts such as lantern and guard rail are attached and road pavement marking is placed on the road surface. For road

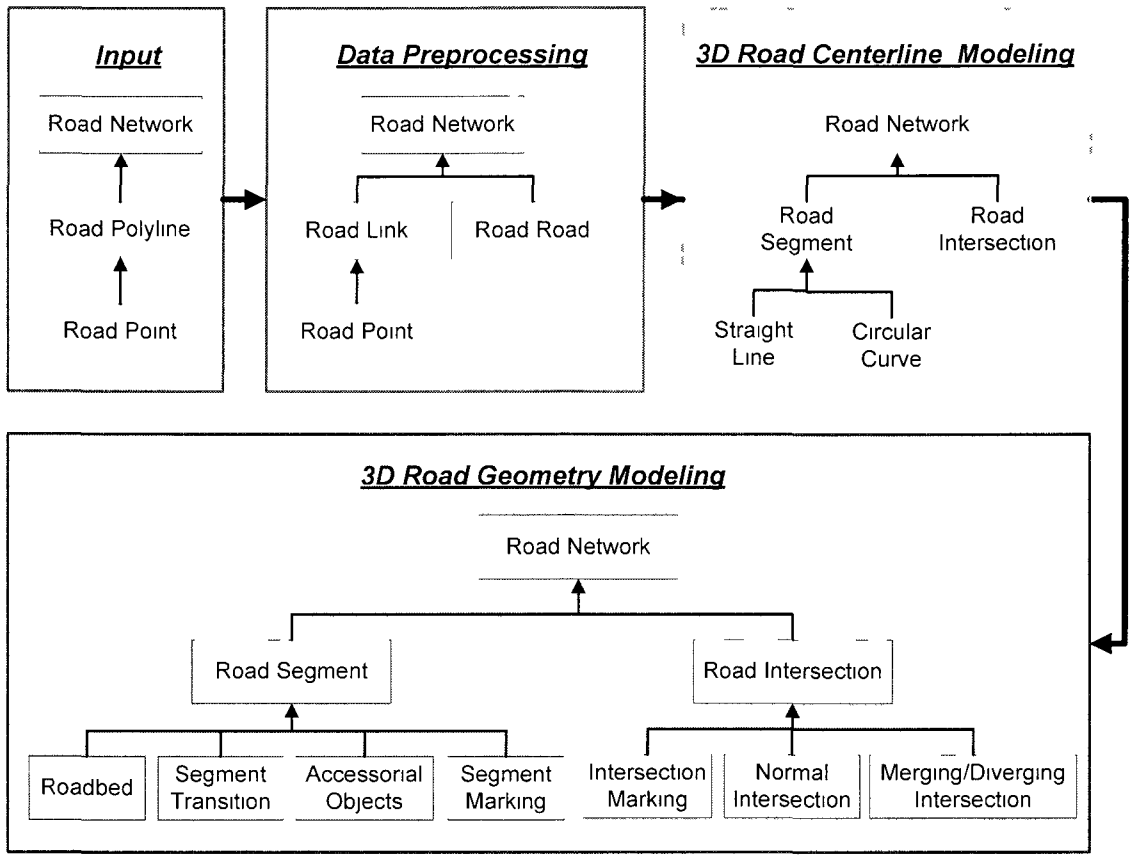

Fig. 52. Evolution of road network data structure

intersections, two kinds of road intersection models are used and road markings are created accordingly, too.

The proposed method was implemented on the Microsoft XNA platform [56] and the whole road network was created based on GIS data automatically using the proposed method and rendered with various shaders. Comparisons between generated traffic interchange models and their corresponding satellite images from top view and side view are shown in Fig. 53 and Fig. 54, and more detailed views of generated models are given in Fig. 55. Fig. 56 gives two examples of road network where different 3D road structures

are generated from the same 2D road data without changing the connection information of this road network. Both these two examples are from the interchange displayed in Fig. 18 and as shown in Fig. 56, all overlapped road segments are placed reasonably Adjacent road segments have the same elevation level so that their corresponding overlapped road segments can extend over or under them smoothly.

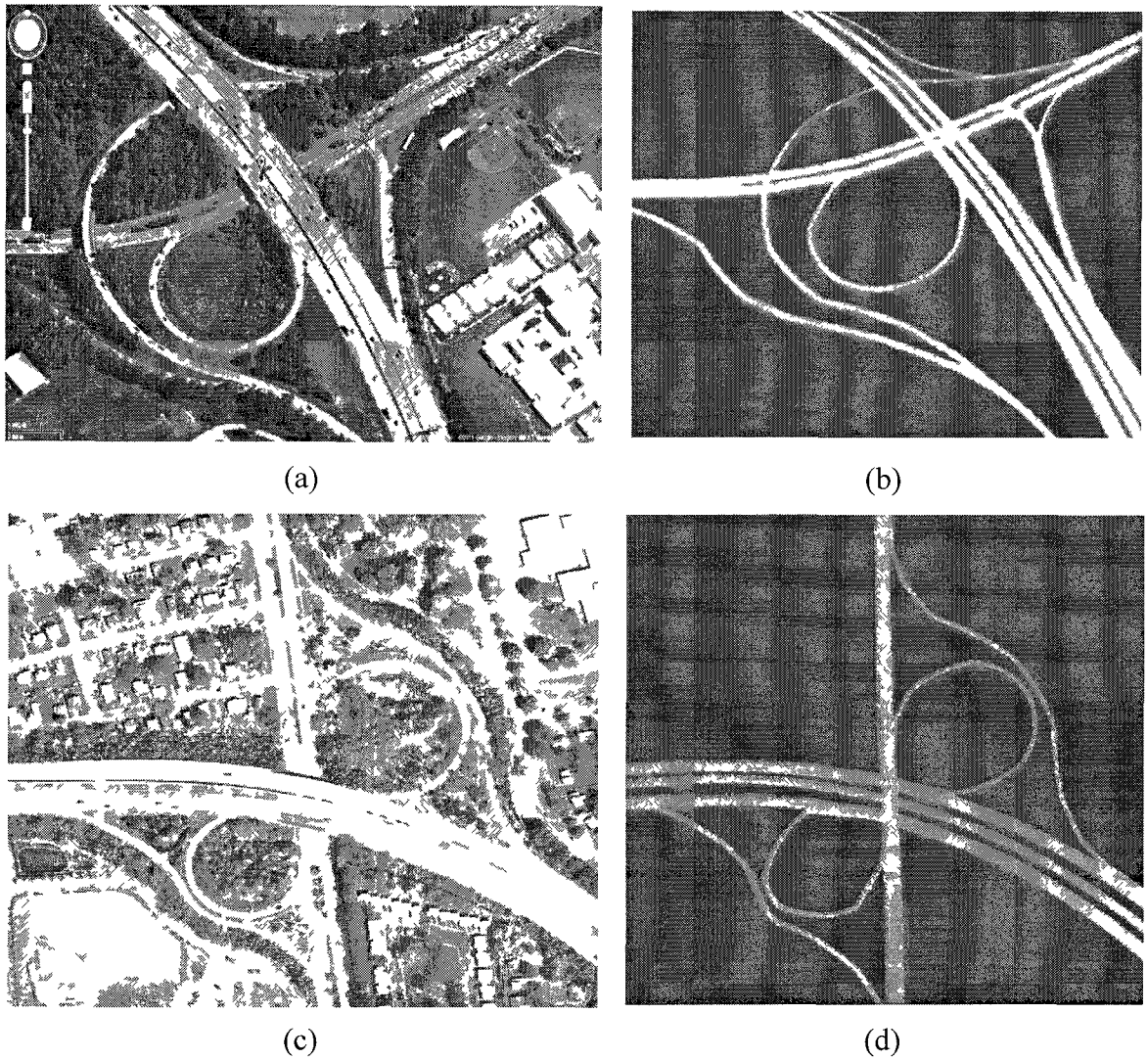

(a) (b)

(c) (d)

Fig. 53. Top view of the whole generated models of two traffic interchanges (right) and their corresponding satellite image from Google Maps (left)

(a)

(b)

Fig. 54. A comparison of the real traffic interchange image and modeling result for an interchange between I-264 and N Military highway, Virginia. (a) Street view image from Google Maps. (b) Modeling result of the corresponding GIS data.

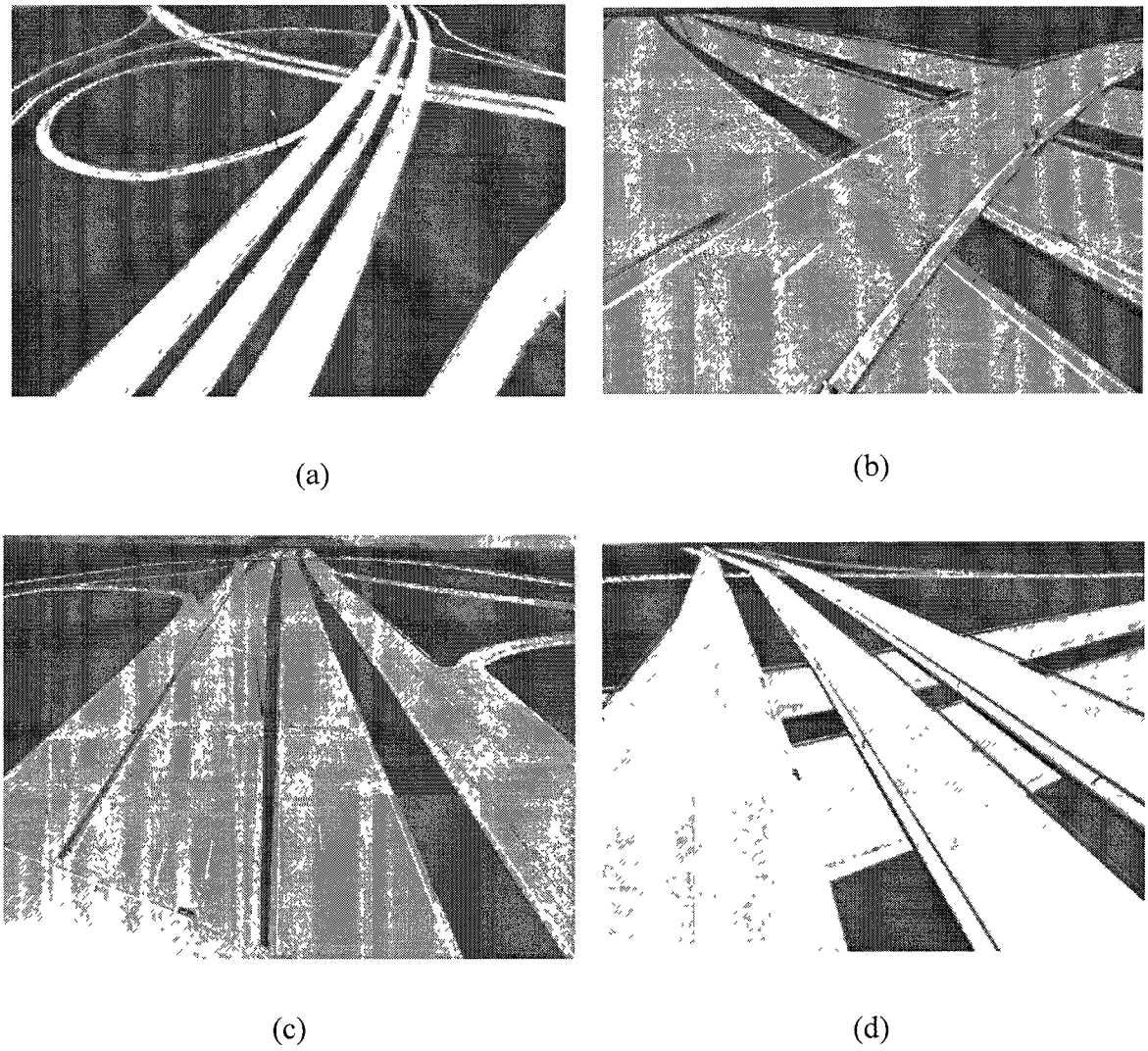

(a) (b)

(c) (d)

Fig. 55. More detailed views of 3D road models generated using the proposed method

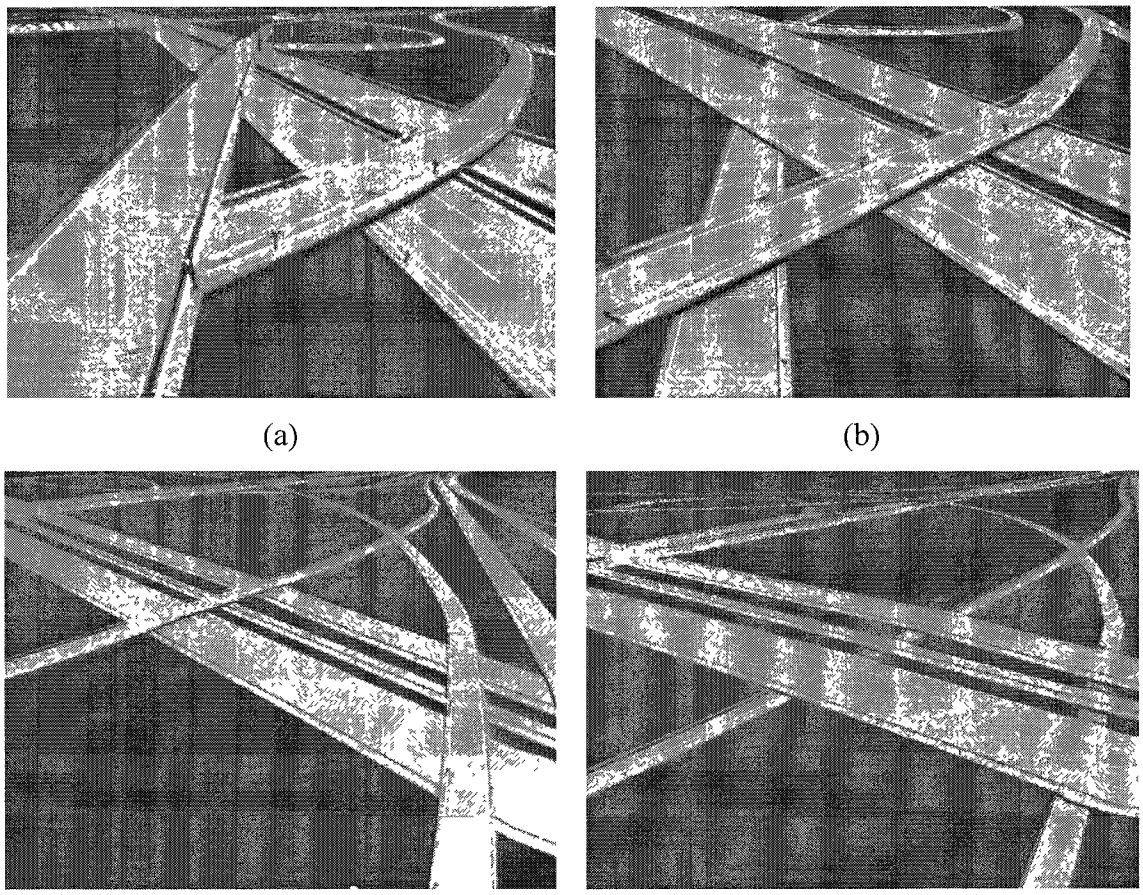

(a) (b)

(c) (d)

Fig. 56. Two examples of road network where different 3D road structures are generated from the same 2D road data

Furthermore, in order to improve the visual effect of the environment around the road network, different rendering methods are utilized to render the surrounding environment, such as terrain and ocean. As shown in Fig. 57, satellite image can be combined with digital terrain elevation and GIS road data in this system through texture mapping. After water areas are identified, an existing water rendering approach [57] was adopted by this research to generate realistic results using programmable shaders. Fig. 58(b) shows a scaled rendering result for the area indicated by the red rectangle in Fig. 58(a).

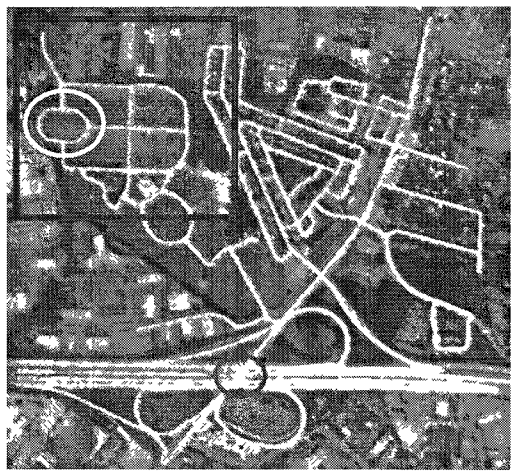

(a)

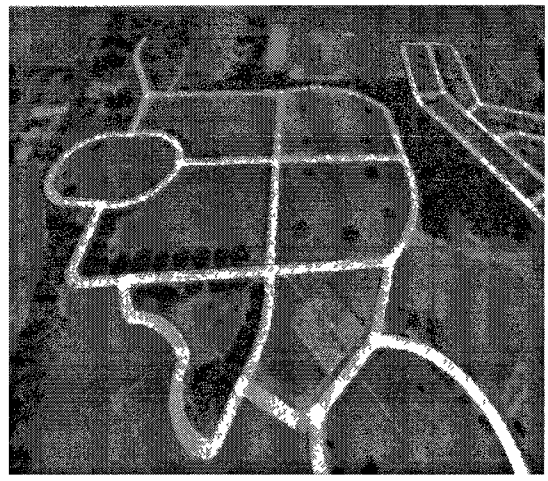

(b)

(c)

(d)

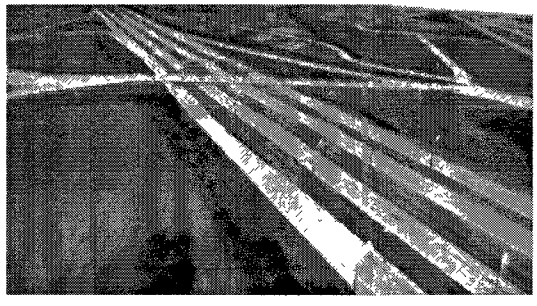

(e)

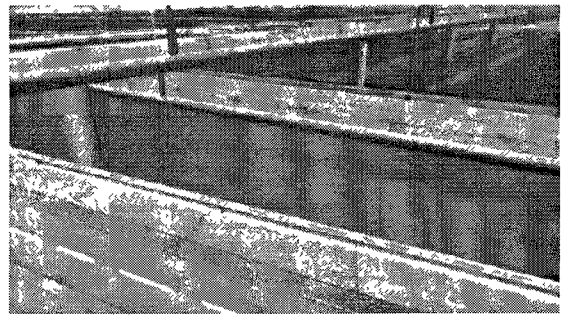

(f)

Fig. 57. Experimental results and comparison. (a) 3D road network generated for the road network shown in Fig. 6. (b) Top view of the area indicated by the red rectangle in (a). (c) Side view of the area indicated by the yellow circle in (a). (d)(e)(f) Different views of the interchange part of the generated 3D road network model.

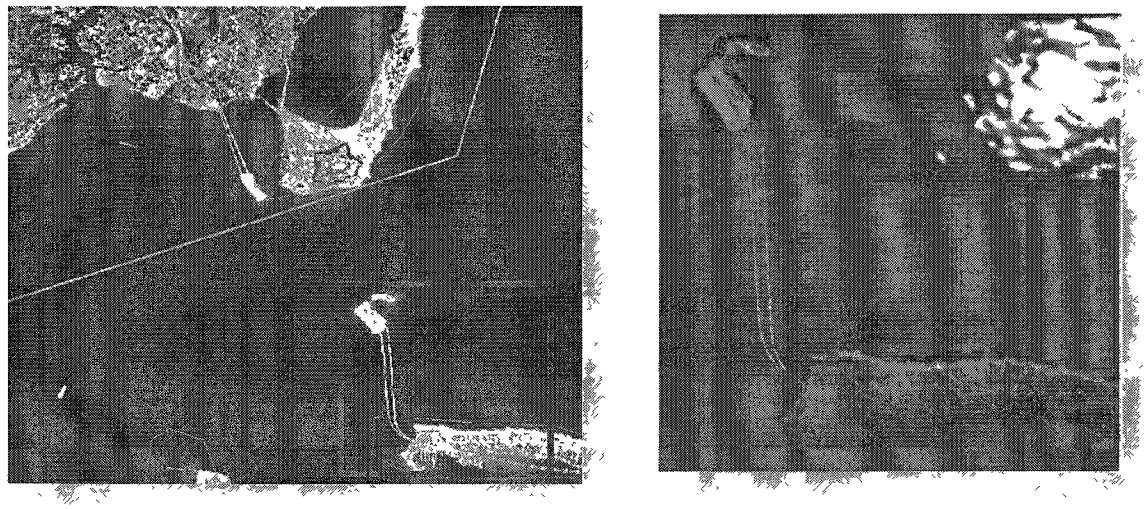

(a) (b)

Fig. 58. An example of the terrain and water rendering for the Hampton Roads Bridge Tunnel in Norfolk, Virginia. (a) Satellite image. (b) Scaled rendered result of the area indicated by red rectangle in (a).

7.2 Discussions

Although civil engineering principles are emphasized in this dissertation research, it is important to note that we do not aim at generating a product that can be used for real road design and construction. Instead the intended audience and users of the proposed work are professionals in the modeling and simulation industry, computer and video game industry, and other computer graphics applications that require realistic roadway models. The purpose is to provide rapid and efficient 3D road modeling for such applications that have higher requirements on high-fidelity road models, such as racing games and driving simulations. As such, not all civil engineering rules on road design are utilized in the proposed work. Since the road surface is the most significant feature of a road, principles and rules on road surface design are of ultimate importance in this

dissertation research. It is also important to note that existing road GIS data do not provide complete information that is needed to generate 3D road models from the GIS data; for example, without elevation (height) information, it is difficult to determine the relative vertical locations of different ramps at a highway interchange. In addition, some existing roads actually do not conform to the design standards (especially some old roads in urban areas). Considering all these factors, although the 3D road models to be produced by the proposed method are still approximations of real roadways, they will have enough fidelity and resolution that are required by high-end modeling and simulation applications.

Since this research is based on 2D road GIS data, errors or missing information in the GIS data affect the results of the proposed method and can cause some serious problems. In the following, we discuss several issues of the road GIS data encountered in this research.

1) The position of centerline is not sufficiently accurate for some parallel road segments, so if these road segments are modeled based on the real number of lanes, they may collide with each other. As shown in Fig. 59, contrary to real a situation where these two road segments are parallel and separated by a median, the edges of these two modeled road segments collide with each other in the middle.
2) In some cases, two parallel roads with different directions are combined into one road polyline in the raw road GIS data. As show in Fig. 60, two traverse roads are represented by just one road polyline in the raw road GIS data.

3) For some places, the road network recorded in raw road GIS data is significantly different from the situation shown in the corresponding satellite image, as exhibited in Fig. 61. This may be caused by new construction; however, obviously it is hopeless to get the same road model as the one shown in a satellite image from such GIS road data.

(a)

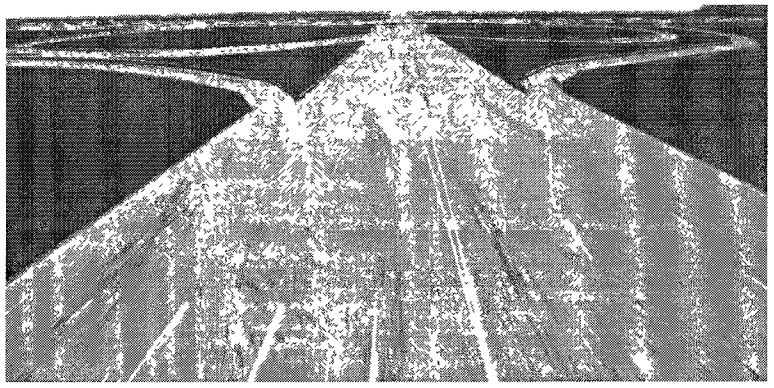

(b)

Fig. 59. An example of the road GIS data without enough accuracy for a traffic interchange in Norfolk, Virginia. (a) The satellite image of this interchange (b) Corresponding generated road segment models colliding with each other

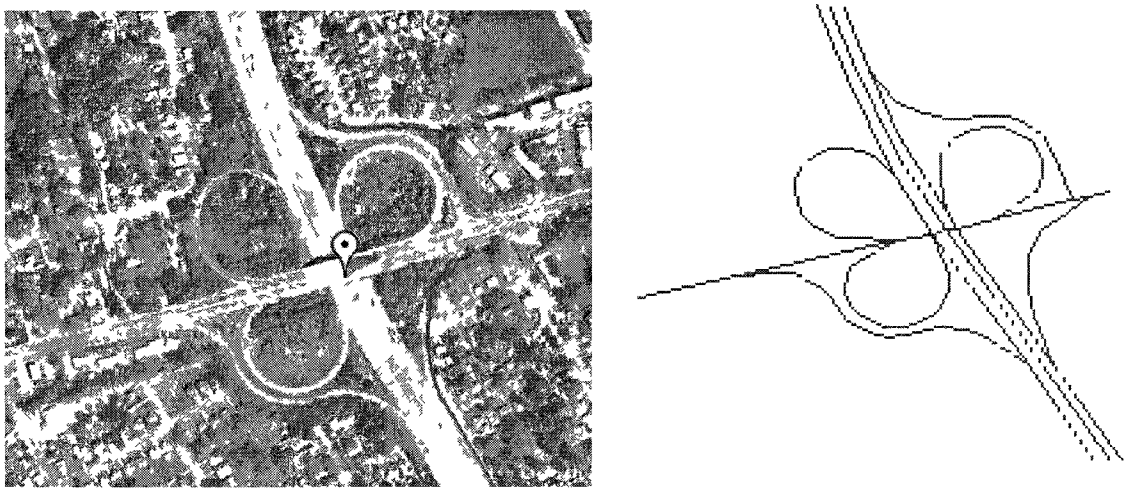

(a) (b)

Fig. 60. An example of road GIS data in which two parallel roads are combined into one road polyline. (a) The satellite image of this interchange (b) Corresponding road GIS data displayed in ArcGIS

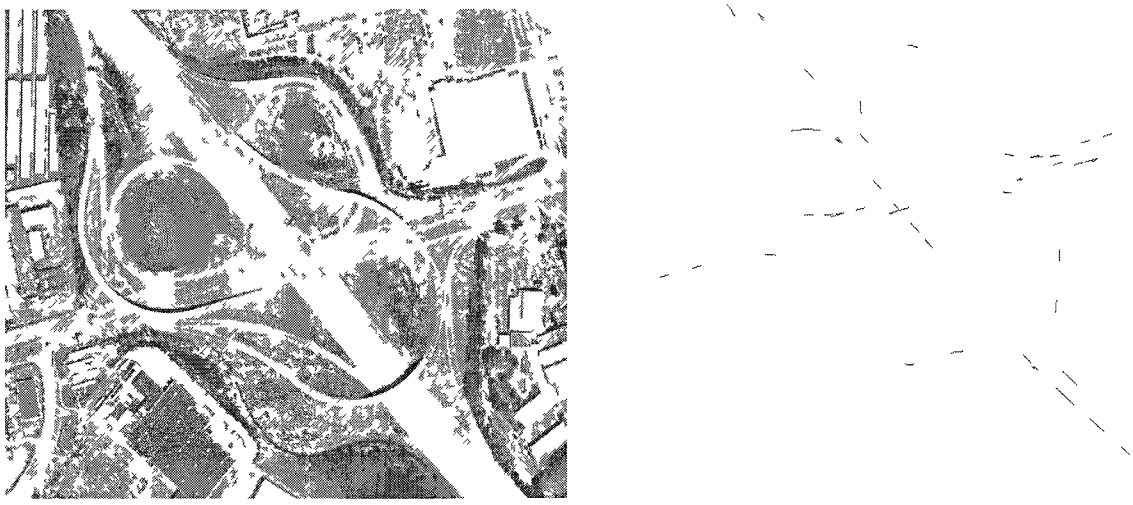

(a) (b)

Fig. 61. An example of road GIS data in which the contained road network is significantly different from the real situation

4) In this research, the overlapped position is identified basing upon an assumption that if there is a road node, there is an intersection. Although for most situations this assumption is correct, some exceptions exist in traffic interchange data as shown in Fig. 62. A road node is placed improperly at the position where two road segments overlapped with each other in raw GIS data and wrong topological information is extracted and used to generate the road network model.

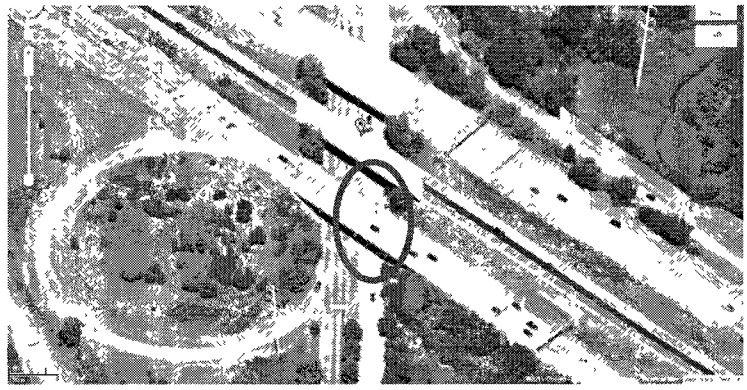

(a)

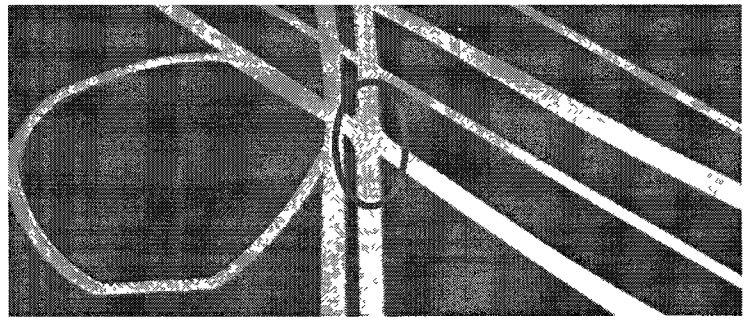

(b)

Fig. 62. An example of road GIS data containing unusable intersection information from an interchange in Norfolk, Virginia. (a) The satellite image of this interchange (b) Corresponding generated model with improper intersection at the place indicated by the red ellipse

CHAPTER 8

CONCLUSION AND FUTURE WORK

This dissertation proposed a method for automatically generating 3D high-fidelity road network models from 2D road GIS data based on carefully selected civil engineering rules for road design and construction. The proposed method consists of several major components, including data preprocessing, 3D centerline modeling, and 3D geometry modeling. The proposed method is especially innovative in traffic interchange modeling by developing several algorithms for overlapped positions identification, interchanges clustering, elevation level determination, and intersection modeling. Many applications, especially the ones that have stringent requirements on high fidelity road networks, can take advantage of the proposed method and the existing vast amount of road GIS data to automatically generate 3D road networks rapidly. Furthermore, with proper modifications, this proposed method can be extended to other areas, such as automatic generation of 3D subway system based on 2D subway maps.

While the results produced by this dissertation research demonstrated the usefulness and potential of the proposed method, more research can be conducted in the future to further enhance the proposed method. The road GIS data utilized by this research only contained information about the positions of the road centerline, limiting the realism of the produced 3D road network. If new road GIS data that contain more information (such as land width and road direction) become available, better results can be obtained with minor modification of the proposed method. Besides straight line and circular curve, more parametric curves such as B-spline, Hermite curve or Cubic curve can be added into the existing program to provide more flexible shape of road segment.

Also in the current proposed method, the road surface is rendered via texture mapping and normal mapping. The geometry of the road surfaces can be further modified to reflect the variations on the road surface by adjusting vertex positions using programmable vertex shaders, which do not use pre-collected textures and generate pixels representing the road surfaces on the fly with carefully designed computer algorithms. For instance, subtle variations of the road surface can be achieved by applying Perlin Noise in terrain modeling as discussed earlier, and significant changes of the road conditions can be obtained through addition of holes to the road surface. The current implementation of the proposed method is fully automated without any user interactions. Sometimes, it is desirable to provide the user with control of some of the parameters of the algorithms. Thus, an interactive user interface for editing and selecting algorithm configurations would be beneficial. Furthermore, if generated road network models from this research are exported as common model files (.obj file, .3ds file, etc.), they can be directly used by some popular 3D modeling software such as Maya and 3D Max as good prototypes for further modification. Compared with generating road models from scratch, numerous manual efforts will be saved by this extension.

REFERENCES

[1] Autodesk, "Autodesk Maya," in *http://usa.autodesk.com/maya/*, 2011.

[2] Autodesk, "Autodesk 3ds Max Products," in *http://usa.autodesk.com/3ds-max/*, 2011.

[3] D. S. Ebert, F. K. Musgrave, D. Peachey, K. Perlin, and S. Worley, *Texturing and modeling: a procedural approach.* San Francisco, CA: Morgan Kaufmann, 2003.

[4] American Association of State Highway and Transportation Official (AASHTO), *A policy on geometric design of highways and streets.* Washington, D.C, 2004.

[5] California Department of Transportation, "Highway design manual from CA," in *http://www.dot.ca.gov/hq/oppd/hdm/hdmtoc.htm*, 2008.

[6] Federal Highway Administration, U.S. Department of Transportation, *Standard highway signs and markings (SHSM)*, 2004.

[7] Federal Highway Administration, U.S. Department of Transportation, *Manual on uniform traffic control devices (MUTCD)*, 2009.

[8] D. Costakis and J. E. Mitchell, "Rapid development of road elevation data to support hurricanes Katrina and Rita operations," Gainesville, FL, 2005.

[9] Presagis, "Creator " in *http://www.presagis.com/*, 2011.

[10] G. Ochoa, "An introduction to Lindenmayer systems," in *http://www.biologie.uni-hamburg.de/b-online/e28_3/lsys.html*, 1998.

[11] Y. I. H. Parish and P. Muller, "Procedural modeling of cities," in *Proceedings of the 28th annual conference on Computer graphics and interactive techniques*, Los Angeles, CA, USA, 2001, pp. 301-308.

[12] J. Sun, X. Yu, G. Baciu, and M. Green, "Template-based generation of road networks for virtual city modeling," in *Proceedings of the ACM symposium on Virtual reality software and technology*, Hong Kong, China, 2002, pp. 33-40.

[13] J. Sun, G. Baciu, X. Yu, and M. Green, "Image-based template generation of road networks for virtual maps," *International Journal of Image and Graphics,* vol. 4, pp. 701-720, 2004.

[14] T. Lechner, B. A. Watson, U. Wilensky, and M. Felsen, "Procedural city modeling," in *1st Midwestern Graphics Conference*, 2003.

[15] T. Lechner, P. Ren, B. Watson, C. Brozefski, and U. Wilenski, "Procedural modeling of urban land use," in *ACM SIGGRAPH 2006 Research posters* Boston, Massachusetts: ACM, 2006.

[16] K. R. Glass, C. Morkel, and S. D. Bangay, "Duplicating road patterns in south African informal settlements using procedural techniques," in *Proceedings of the 4th international conference on Computer graphics, virtual reality, visualization and interaction in Africa*, Cape Town, South Africa, 2006, pp. 161-169.

[17] G. Chen, G. Esch, P. Wonka, P. M¨uller, and E. Zhang, "Interactive procedural street modeling," *ACM Transactions on Graphics (TOG) - Proceedings of ACM SIGGRAPH 2008,* vol. 27, August 2008.

[18] B. E. Artz, "An analytical road segment terrain database for driving simulation," in *1995 Driving Simulation Conference*, 1995, pp. 274–284.

[19] R. R. Mourant and S. Marangos, "A virtual environments editor for driving scenes," in *Proceedings of the International Conference on Computer, Communication and Control Technologies*, Orlando, Florida, 2003, pp. 379–384.

[20] A. Kaussner, C. Mark, H.-P. Krüger, and H. Noltemeier, "Generic creation of landscapes and modeling of complex parts of road networks," in *Proceedings of the Driving Simulator Conference*, Paris, 2002.

[21] C. Mark, A. Kaußner, M. Grein, and H. Noltemeier, "Dynamically changing road networks – modelling and visualization in real time " in *Computational Science and Its Applications – ICCSA 2004*. vol. 3044: Springer Berlin / Heidelberg, 2004, pp. 843-853.

[22] S. Donikian, "Vuems: a virtual urban environment modeling system," in *Computer Graphics International 1997 (CGI'97)*, 1997, pp. 84–92.

[23] G. Thomas and S. Donikian, "Modelling virtual cities dedicated to behavioural animation," *Computer Graphics Forum,* vol. 19, pp. 71-80, 2000.

[24] H. Wang, J. Kearney, and K. Atkinson, "Robust and efficient computation of the closest point on a spline curve," in *5th international conference on Curves and Surfaces*, 2002, pp. 397–406.

[25] H. Wang, J. Kearney, and K. Atkinson, "Arc-length parameterized spline curves for real-time simulation," in *5th international conference on Curves and Surfaces*, 2002, pp. 387-396.

[26] H. Wang, "Efficient roadway modeling and behavior control for real-time simulation," Ph.D. dissertation: The University of Iowa, Iowa City, IA, USA, 2005, p. 126.

[27] H. Wang and J. K. Kearney, "A parametric model for oriented, navigable surfaces in virtual environments," in *2006 ACM international conference on Virtual reality continuum and its applications*, 2006, pp. 51-57.

[28] P. Willemsen, J. K. Kearney, and H. Wang, "Ribbon networks for modeling navigable paths of autonomous agents in virtual environments," *IEEE Transactions on Visualization and Computer Graphics,* vol. 12, pp. 331-342, May-June 2006.

[29] O. Achal and R. M. Ronald, "Use of splines in creating flexible virtual environments," in *ACM SIGGRAPH 2006 Research posters* Boston, Massachusetts: ACM, 2006.

[30] A. Werner, O. Deussen, J. Döllner, H. C. Hege, P. Paar, and J. Rekittke, "Lenné3D - walking through landscape plans," in *Trends in real-time landscape visualization and participation*, Berlin: Wichmann, 2005, pp. 48–59.

[31] S. Ernst, "Inside Biosphere3D - the free digital globe from a developer prospect," in *http://www.fossgis.de/w/images/5/50/InsideBiosphere3D_SteffenErnst.pdf*, 2011.

[32] E-on Software, "Vue 8 - digital nature," in *http://www.e-onsoftware.com/*, 2011.

[33] CommunityViz, "CommunityViz," in *http://placeways.com/*, 2011.

[34] Bentley, "Bentley," in *http://www.bentley.com/en-US/*, 2011.

[35] MultiGen-Paradigm, "Creator road tools," in *http://www.multigen-paradigm.com*, 2011.

[36] D. F. Evans, "High-fidelity roadway modeling for real-time driving simulation." Master thesis: The University of Iowa, 1995.

[37] O. Deusen, D. S. Ebert, R. Fedkiw, F. K. Musgrave, P. Prusinkiewicz, D. Roble, J. Stam, and J. Tessendorf, "The element of nature: interactive and realistic techniques," in *SIGGRAPH 2004 course 31*, 2004.

[38] B. B. Mandelbrot, *The fractal geometry of nature*: Holt, Henry & Company, Inc., 1982.

[39] H. Zhou, J. Sun, G. Turk, and J. M. Rehg, "Terrain synthesis from digital elevation models," *IEEE Transactions on Visualization and Computer Graphics,* vol. 13, pp. 834-848, July/Aug 2007.

[40] A. Fournier, D. Fussell, and L. Carpenter, "Computer rendering of stochastic models," *Communications of the ACM,* vol. 25, pp. 371-384, June 1982.

[41] G. S. P. Miller, "The definition and rendering of terrain maps," in *Proceedings of the 13th annual conference on Computer graphics and interactive techniques*, 1986, pp. 39-48.

[42] K. Perlin, "An image synthesizer," in *Proceedings of the 12th annual conference on Computer graphics and interactive techniques*, San Francisco, 1985, pp. 287-296.

[43] Environmental Systems Research Institute, Inc. (ESRI), "ESRI shapefile technical description," in *An ESRI White Paper*, 1998.

[44] Environmental Systems Research Institute, Inc. (ESRI), "ArcGIS: a complete integrated system," in *http://www.esri.com/software/arcgis/index.html*, 2011.

[45] Shapefile C Library, "Shapelib," in *http://shapelib.maptools.org/*, 2011.

[46] P. H. Dana, "Coordinate systems overview," in *http://www.colorado.edu/geography/gcraft/notes/coordsys/coordsys.html*, 2011.

[47] S. Dutch, "Converting latitude and longitude to UTM," in *http://www.uwgb.edu/dutchs/usefuldata/utmformulas.htm* Natural and Applied Sciences, University of Wisconsin - Green Bay, 2003.

[48] Geography & Geology, University of Wisconsin Stevens Point, "Dig deeper into locational systems: the universal transverse Mercator (UTM) grid," in *http://www.uwsp.edu/geo/faculty/ritter/geog101/textbook/essentials/digging_deeper_UTM.html*, 2011.

[49] S. K. Jakkula, Y. Shen, and J. Sokolowski, "Extraction of road network topology for transportation and GIS applications," in *MODSIM World Conference & Expo* Virginia Beach, VA, 2007.

[50] USGS, "The national map seamless server," in *http://seamless.usgs.gov/*, 2010.

[51] Microsoft, "Bing map," in *http://www.bing.com/maps/*, 2011.

[52] Google, "Google map," in *http://maps.google.com/maps?q=*, 2011.

[53] J. Wang, O. Unal, M. Cetin, Y. Shen, and Y. Papelis, "High-fidelity roadway modeling and simulation," in *MODSIM World Conference & Expo 2009* Virginia Beach, VA, 2009.

[54] W. Mendenhall and T. L. Sincich, *Statistics for engineering and the sciences (4th Edition)*. Denver: Pearson Education, 1995.

[55] W. Gander, G. H. Golub, and R. Strebel, "Least-squares fitting of circles and ellipses," *BIT Numerical Mathematics,* vol. 34, pp. 558-578, 1994.

[56] Microsoft, "XNA," in *http://www.xna.com/*, 2011.

[57] K. Hayward, "Water game component," in *http://graphicsrunner.blogspot.com/2008/11/water-game-component.html*, 2008.

VITA

Ms. Jie Wang

Education Background

- Ph.D. in Modeling & Simulation (Aug. 2011), Department of Modeling, Simulation and Visualization Engineering, Old Dominion Univ., Norfolk, VA, USA

  M.E. in Computer Science & Technology (Mar. 2008), Institute of Computing Technology, Chinese Academy of Science, Beijing, China

  B.S. in Information and Computing Science (July 2004), Beijing Jiaotong Univ., Beijing, China

Publications

J. Wang and Y. Shen, "Automatic 3D High-Fidelity Traffic Interchange Modeling Using 2D Road GIS Data," *IS&T/SPIE Electronic Imaging*, 6 pages, (San Francisco, CA), January 2011.

J. Wang and Y. Shen, "GIS Data Based Automatic High-Fidelity 3D Road Network Modeling," *MODSIM World Conference & Expo 2010*, 8 pages, (Hampton, VA), October 2010.

J. Wang, O Unal, M. Cetin, Y. Shen, and Y. Papelis, "High-Fidelity Roadway Modeling and Simulation," *MODSIM World Conference & Expo 2009*, 6 pages, (Virginia Beach, VA), October 2009.

J. Wang, O. Unal, M. Cetin, Y. Shen, Y. Papelis, "Automatic High-Fidelity Roadway Generation," *2009 Modeling and Simulation Capstone Conference*, 6 pages, (Norfolk, VA), April 2009.

J. Wang and Y. Shen, "Modeling and Visualization of Complex Moon Craters," *MODSIM World Conference & Expo*, (Virginia Beach, VA), September 2008.

J. Wang and Y. Shen, "Synthesizing High-resolution Terrains with Craters," *2008 Modeling and Simulation Capstone Conference*, (Norfolk, VA), March 2008.